UCLA
UCLA Electronic Theses and Dissertations

Title
Communications Networking for Autonomous Vehicle Highway Systems

Permalink
https://escholarship.org/uc/item/8fn8360c

Author
Sunyoto, Yulia

Publication Date
2020

Peer reviewed|Thesis/dissertation

UNIVERSITY OF CALIFORNIA

Los Angeles

Communications Networking for Autonomous Vehicle Highway Systems

A dissertation submitted in partial satisfaction

of the requirements for the degree

Doctor of Philosophy in Electrical and Computer Engineering

by

Yulia Sunyoto

2020

ABSTRACT OF THE DISSERTATION

Communications Networking for Autonomous Vehicle Highway Systems

by

Yulia Sunyoto

Doctor of Philosophy in Electrical and Computer Engineering

University of California, Los Angeles, 2020

Professor Izhak Rubin, Chair

Autonomous driving based systems will improve safety and enhance vehicular traffic flow. A fully-autonomous highway system must make effective use of a reliable and robust communication system. We develop methods for the design of data networking mechanisms that provide for low-latency dissemination of critical messages, as well as enable high system data throughput capacity levels that are used to accommodate the transport of other message flows and sensor data streams.

The data networking mechanisms presented in this dissertation encompass vehicle-to-vehicle (V2V) and/or infrastructure-aided data communication. The latter employs vehicle-to-infrastructure and infrastructure-to-vehicle (V2I) communications. We develop novel networking protocols by considering mobile systems that employ sub-6 GHz spectral resources as well as emerging systems that make use of millimeter wave (mmWave) frequency bands. Data transmissions across sub-6 GHz bands experience lower channel propagation degradations than those incurred across mmWave bands. In turn, mmWave communications channels provide for vastly wider spectral resources, and thus yielding much higher data rates and lower message latencies.

For regions whose transportation networks are not supported by a dense communications infrastructure, we show that an effective use of V2V networking systems can be well realized.

In turn, we show that when a proper infrastructure system, which consists of interconnected road side units (RSUs), is available, highly upgraded networking operations can be realized. We show that such a system, when properly designed, can be configured to yield very low critical data message dissemination delays while assuring ultra high throughput rates for other message classes.

In setting the system schemes and cross layer parameters to induce desired delay-throughput performance behavior, we examine a multitude of scheduling schemes, and properly set the underlying cross layer parameters, including spatial reuse factors, modulation/coding schemes and data rates, and the underlying transmit power levels. We also involve the following system parameters : antenna gains, vehicular formations and speeds, density of the RSU backbone.

The schemes and techniques presented in the dissertation provide system designers with guidelines, protocols and performance evaluation methods to synthesize a network system for the autonomous highway that will guarantee enhanced data networking performance.

The dissertation of Yulia Sunyoto is approved.

Danijela Cabric

Lieven Vandenberghe

Brian D. Taylor

Izhak Rubin, Committee Chair

University of California, Los Angeles

2020

To my family

CONTENTS

xi

ACKNOWLEDGMENTS

First of all, I would like to express my utmost gratitude to my advisor, Professor Izhak Rubin, for helping me throughout my doctorate studies. His guidance has helped me reach the completion of this dissertation. He has shared with me his research expertise, guided me to generate original research ideas, and also given me constant feedback in improving my research work.

I am grateful to have Professor Danijela Cabric, Professor Lieven Vandenberghe and Professor Brian D. Taylor as my doctoral committee members. Their generous comments and valuable suggestions have helped me improve the content and presentation of this dissertation.

I would like to thank Professor Andrea Baiocchi and Ion Turcanu, for their inputs on my research work in Chapter 2. I would also like thank the UCLA Institute of Transportation Studies for providing research grant for my research work in Chapter 3.

I appreciate my lab mates, Yu-Yu Lin and Hung-Bin Chang, who have guided me during the early stages of my doctorate studies.

Last but not least, I would like to thank my parents and sister for their constant support of my academic and professional pursuits.

2015–2020   Ph.D. Candidate (Electrical and Computer Engineering), University of California Los Angeles (UCLA)

2014–2015   M.S. (Electrical Engineering), UCLA

2011–2013   B.S. (Electrical Engineering), UCLA

2019–2020   Teaching Fellow, Electrical and Computer Engineering, UCLA

2018–2019   Teaching Associate, Electrical and Computer Engineering, UCLA

2016–2018   Teaching Assistant, Electrical and Computer Engineering, UCLA

PUBLICATIONS

I. Rubin, A. Baiocchi, Y. Sunyoto and I. Turcanu, "Traffic Management and Networking for Autonomous Vehicular Highway Systems", Ad Hoc Networks, Vol. 83, Pages 125–148, Elsevier, 2019.

I. Rubin and Y. Sunyoto, "Infrastructure-aided Networking for Autonomous Vehicular Systems" In: Arai K., Bhatia R., Kapoor S. (eds) Proceedings of the Future Technologies Conference (FTC) 2019. FTC 2019. Advances in Intelligent Systems and Computing, Vol. 1070. Springer, Cham, 2020.

Y. Sunyoto and I. Rubin, "Infrastructure-based Networking for Autonomous Transportation Systems Using IEEE 802.11p", 2019 IEEE Vehicular Networking Conference (VNC) (IEEE VNC 2019), December 2019.

CHAPTER 1

Introduction

Autonomous driving can improve safety and enhance vehicular traffic flow. A fully-autonomous highway environment must make use of a reliable, robust and delay-aware communication system that enables data networking for the dissemination of both critical and non-critical messages to and from highway vehicles. We study different data networking mechanisms to yield high data throughput for the dissemination of messages across prescribed highway spans under packet delay target levels. The data networking mechanisms include message flow dissemination schemes that use V2V (vehicle-to-vehicle), V2I (vehicle-to-infrastructure) and I2V (infrastructure-to-vehicle) communications. Our methods take into account the different levels of highway coverage provided by the Roadside Unit (RSU) infrastructure. For certain segments of the highway there may be no RSU coverage so that an ad hoc based (V2V) networking mechanism should be used. In turn, under full RSU coverage, infrastructure-based networking (involving V2I and I2V communications) can be utilized. We also consider the deployment of different frequency spectra, namely a sub-6 GHz band and a millimeter wave band. We develop novel networking schemes under the use of these bands. Data transmissions carried out across a sub 6 GHz band experience lower channel propagation degradation than those incurred across the mmWave band. However, a mmWave band based system offers a much wider spectrum resource, leading to significantly higher transmission data rates and much lower packet dissemination latency. The data networking schemes that we develop for operation at a sub-6 GHz band are presented in Chapter 2 and Chapter 3, while those developed for operation at a mmWave band are presented in Chapter 4.

In the first part of the dissertation (Chapter 2), we develop platoon-based Vehicle-to-Vehicle (V2V) cross-layer wireless networking schemes that are used to disseminate messages

1

among vehicles traveling on a multi lane highway within a specified sub-region. Vehicles moving across each lane are organized into platoons. A Platoon Leader (PL) is elected in each platoon and is used to manage its members and their communications with the infrastructure and with vehicles associated with other platoons. For this purpose, we develop algorithms that configure a hierarchical networking architecture for the autonomous system. Certain platoon leaders are dynamically assigned to act as Backbone Nodes (BNs). The latter are interconnected by communications links to form a Backbone Network (Bnet). Each BN serves as an access point for its Access Network (Anet), which consists of its mobile clients. We study the delay-throughput performance behavior of the network system and determine the optimal setting of its parameters, assuming both TDMA and IEEE 802.11p oriented channel sharing (MAC) wireless schemes. We demonstrate the performance tradeoffs available to the system designer and manager when aiming to configure the data communications network system to meet targeted message throughput and delay objectives.

In the second part of the dissertation (Chapter 3), we study infrastructure-based vehicular data networking for autonomous highway transportation systems. The infrastructure backbone consists of roadside units (RSUs) that act as access points for vehicles traveling along a segment of a highway system. The RSUs are interconnected by high-capacity point-to-point links. It is assumed that RSU transmissions reach all vehicles traveling along the highway. We present a data networking protocol that enables geocasting so that source vehicles aim to disseminate their data packets to vehicles that travel within a specified span. The dissemination route includes vehicle-to-infrastructure (V2I) and infrastructure-to-vehicle (I2V) wireless communication uplinks and downlinks. We study the performance behavior of the synthesized data network as a function of the average inter-RSU distance (and thus impacting the density of the RSU backbone). For each case, we set the structure of the medium access control scheduling scheme and configure the employed Modulation Coding Schemes (MCS) and corresponding data rates, the transmit power levels and the spatial-reuse factors. TDMA and IEEE 802.11p based Medium Access Control (MAC) scheduling schemes are used for vehicles and RSUs to efficiently share the system's communications links. We

aim to obtain high throughput rates under prescribed packet delay limits. In addition, we impose high packet successful reception rate requirements for assuring reliable dissemination of packet flows.

In the third part of the dissertation (Chapter 4), we develop millimeter wave (mmWave) based data networking multicast schemes for autonomous vehicle highway systems. An ultra reliable, robust and low-latency communications networking facility is essential for the support of safe and rapidly adaptive autonomous operations. This is of critical importance for the dissemination of safety messages and for the maintenance of platoon based vehicular formations. The availability of high data throughput rates is also essential for maintaining the dissemination of sensor data and non-critical message applications. The availability of wide spectral resources when using a mmWave band enables the support of low latency critical messaging as well as high throughput data flows. In considering mmWave signal propagation characteristics, directional transmissions are employed. In implementing data multicast dissemination of critical messages over mmWave bands, we present and study two networking algorithms: a RSU-aided mmWave multicast dissemination protocol (RAMDA), and a V2V based mmWave multicast dissemination protocol (V2VDA). The RAMDA scheme uses joint V2V and V2I mmWave data links, as well as RSU-to-RSU transmissions across an infrastructure backbone. In turn, communications links employed under the V2VDA scheme are used for V2V intralane and interlane transmissions. We evaluate the performance of RAMDA and V2VDA protocols by considering several parameters, namely the inter-RSU distance, inter-vehicular distance, underlying modulation/coding scheme (MCS) and associated link data rate, the transmit power level and the antenna beamwidths used by RSUs and vehicles, as well as FDMA / TDMA based resource allocation medium access control (MAC) schemes and the employed spatial reuse factors (SRFs). We derive and study the system's delay vs. throughput performance behavior, under prescribed strict message delay requirements. In comparing the performance behavior of the underlying RSU aided and V2V algorithms, we show that under a RSU density that is higher than a demonstrated level, data messages will experience much lower dissemination delays under the RSU aided

3

scheme, When lower priority non-critical data flows are involved, we note the two algorithms to yield similar throughput capacity rate levels.

CHAPTER 2

Vehicle-to-Vehicle Data Networking for Autonomous Vehicle Highway Systems on the Sub-6 GHz Band

2.1 Introduction

Automated vehicle technology is advancing rapidly. The Society of Automotive Engineers classifies six levels of vehicle automation, from Level 0 (no automation) to Level 5 (full automation). Nearly every vehicle sold today can operate at Level 1 (driver assistance), many at Level 2 (partial automation), and and a few of the most advanced new vehicles are close to Level 3 (conditional automation). Given this rapid pace of change, increasingly autonomous vehicles need to not just sense other vehicles and the physical environment, but also to communicate with other vehicles and the smart urban and transportation infrastructure. To enable these advances, technologies and regulation procedures need to be developed and enacted.

Among the multitude of technical aspects that dominate the design, management and control of high performance autonomous driving systems, vehicular data networking is of paramount importance. This involves communications and data dissemination among vehicles, i.e. Vehicle-to-Vehicle (V2V), and between vehicles and fixed infrastructure, i.e. Vehicle-to-Infrastructure (V2I). High performance reliable communications networking of data messages among moving vehicles is a key ingredient in enabling the learning by autonomous vehicles of their surrounding environment, the rapid reaction to critical events assure the safety of the operation, coordination among vehicles to synchronize mobility and maneuvering. It facilitates in the execution of processes that serve to optimize travel safety, reduce transit

delays, disseminate sensed data reports to nearby vehicles that include environmental and congestion conditions, upload data to remote cloud servers, and enable remote monitoring, supervision, management and control of the autonomous vehicle system.

In this chapter, we consider a highway populated with autonomous vehicles [1]. We regulate vehicles that move in each lane into platoon formations. Key advantages offered by the use of autonomous vehicle platoon formations [2] include distinct upgrades in vehicular throughput rates and higher energy efficiency levels. Autonomous vehicle platoon formations enhance the efficiency of realized cooperative interactions between vehicles. Such interactions enable the maintenance of effective inter-vehicular distances, promoting lower variations in vehicular speeds and inter-vehicular distance variations. The latter also lead to improved energy / fuel and emission efficiency levels.

Such formations are advantageous in that an elected vehicle within the platoon, identified as the Platoon Leader (PL), can be used to rapidly and efficiently regulate mobility and maneuvering of its platoon vehicular members. Furthermore, we make use of these formations in synthesizing a dynamically adaptive V2V networking architecture. We develop models that provide system design guidelines and that demonstrate the performance tradeoffs characterizing the system when integrating the embedded traffic management and data communications networking operations. The major contributions of this work can be summarized as follows:

- We investigate the design of a V2V data communication networking system that is aided by the formation of autonomous vehicle platoons along the highway. For this purpose, we introduce a two layer hierarchical network architecture that consists of a dynamically formed Backbone Network (Bnet) and Access Networks (Anets). Bnet is dynamically synthesized through the election of PLs that are elected to serve as Backbone Nodes (BNs). Each Backbone Node (BN) manages its Access Network (Anet), which consists of its mobile clients. We examine the use of mixes of candidate Medium Access Control (MAC) schemes across the Bnet and the Anets, in considering Time-Division Multiple Access (TDMA) and IEEE 802.11p based protocols. We carry out extensive analyses to determine the optimal parameter settings to be set for each candidate scheme,

6

determining the highest data communication throughput levels that are attainable in each case, under specified packet delay limits. To demonstrate the underlying design options, we assume data applications that require the packets generated by a vehicle that is active in producing a data flow to disseminate the ensuing data packets across a specified distance span.

- We study the tradeoffs involved in integrating the mechanisms developed by us to induce an effective traffic management operation, which strives to produce high vehicular flows along the highway under vehicular delay constraints, and those developed to attain a high capacity V2V data communications network system.

The remainder of the chapter is organized as follows. In Section 2.2, we present related works and the motivation for platoon-based traffic management and for the employed networking schemes. In Sections 2.3 to 2.7, we present our data networking models, and carry out optimal design and performance analyses. In Section 2.3, we describe our network system assumptions and the Mobile Backbone Network (MBN)-based networking protocol. In Section 2.4, we outline the involved platoon management systems and network synthesis functions, and discuss an approach to the synthesis of communication network systems. Network parameters and performance metrics are defined in Section 2.5. In Section 2.6, we present the different MAC schemes that we employ in our network study for sharing the communications channel resources along the Anets and the Bnet. Network performance results are presented and discussed in Section 2.7. In Section 2.8, we demonstrate and discuss the design tradeoffs available to the system manager when considering the integrated system operation, in combining traffic management and networking performance objectives. Conclusions are drawn in Section 2.9.

2.2 Related Work

The impact of vehicular platoon applications on traffic flows and road safety have attracted significant interest. Published works have shown that organizing vehicles in platoons can

7

Focus	Approach	References	Features
Networking & communications	VBN-based	[3, 4, 5, 6]	• Focus on dynamic formation of multi-hop vehicular backbone network. • Vehicles residing at preffered locations act as backbone relay nodes and are in charge of handling the network data flows. • The vehicular traffic flow optimization problem is not tackled.
	TDMA-based	[7, 8]	• Use TDMA wireless access scheme to coordinate the access of vehicles that travel in platoon formations. • Targeted performance metrics include message transport latency and throughput rate. • Only vehicles within the same platoon are assumed to be synchronized.
	IEEE 802.11p-based	[9, 10, 11]	• Employ IEEE 802.11p schemes to study the impact of different beaconing frequencies, platoon sizes, intra-platoon distances, and various vehicular highway loading levels on the communication channels. • Typical measured metrics are probability of successful transmission and platoon stability. • Communication problems due to inter-platoon coordination are not considered.
	Hybrid TDMA and IEEE 802.11p-based	[12, 13]	• Exploit TDMA-like schemes for platoon stability preservation and CSMA/CA for disseminating event-based safety messages. • Vehicular traffic management problems are not considered.

Table 2.1: Summary and classification of the related works

improve traffic flows and reduce fuel consumption [8, 14, 15], while increasing safety and enhancing driving experience [11, 16, 13]. Such advantages of vehicular platoon formations motivate the platoon-based data networking schemes developed in our study.

A common approach of vehicular network communications found in the literature is to dynamically select a subset of vehicles to be in charge of the communication operations in order to reduce the network load [3, 4, 5, 6]. In [3], the authors describe a high throughput dissemination scheme for Vehicular Ad Hoc Networks (VANETs) based on dynamic formation of a multi-hop backbone network. Analysis and design is performed of such a networking protocol when used to broadcast message flows that are generated by a Roadside Unit (RSU) along a linear road, forming a VANET structure that is identified as a Vehicular Backbone Network (VBN). The main idea behind the VBN approach is to use vehicles that reside at preferred locations to act as backbone relay nodes. These relay nodes are optimally configured to operate at designated link data rates, modulation/coding schemes and spatial reuse factors. Presented results demonstrate the significant performance enhancement achieved under a VBN architecture in attaining enhanced throughput capacity rate and in providing for a wider dissemination coverage span. Admitted packets are assured low end-to-end packet delays through the employment of a flow control scheme.

In [4], a topology synthesis algorithm is presented for the synthesis of the Bnet for an MBN based mobile ad hoc network. The algorithm is shown to be highly scalable and fast converging to a solution of an effective connected backbone network that consists of elected mobile nodes. The use of multicast protocols over a mobile ad hoc network is discussed and studied in [5]. A VBN-based scheme is also employed in [6], where the authors exploit the created backbone network to periodically disseminate and collect floating car data from vehicles roaming inside an area of interest. The advantage of multicasting over an ad hoc network through the dissemination of messages over a VBN oriented synthesized backbone has been well demonstrated. In this chapter, our study on platoon based data networking schemes uses a VBN-oriented backbone. However, a major difference between this study and the above mentioned VBN related studies is that we develop joint routing and scheduling mechanisms as

well as analyze the performance behavior of the setting of cross-layer networking parameters for nodes which belong to the backbone and active nodes which do not belong to the backbone.

For platoon-based communications networking studies, whereby a TDMA wireless access scheme is used, we note the following references. In [7], a TDMA scheme is employed to coordinate the access of vehicles that travel in platoon formations. Time slots are arranged in accordance with the relative distance of the message source to the location of a crash. Vehicles that are located closer to a crash location are granted earlier slots, aiming to reduce data message transport latency. An interference reduction mechanism is also illustrated. The employed protocol uses hop-by-hop routing within a platoon. No use is made of platoon structures to execute inter-platoon communications.

In [8], vehicles traveling along a single lane highway are arranged in platoon formations. Platoon formation parameters include inter-platoon and intra-platoon distances, vehicular speeds and the number of vehicles included in a platoon. The desired values of these parameters are determined in relation to performance considerations that are based on the trade-offs between two categories of performance metrics: realized vehicular throughput rate and underlying V2V wireless network performance. A vehicle that produces a packet flow aims to disseminate its packets across a span of the highway whose scope is specified in accordance with the engaged application type. For critical event-driven (Class I) packet flows, the key performance metric is the packet end-to-end dissemination delay. For periodic status-update type (or other stream types of) packet flows (Class II), the attained message throughput rate serves as the key metric. The authors employ a spatial-reuse TDMA protocol, using hop-by-hop communications among vehicles inside and outside a platoon. Multiple information sources can be simultaneously active. Optimal platoon formations are determined, aiming to preserve Class I message delays prescriptions while attaining high Class II message throughput rates and high vehicular throughput rates. Only vehicles that are members of the same platoon are assumed to be synchronized.

In contrast, we assume in this chapter, that when TDMA-based transmissions between platoons are executed, time synchronization information is made available to platoon leaders

10

(e.g., by using a Control Channel (CCH) or a road side backbone). Also we note that in this chapter, we do not impose hop-by-hop transmission of messages among platoon mobiles. In turn, a message transmitted by a platoon leader is broadcasted over a specified range, reaching also its platoon members.

Relating to papers that employ IEEE 802.11p-based schemes, we note the following studies. The study in [9] presents analytical and simulation models that are used to calculate the probability of successful transmission of beacon messages within a platoon. The study explores the effect on system performance of using different beaconing frequencies, fixed platoon sizes and various vehicular highway loading levels. The study also determines the minimum beacon rate. This study does not consider the impact of different platoon configurations on data throughput. It also does not involve inter-platoon communications.

The study presented in [10] presents analytical and simulation models for capturing the impact of Cooperative Awareness Message (CAM) exchange process, when applied for platooning control. The authors assume both platoon-organized and non-platooned vehicles traveling on a highway and periodically exchanging CAM messages. From a network communication perspective, the probability of a successful transmission is computed under varying traffic density levels. The impact of the communication process on platoon stability is also analyzed by the authors of [10]. The parameters taken into account include the highway density, intra-platoon distance values, and beacon frequency. The employed analytical model neglects the hidden node terminal problem and considers synchronous communications. This work does not study routing of message flows and optimal platoon formations.

In [11], the authors propose a distributed consensus-based control algorithm for performing vehicular platooning with Inter-Vehicle Communication (IVC). Generally, the coordination of a platoon of vehicles involves the use of a control algorithm that adjusts the relative distance among adjacent vehicles in the platoon, and a communication network that allows vehicles to exchange information. This paper considers the IEEE 802.11p protocol as the main scheme used for executing V2V communications networking. The proposed control algorithm is proved to be robust with respect to variations in logical communications topologies (e.g.,

predecessor-following, leader and predecessor-following bidirectional), as well as with respect to communication delays and losses. The authors provide a theoretical analysis of the stability of their proposed algorithm and validate their solution through simulations that consider detailed physical characteristics of vehicular dynamics. In contrast to our study in this chapter, the inter-platoon coordination and communications problem is not considered.

Several papers include the use of both TDMA and IEEE 802.11p protocols for V2V networking. In [12], just two types of communication scopes are involved: broadcasting from a platoon leader to all platoon vehicles, and transmission of a message from a vehicle to its neighboring vehicles. Protocols include slotted beaconing within a platoon (intra-platoon TDMA) and beaconing using Carrier-Sense Multiple Access with Collision Avoidance (CSMA/CA). The number of vehicles on the highway serves as a parameter, under fixed platoon size and intra-platoon distance values. This study also explores the effect of varying the beacon frequency on the minimum intra-platoon distance levels, under targeted data communication delay constraints. The paper does not perform a study on communication between platoons and it does not account for message routing between different platoons. It also does not investigate the setting of platoon configurations for the aim of optimizing communications and/or vehicular throughput metrics, as performed by us in this chapter.

The study in [13] presents a consensus-based control algorithm for vehicular platooning and an adaptive message dissemination scheme to guarantee a platoon stability requirement. The study considers a scenario that involves both platoon-organized and individual vehicles traveling along a highway. The theoretical analysis of the proposed control algorithm shows that the state error (position and speed) function incurred between platoon members and platoon leader can converge within a prescribed time bound in presence of beacon packet loss. This bound depends on the platoon size, beacon delivery ratio, and magnitude of the acceleration perturbation component. The proposed message dissemination scheme uses the current channel quality and the leader's dynamics to adaptively select beacon sending time slots for each platoon member. A TDMA-like MAC mechanism is used for intra-platoon beaconing, while a CSMA/CA-based approach is considered for disseminating event-based

safety messages. An inter-platoon communication management mechanism is also proposed. The authors perform analytical and simulation-based evaluations to validate the effectiveness of their proposed solution. A summary of these related works can be found in Table 2.1.

2.3 Network Systems

In the following sections, we illustrate the configuration and performance behavior of a V2V wireless network system that we synthesize by taking advantage of the organization of vehicles flowing along the highway lanes into platoon formations. As often assumed, the wireless medium assigned for communications among vehicles is divided into distinct communication channels. Included in our models are thus a Control Channel (CCH) and a Service Channel (SCH). As performed by IEEE 802.11p systems, vehicles use the CCH to periodically (such as every 100 ms) transmit and disseminate status updates to other vehicles in their neighborhood. The type of CCH under consideration can be similar to that used by WAVE [17] and other currently examined architectures, where CCH is used by vehicles and/or infrastructures to broadcast in each area status and system management and control messages [18],[19],[20] as well as to allocate time slots for contention-free MAC schemes [21],[22]. To illustrate, we use wireless communications radios that employ the 5.9 GHz band, as often used for testing autonomous vehicle system technologies such as DSRC and C-V2X [23] [24].

To demonstrate the performance behavior of a platoon-based V2V communications network that we hereby introduce, we consider two classes of event-driven messages produced by highway vehicles that are targeted for dissemination to other highway vehicles for dissemination within the SCH. To illustrate, we assume that each such message has a dissemination span of a range of at least $d_{\mathrm{span}} = 300\,\mathrm{m}$. We note that for protocol simplification, the dissemination span may at times somewhat exceed this range. Also, to simplify we assume in the following that messages produced by a source vehicle are disseminated to vehicles that travel in the specified span behind the source vehicle (i.e., behind its direction of motion). Our protocols and basic models are noted to readily extend to apply to scenarios whereby the dissemination span bi-directionally covers vehicles that move behind and ahead of the source vehicle. We

13
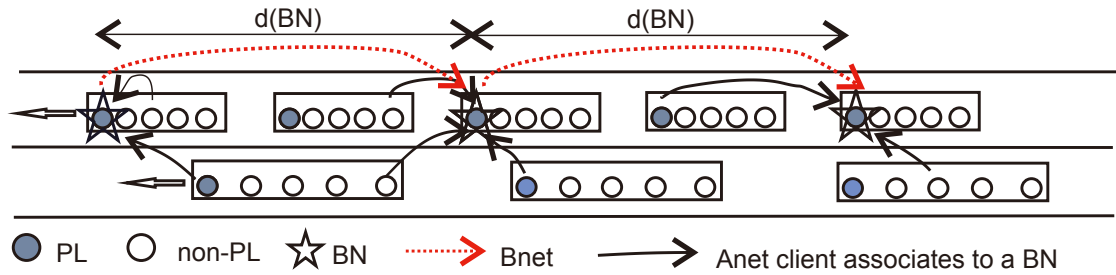
Figure 2.1: Network Architecture: BNs and associated Anet clients. The solid arrows represent association of Anet clients to BN and the dotted arrows represent Bnet communications

assume Class 1 messages to include critical (e.g., safety) messages and to thus be granted higher priority. The throughput rate of such event-induced message flows is relatively low. However, such a message should be disseminated across its span aiming to achieve a Packet Delivery Ratio (PDR) across the complete span that is at least 0.95. Successfully delivered messages should complete their dissemination within a 95-percentile time delay requirement of 50 ms. Class 2 message flows are of lower priority. Yet, they tend to produce message flows that impose high throughput rate requirements on the wireless network.

The network architectures and protocols presented in this chapter, extend the concepts and techniques introduced by us in developing a class of mobile ad hoc networks that move in two or three dimensions, identified as MBNs and a class of V2V wireless networks identified by us as VBNs. Yet, in contrast, the network systems introduced in this chapter involve the autonomous mobility of highway vehicles and are based on the formation of vehicular platoons across highway lanes. Otherwise, the networking systems studied in this chapter assume a two layer hierarchical architecture similar to that used in our MBN and VBN-based systems: certain vehicles are elected to act as BNs forming an interconnected wireless Bnet; each BN manages the access of its client mobiles across its wireless Anet. Figure 2.1 illustrates the network systems which we use in this chapter. We assume the wireless communications channels forming the Bnet and Anet systems to be shared in accordance with one of the following joint MAC protocols:

1 Demand-assigned (DA) TDMA scheme across each Anet and TDMA scheme across the

Bnet (MAC 1);

2 IEEE 802.11p oriented protocol across each Anet and TDMA scheme across the Bnet (MAC 2);

3 IEEE 802.11p oriented protocol across each Anet and IEEE 802.11p protocol across the Bnet (MAC 3).

2.3.1 MBN-based Networking Protocol

As noted above, the network architecture studied in this chapter consists of the Bnet and its BNs and the corresponding Anets. An Anet client always associates itself with a BN which the Anet client determines to be the closest to it (or, generally, from which it receives radio signals at the highest power or quality, as often done in a cellular system). The messages produced by a vehicle that is a client of a BN are transmitted by the source vehicle across its Anet to its associated BN (identified as the corresponding source BN). The distance between two adjacent BNs located along the same lane (i.e., the inter-BN distance) is denoted as d_{BN}. The later disseminates the messages across the Bnet, across BN-to-BN links, covering its targeted d_{span} range, in a multi-hop fashion across $n_{\mathrm{hops}} = \lceil d_{\mathrm{span}}/d_{\mathrm{BN}} \rceil$ hops. The destination Anet client is assumed to be able to receive that message sent to the destination BN that manages its Anet. For simplification of the analysis, we skip hereby cases under which the number of Bnet hops may exceed by 1 the later value, as it does not affect much our analyses and performance results. By using BNs (among elected PLs) to forward messages, rather than performing hop-by-hop forwarding, we reduce in a significant manner the number of hops that are used for the V2V dissemination of data messages and thus increase the energy efficiency of the networking operation.

Under a borderline case, such as when $d_{\mathrm{BN}} > d_{\mathrm{span}}$, the destination Anet client is a member of the source Anet. The performance metrics are calculated in a similar manner for this case under the setting of $d_{\mathrm{BN}} = d_{\mathrm{span}}$. The overall system throughput is scaled by using a factor that is proportional to the number of system BNs, N_{BN}, similarly for the case where

15

the source and destination mobile nodes are members of the same Anet, sharing the same BN. In case the distance from Anet client to its BN is greater than its d_{span}, the Anet client can proceed to directly reach its destination through a sole transmission across its Anet. To simplify, we focus on dissemination span coverage ranges that exceed the Anet diameter span.

2.4   Synthesis of Network Hierarchical Architecture

We assume that vehicles are organized in platoons when traveling on a highway of length l. The vehicle that travels at the head of a platoon is identified as the PL. We note that our schemes and protocols are also readily applicable when a vehicle that occupies a different position within a platoon is selected as the PL. We introduce the following notation:

d_{PL} distance between two successive platoon leaders.

d_{V} minimum distance between vehicles that are members of the same platoon.

d_{P} minimum distance between platoons, i.e, the minimum distance required between the ending location of a platoon and the starting location of a subsequent platoon; it is set as $d_{\text{P}} = d_{\text{V}} + g$, where g represent an excess gap range, beyond d_{V}.

g excess minimum gap distance between two subsequent platoons; its value is a function of the rate of vehicles that need to merge into and/or out of a given lane and/or maneuver through the lane to change lanes; higher such gap margins are typically required for setting platoon formations across slower lanes, as they need to accommodate vehicles that cross the lane as they enter to join flows across a faster lane, or vehicles that enter the lane from faster lanes as they are in the process of exiting the highway, or switching to another highway.

n maximum number of vehicles that are allowed to form a platoon.

v mean velocity of vehicles on the considered highway link.

s mean length of a vehicle.

u deceleration of a vehicle.

Δu deviation of the deceleration level from its nominal value.

The platoon leader of platoon k, denoted as PL_k, is the leading vehicle in platoon k. The platoon trailer of platoon k, denoted as PT_k, is the trailing vehicle in platoon k. The distance spanned between PL_{k-1} and PL_k, defined as the distance between consecutive platoon leaders, d_{PL}, assuming each platoon to have full occupancy of n vehicles, is given by

$$d_{\text{PL}} = (n-1)d_{\text{V}} + d_{\text{P}} = nd_{\text{V}} + g = ns + n\zeta\frac{v^2}{2u} + g \qquad (2.1)$$

where the second term in the rightmost side of the equation is calculated by using the same model as that presented in [25], which accounts for a safe distance that must be maintained between adjacent vehicles, and uses the factor $\zeta \equiv 2\Delta u/u/[1 - (\Delta u/u)^2] \leq 1$ to account for the range of dispersion of deceleration factor values realized by different vehicles. Thus, platoon formations are characterized by three key parameters: the maximum number n of vehicles that are members of a given platoon, the inter-platoon distance factor ψ, which accounts for the inter-platoon gap $(g = \psi d_V)$ required to handle add/drop mergers and transit movements, and the velocity parameter v. To illustrate, the parameter values are set to $s = 6\,\text{m}$, $u = 3\,\text{m/s}^2$ and $\Delta u/u = 0.1$.

2.4.1   Platoon Management for Network Synthesis

We assume that vehicles traveling across each lane of the highway are organized into platoon formations. Each platoon is managed by its PL. Alternatively, another member of a platoon may also be elected to act as the PL. The corresponding management architecture includes the following management entities (whose functionality may be physically realized to reside in a single or separate nodes): the Highway System Manager (HSM) and the Ramp Access Manager (RAM).

HSM collects and stores status and capability information about vehicles under its supervision; for this purpose, it also monitors the periodic status messages disseminated by highway

17

vehicles. The information includes vehicles' location coordinates, speeds, destination, communications channel, radio, memory, processing and energy resource capabilities, environmental status, and management responsibilities, including whether it currently serves as a PL. This allows the system manager to also regulate the admission process of vehicles waiting on-ramp for being admitted into the system. It also computes optimum traffic management parameters including: d_V, d_P, n, d_{PL}. These parameters can be adapted to different vehicular traffic loads. The status of vehicle i (among N vehicles currently admitted into the highway segment under consideration) is represented by a status vector that includes the following components: $x_i = (pl_i, c_i, bn_i, v_i)$, i = 1, ..., N. The pl_i state variable indicates whether vehicle i is a PL, c_i represents the coordinates of the location of vehicle i, bn_i indicates whether a vehicle currently serves as BN, v_i represents the vehicle's velocity.

In considering the mobility of platoons relative to an access point of a ramp (that is used for vehicles entering the highway as well as for vehicles departing the highway), we identify the following platoon status indicators. A departing platoon is identified as a platoon which is either in the process of passing through a ramp's access point while its tail has not yet passed this access point, or has completely passed this access point (so that its tail vehicle passed it as well). A departing platoon may incur vehicle departures and admissions as the platoon passes by the ramp's access point. An arriving platoon is identified as a platoon whose leader has not yet arrived at the ramp's access point (which is located upstream relative to its mobility). The state of the system at ramp k at time t that corresponds to the time that a departing platoon on a given highway reaches the ramp, is represented by the vector $X_t = ((P_d, P_a)^{(k)})$, where $1 \leq k \leq N_{PL}$. The components of the vector $P_d(n_d, c_d, v, bn_d)$ identify the states of a departing platoon. The component n_d represents the number of vehicles belonging to a departing platoon, c_d represents the coordinates of the last vehicle of this platoon, bn_d indicates whether the platoon leader serves as a BN. The vector $P_a(n_a, c_a, v, bn_a)$ stores the states of the arriving platoon, whereby n_a is the number of vehicles within the arriving platoon, c_a are the coordinates of leading vehicle of the platoon, bn_a indicates whether the platoon leader serves as a BN.

The HSM computes and disseminates the optimal values of the communications network parameters, such as d_{BN}, in considering the system's desired vehicular traffic and communications networking performance features, using the formulas and approaches described in this chapter. The RAM receives state information from the HSM, as well as the outcome of its computations that convey the desired system traffic management parameters, including recommended platoon formation parameters, the optimal networking parameters (including d_{BN}), and the states of vehicles which are subjected to its local management. The RAM uses the local vehicular state updates that it periodically receives from the HSM to regulate the admission of vehicles into the highway, to determine the structure of new platoons that it forms, to control the admission of vehicles in joining existing platoons, to merge platoons, and to elect PLs and BNs.

For purpose of forming platoons and managing vehicle admissions, the RAM computes several time spans. It calculates the time elapsed between the tail of a departing platoon and the time of arriving PL at its access point, denoting it as $T_{\mathrm{d,a}} = \frac{c_{\mathrm{d}} - c_{\mathrm{a}}}{v}$). It also calculates the time parameter T_{p} that represents the minimum time required to elapse between the traversal time at its access point of the tail vehicle of a departing platoon and the time of arrival of the subsequent leader of an arriving platoon; $T_{\mathrm{p}} = \frac{d_{\mathrm{PL}} + d_{\mathrm{P}}}{v}$, corresponding to the gap required to be set between such instants of time. The later parameter is used in its decision as to whether there exists a sufficient gap that allows it to form a new platoon.

2.4.2   Synthesis of Platoon Formations

The principles that we have used for platoon formation include the following assumptions:

- The RAM considers only arriving platoons in determining the admission of vehicles onto the highway. Vehicle admissions take place at instants of time at which the arriving platoons arrive at and then pass by a ramp access point; a platoon that passes by the ramp access point is identified as a departing platoon.

  It is noted that, with no loss in generality, our protocol and analysis can be readily

applied, with corresponding adjustments made, if admission decisions at a ramp access point incorporate the number of vehicles that depart from the highway at an exit ramp located at or near the underlying entry ramp.

The RAM does not consider the admission of a new vehicle with the purpose that it would accelerate to catch up with a departing platoon.

- Vehicles within a platoon move forward to occupy vacant platoon spaces, if any. Vehicles which are admitted from the ramp join a platoon in occupying its tail positions.

- The computed optimal platoon parameters apply to all platoons and vehicles that travel in the same lane, but can be different for different lanes.

- When there are multiple lanes, an admitted vehicle would be routed to a platoon traveling in a designated lane, based on the routing schemes described in the Traffic Management sections of [25]. Yet, due to space limitations, we describe in the networking sections a single lane operation.

The following principles govern the process used by a vehicle admission and platoon formation algorithm (clearly, other versions can be similarly composed):

1. If no platoon is currently passing at a ramp's access point, and if the time to elapse between the last departing platoon and the next arriving platoon is sufficiently long, such that $T_{d,a} \geq T_p$ and at least one vehicle is queueing in ramp, the ramp manager would then admit queued on-ramp vehicle(s) to form a new platoon, electing the first one admitted under this event as the platoon's PL. The manager would proceed to subsequently admit other queued vehicles to join this platoon, assuring that the new platoon contains no more than a total of n vehicles.

2. If no platoon is currently passing by the ramp, and $T_{d,a} < T_p$, the ramp manager waits until the next platoon arrives at its access point prior to making new admission decisions. If the platoon that will subsequently arrive is not full (accounting for current departures as well), so that $n_a < n$ and there is at least one queueing vehicle, the ramp

manager admits new vehicles to join this in-transit platoon, assuring its membership to not exceed its designated capacity n.

3. If an arriving platoon is currently passing by the ramp access point, and if there is at least one queueing vehicle, the platoon manager admits new vehicles to join the platoon in accordance with the principles stated above.

2.4.3 Backbone Network Synthesis

In this section, we illustrate a protocol that is used for the formation of a Bnet. Depending upon the managers objectives, other synthesis protocols can be readily applied. Furthermore, RSUs, including Base Station or Access Point nodes, that are installed at road-side may also be employed and embedded into our models and analyses. To simplify the discussion, we hereby assume that BNs are elected among PLs.

For multi-lane highway systems, BNs can be elected by considering PLs of platoons that travel across any lane or in preference of PLs that travel in certain lanes. For example, the advantage of electing BNs from PLs that are members of platoons that travel along the slow lane is that a lower rate of re-elections of PLs and BNs may be invoked. Slower lane vehicles will then also incur lower rate of re-associations (of a mobile with an elected BN). Furthermore, the slower lane is usually denser, allowing more flexibility when wishing to elect a higher density Bnet. On the other hand, the advantage of electing BNs from PL vehicles that travel along a fast lane is that such vehicles tend to travel longer distances, and thus staying longer on the highway and serving an assigned BN role. For illustrative and discussion purposes, we assume that the RAM assigns higher priority for electing BNs among PLs that travel along a slower lane. If at an underlying period of time there is no PL that travels along a slow lane, the RAM proceeds to choose one that travels along a faster lane.

Each RAM receives information from the HSM regarding the status of vehicles that it manages, including the residual lifetime (time to destination) and entry and departure locations of these vehicles. As noted above, BNs are elected from the group of underlying

PLs, including PLs which have already entered the highway or vehicles queued on the ramp which will be admitted into the highway. The rules for BN election for association of mobiles with a BN are as follows:

1 If a RAM observes that there is no vehicle that assumes a BN role traveling across its highway link, in upstream or downstream direction, it will elect a PL whose location is closest to its access point to serve as a BN, preferring one that travels along the slowest lane.

2 If the RAM detects at least one vehicle that acts as a BN to transit its location but determines that there is no other vehicle that serves as a BN which is located d_{BN} away from the latter BN, in either upstream or downstream direction, the RAM proceeds to elect a PL to serve as a BN, aiming this PL to be located a range of d_{BN} away from the preceding detected BN. For this election, it can consider vehicles that travel in either upstream or downstream direction from the existing BN, in its vicinity.

3 If the above process results in $d_{\mathrm{BN}} \leq d_{\mathrm{PL}}$, the RAM attempts to elect a PL from another lane to serve as a BN, provided the latter is at a distance that is closer to the targeted distance of d_{BN}, to ensure the desired Bnet connectivity throughout the highway. It is noted that in periods during which the vehicular flow density levels along the lanes are low, it could help to elect BNs from PLs that belong to multiple lanes in aiming to synthesize a high capacity connected Bnet. If no available PL which satisfies the latter d_{BN} distance requirement can be detected, PL that travel along the slow lane are configured to serve as BN.

4 A PL which is elected to serve as a BN advertises this role by indicating it within its periodic status message. It is thus detected by all neighborhood mobiles (including PLs, BNs and other mobiles).

5 The RAM initiates election of a new BN upon departure of a PL which was elected as a BN.

6 A non-BN regularly listens to periodic status message advertisements on the CCH. It uses this information to identify the identity of the BN which it receives at the highest communications quality; often the one that is closer to it. It then associates itself with the Anet managed by the latter BN.

2.5 Network Parameters and Performance Metrics

In the following, we study the performance behavior of the network under several Anet and Bnet MAC protocols, determining for each case the best configuration of the platoons and the best inter-BN distances to be configured. Platoon compositions and velocity parameters setup conditions that correspond to attaining high vehicular flow rates, as determined by the traffic management models presented in this chapter, are also incorporated. For configuring the communications network to achieve high performance, we aim to synthesize a network system that yields a high message throughput rate in disseminating Class 2 message flows while disseminating Class 1 message flows under strict message delay objectives. To characterize the highest achievable such throughput capacity rate, we assume the nodes to be highly loaded by Class 2 application flows.

When analyzing multiple lane scenarios, a selective set of PLs are elected as BNs. As noted above, we select BNs from PLs that travel along the slow lane. Through our simulation and analysis based evaluations, we have found that parametric results presented for a single lane can point to performance attained in a multi lane environment. However, due to space limitations, we focus here on performance results for vehicles that travel along a single lane. The total number of clients served on the highway is set to N. Each BN serves across its Anet n_{clients}. We determine the best configuration of each network scenario by varying the inter-PL and inter-BN distance levels, and by varying the employed Anet and Bnet MAC schemes, and their corresponding transmission data rates and reuse (coloring) levels.

To illustrate the performance tradeoffs available to the designer under various network configuration options, our simulations and analysis based performance evaluations employ

the following parameter ranges. We consider Bnet link ranges, d_{BN}, to range from 100 m to 500 m. The number of vehicles N admitted to the single lane system under consideration is set to range from 100 to 500, representing highway congestion levels that vary from light to heavy loading conditions. The inter-vehicular distances within a platoon, d_{V}, is varied from $d_{\text{PL}}/20$ to d_{PL}/n, and the transmit power level P_{tx} is varied between 23 dBm and 33 dBm.

The simulations for IEEE 802.11p-related MAC schemes are implemented by using the NS-3 simulator. For TDMA-related MAC schemes, we use analytical models and MATLAB based evaluations. For performance comparisons, we focus our evaluations on setting d_{BN} levels at 100, 150 and 300 m, noting that the assumed d_{span} for flow dissemination is assumed to be equal to 300 m, and under the later d_{BN} levels Bnet disseminations traverse an integral number of inter-BN hops. The results however well illustrate the performance trends to be incurred under other setting levels.

We assume throughout a gap factor of $\psi = 2$. We found out that when using a larger ψ value, for example, setting it to 3, yields generally better or similar network performance behavior, for all the MAC schemes that we have studied. Note however that, as shown above in the traffic management sections, higher ψ values, which may have to be imposed to accommodate trans-lane movements, lead to lower vehicular flow rates.

The employed communications propagation loss model is based on that used in [26]:

$$P_0 = P_{\text{r,dB}}(d_0) = P_{\text{t,dB}} + 10log(\frac{\lambda^2}{(4\pi)^2 d_0^2})$$

$$P_{\text{r,dB}}(d) = \begin{cases} P_0 - 10\gamma_1 log_{10}\frac{d}{d_0}, \text{ if } d_0 \leq d \leq d_{\text{c}} \\ P_0 - 10\gamma_2 log_{10}\frac{d}{d_{\text{c}}} - 10\gamma_1 log_{10}\frac{d_{\text{c}}}{d_0}, \text{ if } d > d_{\text{c}} \end{cases}$$

The network parameters and performance metrics that we have used are summarized in Table 2.2.

Acronym	Definition	Values	Reference
N	total number of vehicles served by the BNs along the highway	100–500	
N_{PL}	number of PLs on the highway $\lfloor L/d_{\text{PL}} \rfloor$		
d_{BN}	distance between BNs along and parallel to the highway	100–500 m	
N_{BN}	number of BNs on the highway $\lfloor L/d_{\text{BN}} \rfloor$		
R	transmission rate used by the Anet R_{Anet} or Bnet R_{Bnet}	6, 12 and 24 Mbit/s	[27]
$SINR_t$	minimum SINR to receive packets correctly for different R	7, 11 and 20 dB	[28, 29]
rv_t	minimum receiver sensitivity for 10 MHz channel for different R	-85, -82 and -77 dBm	[27]
P	packet length	3024 bit	[30]
d_{span}	targeted message dissemination span opposite to travel direction	300 m	[8, 31]
P_{tx}	transmission power used by all communicating nodes	23 and 33 dBm	[32]
M	reuse-M factor used for the Bnet using TDMA	3, 4 and 5	
k_{c}	coloring applied on the Anet using TDMA	1, 2, 3 and 4	
CS_t	carrier sensing threshold	-85 dBm	[27, 26]
d_{CS}	carrier sensing radius assuming single farthest transmission sensed with CS_t	346 m ($P_{\text{tx}} = 23$ dBm)	
γ_1, γ_2	path gain coefficients used in the used propagation loss model	1.9 and 3.8	[26]
d_0, d_c	reference distance and cut-off distance in the used propagation model	10 and 80 m	[26]
TH_{Anet}	aggregate throughput at BNs from Anet clients along L km		
TH_{Bnet}	aggregate throughput at BNs d_{span} from source BN along L km		
$TH_{\text{Anet,Bnet}}$	aggregate throughput at BNs d_{span} from message source along L km		
D_{P}	end-to-end communication delay from source node to destination node		
$D_{\text{P,max}}$	maximum end-to-end packet delay	50 ms	[8]
PDR	packet delivery ratio: fraction of packets successfully received d_{span} from the source	≥ 0.95	

Table 2.2: Network parameters and performance metrics.
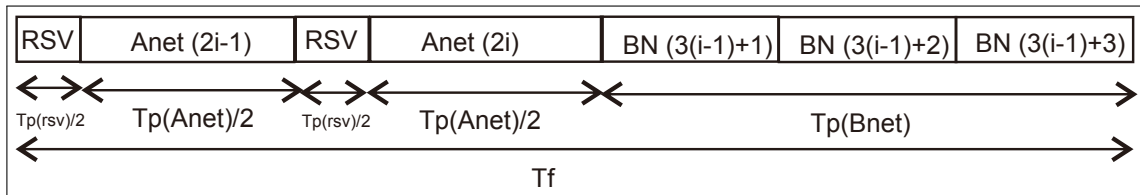
Figure 2.2: Time Slot Allocation in a DA/TDMA Anet-TDMA Bnet Time Frame for Anet coloring $k_{\text{c}} = 2$ and TDMA Bnet reuse-M $= 3$ and $i \geq 1$

2.6 Anet and Bnet MAC Schemes

2.6.1 DA/TDMA Anet - TDMA Bnet (MAC 1)

Under this joint MAC configuration, allocated Anet and Bnet bandwidth resources are shared on a TDMA basis. Also, as shown in Figure 2.2, we assume the overall bandwidth allocated for data communications to be shared by Anets and the Bnet on a TDMA basis (equivalently, one could use an FDMA configuration to separate Bnet and Anet transmissions). We assume BNs to acquire time synchronization, as required for the implementation of the underlying time division schemes. This can be attained by using the periodic broadcasting of a master clock in beacons that are disseminated across the region by using a control channel, or by such message beacons that are periodically transmitted by road-side or other units. In each time frame, time slots are allocated for data transmissions made by Anet clients and by BN nodes. Also, during Anet periods, time slots are allocated for the transmission of reservation packets (that are embedded as reservation indicators sent to the BN by a client that transmits the first message of a new flow during the reservation slot). Thus, each time frame T_f consists of a time period allocated to Anet clients to make reservation requests, Tp_{rsv}, time allocated for Anet transmissions, Tp_{Anet}, and time allocated for Bnet transmissions, Tp_{Bnet}. Hence:

$$T_f = Tp_{rsv} + Tp_{Anet} + Tp_{Bnet}$$

To reduce interference caused by transmissions that are executed simultaneously across neighboring Anets, a k_c-coloring MAC scheduling scheme is employed. Hence, during a Tp_{Anet} period, clients in a given Anet can transmit for a fraction of time that is equal to $\frac{1}{k_c} Tp_{Anet}$, so that during such a period only 1 out of k_c consecutive Anets can allow Anet transmissions to take place. We have determined the proper Anet reuse level k_c to use to mitigate inter-Anet interference, in aiming to assure a high PDR level, $PDR \geq 0.95$ while attaining the highest feasible throughput level. The coloring value to be properly used depends on the employed Anet data rate, R_{Anet}. Under such higher data rate values, a higher reuse k_c level is typically required induced by the higher SINR threshold required at the intended BN receiver.

We allocate within each $\frac{1}{k_c} Tp_{Anet}$ period, a single Anet time slot of duration $Ts_{Anet} = \frac{P}{R_{Anet}}$

to each one of the n_{served} actively served Anet clients, where n_{served} represents the configured number of active Anet clients that can be served by a BN during a time frame.

As noted, our throughput analysis has been performed by assuming heavily loaded BNs. The allocation of Anet slots to a newly active application flow is made on a first-come first-serve basis depending on the arrival time of the first packet of a stream flow. Hence, the index of the transmitting Anet client in each Anet is effectively random. Some transmissions may fail due to interference between Anets (as they may then to not meet minimum SINR level requirement).

The Anet MAC scheme is based on the use of a Demand-assigned (DA) TDMA. The Anet data rate used by Anet clients is denoted as R_{Anet}. Anet clients need to send reservation requests if the number of active clients associated to a BN is higher than than the number of clients which can be served in a single time frame. When the number of active clients n_{active} is lower than the n_{served}, all time slots can be allocated to these n_{active} mobiles on a dedicated basis. Otherwise, if $n_{\text{active}} > n_{\text{served}}$, Anet clients must send reservation packets to the associated BN. Reservation transmissions use the allocated time periods using the bandwidth allocated to the SCH. Class 2 message flows can employ a slotted ALOHA MAC to transmit reservation messages during the reservation slots. In turn, Class 1 messages, may use periods allocated within the CCH to assure a very high success rate in sending reservations. For this purpose, a high priority access mechanism employed by a priority-based IEEE 802.11p protocol can be employed. To well accommodate real-time flows, the BN allocates available data slots for the subsequent transmission of all packets that are members of the flow for which reservation has been successfully carried out. The BN may change the allocation of slots to its client mobiles if slots are required for the support of a new high priority flow.

Across the Bnet links, each BN transmits its packets to its BN neighbor at the R_{Bnet} data rate. To mitigate interference among simultaneously transmitting BNs, and reuse-M level is used. We select the optimal M value, considering the most effective levels, which are established to be equal to the set of values M = 3,4,5. It is noted that for a radio receiver

to effectively receive messages at a prescribed bit error rate, for the underlying employed modulation/coding scheme, one needs to assure the receiver to satisfy minimum SINR and minimum receiver sensitivity level requirements.

The throughput rate achieved along the Bnet is calculated as follows:

$$TH_{\text{Bnet}} = \begin{cases} R_{\text{Bnet}} \frac{N_{\text{BN}}}{M.E[n_{\text{hops}}]} & \text{, if (1) and (2)} \\ 0 & \text{, otherwise} \end{cases}$$

The aggregate Bnet-only throughput TH_{Bnet} is computed based on the assumption that the following conditions are met under the selected reuse-M and d_{BN} values: (1) $SINR > SINR_{\text{t}}$ setting to meet minimum SINR value requirements. Since distance between BNs are fixed with respect to each other being d_{BN}, reuse-M value which is selected to fulfil minimum SINR requirement by assuming a conservative case that all BNs are busy results in transmissions on the Bnet being always successful. For example, to meet this requirement under $R_{\text{Bnet}} = 6\,\text{Mbit/s}$, a minimum reuse $M = 3$ level is required; under $R_{\text{Bnet}} = 12\,\text{Mbit/s}$, a minimum $M = 4$ value is required; under $R_{\text{Bnet}} = 24\,\text{Mbit/s}$, a minimum $M = 5$ value must be configured; (2)$rv > rv_{\text{t}}$ is required to satisfy minimum receiver sensitivity value. For example, under $R_{\text{Bnet}} = 6\,\text{Mbit/s}$ the latter requirement induces a maximum transmission range (under the employed transmit power level of $P_{\text{tx}} = 23\,\text{dBm}$) of about $340\,\text{m}$, while under $R_{\text{Bnet}} = 24\,\text{Mbit/s}$, the maximum transmission range is reduced to about $220\,\text{m}$.

We coordinate the joint allocation of bandwidth resources to the Anet and Bnet components, noting that the Bnet must carry the traffic that is fed to it by Anet clients. Hence, the corresponding time periods Tp_{Anet} and Tp_{Bnet} allocated to Anet and Bnet transmissions in each frame, are set to the proper values, such that one guarantees that the average rate of data messages successfully received by a randomly selected BN from its Anet mobile clients, supplemented by the rate of disseminated messages that arrive from its neighboring BNs, is equal to the average rate at which data can be served by a BN. Consequently, time period allocations must satisfy the following ratio:

$$\frac{Tp_{\text{Bnet}}}{Tp_{\text{Anet}}} = \frac{E[n_{\text{hops}}]R_{\text{Anet}}PDR_{\text{Anet}}M}{R_{\text{Bnet}}k}$$

Accordingly, in considering a BN, the above noted ratio is determined by the time that it requires to transmit messages across the Bnet (which is proportional to $\frac{ME[n_{\text{hops}}]}{R_{\text{Bnet}}}$) vs. the time needed to receive messages transmitted by its Anet clients (which is proportional to $\frac{R_{\text{Anet}}PDR_{\text{Anet}}}{k_c}$) , where PDR_{Anet} is the probability that a packet is successfully transmitted across the Anet, subject to fulfilling minimum SINR and received power constraints.

It is noted that active BNs are allocated Bnet slots on a reuse-M basis so that the corresponding data rate and M values are set to assure the BN receiver's SINR is higher than the minimum level required to assure a specified error rate level. In turn, active Anet clients may be located at varying distances from their associated BN. By properly selecting the number of colors k_{c}, one can ensure that at least $95\,\%$ of the packets will meet the minimum SINR (and thus targeted error rate) requirement.

Assuming the system and access channel to be highly loaded, so that admitted Anet clients are continuously busy, we deduce the following. The aggregate Anet throughput is equal to: $TH_{\text{Anet}} = N_{\text{BN}}\frac{R_{\text{Anet}}PDR_{\text{Anet}}}{k_c}$. The aggregate Bnet throughput is given by: $TH_{\text{Bnet}} = N_{\text{BN}}\frac{R_{\text{Bnet}}}{Mn_{\text{hops}}}$. The aggregate joint Anet-Bnet throughput rate is equal to the average data rate received at the destination BNs. It is equal to: $TH_{\text{Anet,Bnet}} = TH_{\text{Anet}}\frac{Tp_{\text{Anet}}}{T_{\text{f}}}$, representing the effective data rate carried by the Anets.

To assess the packet delay components, we note the following. The Frame Latency (FL) delay component represents the time elapsed between the arrival (or production) time of a packet at the source Anet client and the time instant at which the mobile transmits its reservation packet. The average FL value is set equal to approximately half of the time frame. FL is incurred only at the start time of a stream flow. We assume that the first packet piggybacks a reservation request. Subsequent flow packets will not experience such FL delays, as we assume that the flow is allocated slots at a rate that matches its requested rate. To state an upper bound, we set a worst case frame latency value of $FL = T_{\text{f}}$.

The time allocated for Bnet operation, as it applies for transmissions carried out by each BN, has been calculated to include the time taken to serve the traffic arriving from its Anet and the multi hop traffic arriving from other BNs. Based on the location of the associated BN

relative to its Anet clients, the data traffic disseminated across the Bnet will be distributed by using a number of hops that can vary between n_{hops} and $n_{\text{hops}} + 1$. In our simulation based analyses, the actual measured average value has been incorporated and used to allocate the corresponding Tp_{Anet} and Tp_{Bnet} periods.

Assuming all message flows to traverse the Bnet, we note that the internal traffic rate traversing the Bnet is higher than the incoming traffic rate from the Anets by a factor of n_{hops}. Yet, if we account for the last hop of message flows across the Bnet to include reception by the destination BN (and its associated destination Anet clients), the traffic load that is forwarded by BNs (to other BNs) involves traversal of $n_{\text{hops}} - 1$ Bnet links. Hence, the fraction of time that is used by a BN to forward traffic across the Bnet is given by $\frac{(n_{\text{hops}} - 1)}{n_{\text{hops}}}$, relative to its assigned period Tp_{Bnet}, while the time used by a BN to serve traffic from its Anet clients is equal to a fraction $\frac{1}{n_{\text{hops}}}$ of its allocated period Tp_{Bnet}. However, it is noted that the Tp_{Anet} and Tp_{Bnet} time periods were calculated by us above based on Bnet flows traversing $\text{E}[n_{\text{hops}}]$. To regulate the loading of the Bnet under conditions whereby different flows may require dissemination along a different number of Bnet hops, the system would employ a flow control mechanism that serves to block the admission of flows which induce overloading of the backbone.

In calculating the end-to-end delay incurred by packets across the system, we account for the delay incurred in traversing the source Anet, D_{Anet}, and for the delay associated with the dissemination of the packet across the Bnet and reception by the destination Anet client, D_{Bnet}.

For example, consider an Anet client that produces a stream flow whose application produces packets at a rate of a single packet every r_{app} time frames. Such a flow requires the allocation of a single Anet slot every r_{app} time frames. The allocation will last for the duration of the flow; say, for n_{flow} packet transmissions. The first packet will incur reservation delay, including a FL component and further delay until its reservation packet is successfully received at its BN (using, for example, a slotted ALOHA reservation access protocol). Once the reservation / first packet has been successfully sent, subsequent flow

packets are transmitted at periodically assigned time slots, so that no further latencies are incurred. Other models, including such that account for random reservation delays, could be readily included as well. For example, when its Anet is not highly loaded, the BN can proceed to announce also idle service slots to be available for the transmission of reservation packets, yielding a much reduced reservation latency. As the traffic loading increases, the BN can announce the assigned reservation slot(s) to be available for reservations made by only the highest priority client mobiles, assuring a targeted lower reservation delay level for such messages. Clearly, as a higher capacity is allocated for reservations, a lower residual capacity remains available to support the transmissions of data packets with reservations. In the performance analyses presented in the following sections, we however focus on determining an upper bound on the throughput performance rate attainable under the demand-assigned scheme. Hence, we assume there that just a single reservation slot per frame is allocated, when the system is subjected to high loading. Furthermore, by implementing the above described dynamic scheme to allocate reservation slots, by employing flow admission controls, and by assuming flow durations to be of the order that assures otherwise high probability of success in reservation transmissions across the allocated reservation slot in each frame, we further assume there that the targeted reservation latencies are met. Other analyses are readily carried out when making other reservation process or delay assumptions.

By using the following flow control scheme, we provide admitted packets with a bounded delay level. All packets that reach a BN during a period (of time frame duration) that precedes the Bnet service period (whose duration is equal to Tp_{Bnet}) and are targeted for transmission across the Bnet, are targeted for service during the current Bnet service period. Such packets include all packets that arrive across the Bnet from neighboring BNs and must be forwarded to other BNs, which can be provided higher priority for service by the BN. It also includes Anet packets that are received by the BN from its Anet clients during the preceding Anet period (whose duration has been set to Tp_{Anet}). By using flow admission control for regulating the admission of new Anet flows to a BN, using sliding window measurements of transit traffic and thus concluding the rate available to support newly admitted flows, one

can assure an end-to-end packet delay of the order of $D_\mathrm{p} \leq FL + T_\mathrm{f} \leq 2T_\mathrm{f}$ (plus the impact of reservation delay when applicable, normalized in relation to the average flow duration as only the first packet of the flow incurs such delay). In turn, if a higher end-to-end packet delay level is acceptable, a more relaxed access regulation scheme can be employed.

2.6.2 TDMA Bnet - IEEE 802.11p Anet (MAC 2)

In this section, we discuss the performance features of a system that employs an IEEE 802.11p type CSMA/CA MAC scheme for Anet access and a TDMA scheme in sharing the Bnet communications resources. Anet clients thus use a contention based CSMA/CA access scheme. We assume the carrier sensing range to be set at d_CS. A mobile that is currently in the process of transmitting its message, prevents other mobiles (which may be located in the same Anet or in neighboring Anets) that are within carrier sensing range from it from initiating new transmissions. To reduce interference signals caused by simultaneous transmissions occurring in neighboring Anets, we employ a reuse-k_c Anet coloring scheme. Through the execution of system simulations, we have determined that the highest achievable Anet throughput rate, TH_Anet, is attained when using $k_\mathrm{c} = 1$ or $k_\mathrm{c} = 2$ scheme. Furthermore, the ensuing throughput rate values were noted to be about the same. At low loading rates, the carrier sensing blocking effect is noted to be equivalent to a coloring level of approximately $d_\mathrm{CS}/d_\mathrm{BN}$. At high data traffic rate, the PDR value attained by using $k_\mathrm{c} = 2$ is noted to be about twice higher but the nodes are noted to be able to initiate transmissions only half the time, resulting in comparable overall throughput rates.

The Bnet is configured to use a properly configured TDMA based reuse-M and R_Bnet levels, considering $M = 3$, 4 and 5. As discussed above, the reuse-M level is configured to attain sufficiently high SINR and receiver sensitivity levels, while achieving high throughput rates.

Anet and Bnet periods share the SCH resources on a time division basis. Thus, each time frame T_f consists of disjoint time slots and periods allocated for Bnet and Anet transmissions. The durations of Anet and Bnet time periods are denoted as Tp_Anet and Tp_Bnet, respectively.

Corresponding time periods are allocated within each frame for Anet and Bnet packet transmissions:

$$T_f = Tp_{\text{Anet}} + Tp_{\text{Bnet}}$$

The corresponding periods are sized to accommodate the transmission of admitted Anet and Bnet packets. A flow control mechanism is employed to guarantee that the average packet rate received at each BN (from its Anet and from other BNs) is lower than the effective service rate (i.e., packet transmission rate) that can be executed by the BN. Accordingly, we set the durations of the corresponding periods to satisfy the following relationship:

$$\frac{Tp_{\text{Bnet}}}{Tp_{\text{Anet}}} = \frac{TH_{\text{Anet}} E[n_{\text{hops}}] M}{N_{\text{BN}} R_{\text{Bnet}}}$$

The explanation of this expression is similar to that outlined for the TDMA/TDMA case, except that here employed Anet throughput performance is based on our simulation results.

The maximum aggregate throughput rate attainable by the system, when no packet delay constraints are imposed, denoted as $TH_{\text{Anet,Bnet,max}}$, is expressed in terms of the aggregate Anet throughput rate as

$$TH_{\text{Anet,Bnet,max}} = TH_{\text{Anet,max}} \frac{Tp_{\text{Anet}}}{T_f}$$

When packet delay constraints are imposed, the aggregate delay-capped throughput of the system is approximated as:

$$TH_{\text{Anet,Bnet}} = \rho_{\text{BN}} TH_{\text{Anet,Bnet,max}}$$

where

$$\rho_{\text{BN}} = \frac{\lambda_{\text{BN}}}{\mu_{\text{BN}}}$$

The arrival rate of traffic at each BN is contributed by traffic from the Anet and from neighboring BNs involved in the multi-hop flow. In total, $\lambda_{\text{BN}} = E[n_{\text{hops}}] \frac{TH_{\text{Anet}}}{N_{\text{BN}}} \frac{Tp_{\text{Anet}}}{T_f}$.

The service rate of each BN , μ_{BN} is expressed as $\mu_{\text{BN}} = \frac{R_{\text{Bnet}} Tp_{\text{Bnet}}}{M(T_f)}$ (bit/s). It is noted that μ_{BN} depends on the proportion of time allocated for Bnet transmissions in a time frame, on the reuse-M factor used by the Bnet's TDMA mechanism, and on the employed Bnet data

rate R_{Bnet}. The packet arrival rate at each BN depends on the number of hops taken by a flow to reach the destination BN, on the coloring factor k_{c} and on the employed Anet data rate R_{Anet}.

The time delay incurred by a packet across its source Anet, denoted as D_{Anet}, is measured from the instant of its generation to the instant that it is successfully transmitted to the associated BN (given that its flow has been admitted) is obtained through the execution of Monte Carlo simulations. The delay time incurred by a packet at each BN, denoted as d_{BN}, has been approximated by using analytical calculations.

The waiting time incurred by a packet at each BN, denoted as W_{BN}, has been evaluated by using the following approximations. Within the Bnet per-frame service period, which is of duration Tp_{Bnet}, each BN forwards a fraction $(n_{\text{hops}} - 1)/n_{\text{hops}}$ of the packets that it receives from another BN and also forwards packets that it receives from its Anet clients (of the corresponding fractional order of $1/n_{\text{hops}}$). The latter also represents the assumed fraction of packets that are received by the BN as their destination, and are not forwarded.

As noted above for the previously considered MAC scheme, a flow control scheme is enacted to ensure that traffic with higher than average number of hops is admitted only if under current conditions it can be served while incurring acceptable packet delay levels. Also, a possible service policy at the BN would be for the BN to grant higher service priority to transit packets (that arrive from other BN) and then serve (and flow control the admission of) Anet packets at a lower priority level. Then, when sized properly, transit packets incur limited delay that is of the order of a frame latency.

On the other hand, packets received by each BN from its Anet clients arrive to the BN in a stochastic manner that is induced by the random times at which successful transmissions occur across the IEEE 802.11p based channel sharing scheme. We approximate the queueing delays incurred by Anet packets at a BN by modeling the associated BN service system for Anet packets as an M/M/1 queueing system. Consequently, the cumulative distribution function of the Anet packet waiting time at a BN is given by:

$$W_{\text{x}} = 1 - \rho_{\text{BN}} e^{-\mu_{\text{BN}}(1-\rho_{\text{BN}})x}$$

To illustrate, we size the system to guarantee Anet packets with a waiting time (at the BN queue) that is lower or equal to x for 95 % of the packets, so that we set $W_x > 0.95$.

The targeted packet delay is then expressed as the sum of the FL and delay time level (D_{Anet}) incurred at the Anet client, supplemented by the waiting time (x) incurred at the source BN and the total transmission time experienced by disseminating the packet across the Bnet, which is expressed as $E[n_{\text{hops}}]\frac{P}{R_{\text{Bnet}}}$.

$$D_{\text{P}} = FL + D_{\text{Anet}} + D_{\text{Bnet}}$$

In our simulations runs, we examined varying TH_{Anet} levels, determining the highest allowable packet arrival rate from the Anet that yields an acceptable BN delay waiting time value x, aiming to satisfy the targeted end-to-end delay value D_{P}.

2.6.3   IEEE 802.11p Anet and IEEE 802.11p Bnet (MAC 3)

The third MAC scheme examined assumes the use of an IEEE 802.11p protocol in sharing the Anet channels and the Bnet links. In fact, we assume that the same communications channels are shared by all BNs and non-BNs (clients) on an IEEE 802.11p contention basis. An entity that wishes to gain access to the channel for the successful transmission of its packet must contend with currently active nodes that reside within a range of d_{CS}. Yet, active nodes that are located even further may also cause interference at the intended receiver when the total interference energy detected at the receiver is sufficiently high. To simplify our evaluation, we assume that the same transmission data rates are used across each Anet and the Bnet.

2.7   Performance Results

2.7.1   DA/TDMA Anet - TDMA Bnet (MAC 1)

In this section, we discuss the performance behavior of the DA/TDMA-Anet / TDMA-Bnet scheme. First, we display the performance of a sole Anet system, showing the dependence of the attained throughput TH_{Anet} on the data rate R_{Anet} and k_c reuse factor. In Figure 2.3,
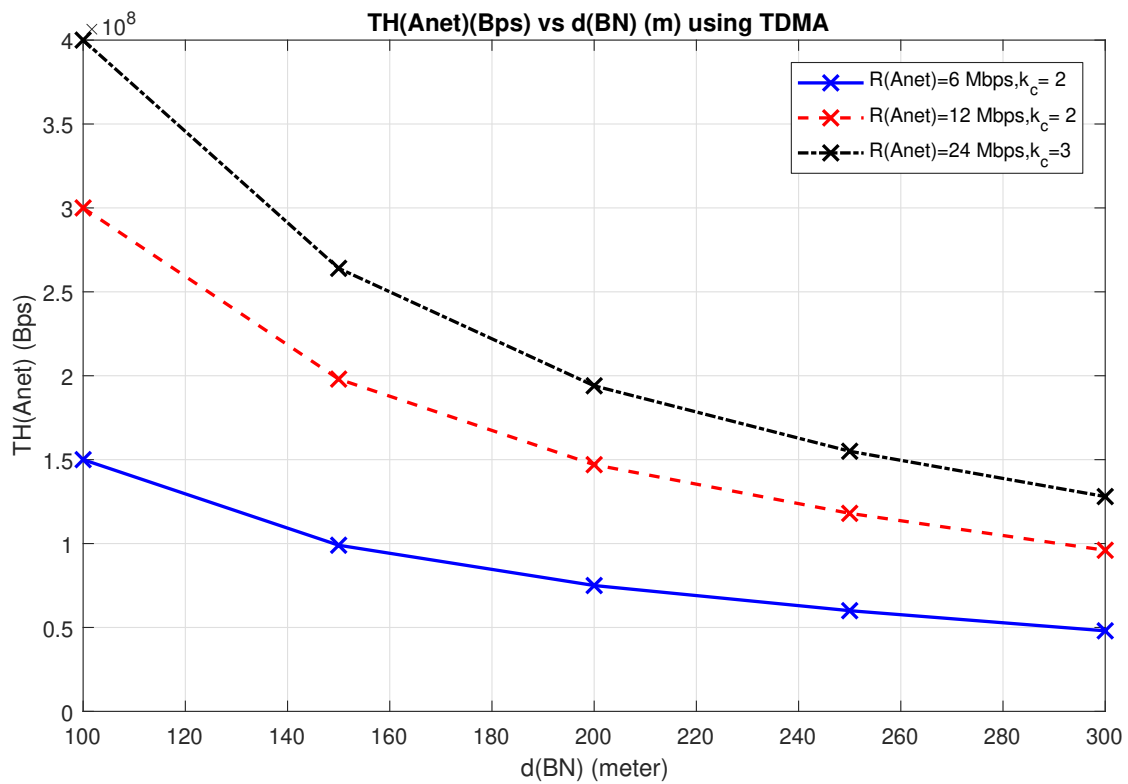
Figure 2.3: Aggregate Anet Throughput TH_{Anet} (bit/s) vs d_{BN} (m) using DA/TDMA, $l = 5\,\mathrm{km}$

we show the corresponding performance, assuming the following parameter values: $N = 250$, $l = 5\,\mathrm{km}$, $\psi = 2$ with $d_{\mathrm{BN}} = 100$, 150 and 300 m, inducing the respective number of clients served per BN to be $n_{\mathrm{served}} = 5$, 7 and 15. The performance evaluations of TH_{Anet} are based on running Matlab-based Monte Carlo simulation. The simulation is used to determine the interference signal power induced by simultaneous Anet clients uplink transmissions to the BNs (note that since Anet and Bnet operations are carried out during separate time periods) according to reuse-k_c scheme, which impacts the SINR levels detected at the receiving BNs and subsequently determine whether the Anet uplink transmissions are successfully received. k_c is selected such that $PDR \geq 0.95$. The higher the R_{Anet} value, the higher one must set the number of Anet k_{c}, as a higher R_{Anet} value requires the receiver to detect a higher minimum SINR value, noting that a higher Anet coloring value leads to better mitigation of inter-Anet interference. For example, specifying a $PDR \geq 0.95$, and setting $R_{\mathrm{Anet}} = 24\,\mathrm{Mbit/s}$, induces an optimum setting (yielding the highest Anet throughput) of $k_{\mathrm{c}} = 3$ colors. The latter value is higher than that required when a lower data rate $R_{\mathrm{Anet}} = 6\,\mathrm{Mbit/s}$ is used, which requires setting $k_{\mathrm{c}} = 2$ colors. As shown in Figure 2.3, the throughput TH_{Anet} is reduced as the inter-BN range d_{BN} increases. This main cause for this drop is attributed to the ensuing decrease in the number of elected BNs, which in turn reduces the total Anet and Bnet communications capacity that is made available since each BN makes use of its own associated transmission channel resources. Under a set d_{BN} value, the attained TH_{Anet} increases as the employed data rate R_{Anet} increases. Yet, this increase is moderated by the need to use a higher number of Anet colors.

The behavior of the attained Bnet only throughput rate as a function of the inter-BN distance is depicted by Figure 2.4. The performance analyses is based on the mathematical formula presented in Section 2.6.1.

For inter-BN ranges of $d_{\mathrm{BN}} = 100\,\mathrm{m}$ and $d_{\mathrm{BN}} = 150\,\mathrm{m}$, the highest throughput is obtained by setting $R_{\mathrm{Bnet}} = 24\,\mathrm{Mbit/s}$, $M = 5$. In turn, when configuring $d_{\mathrm{BN}} = 300\,\mathrm{m}$, the highest throughput is obtained by setting $R_{\mathrm{Bnet}} = 6\,\mathrm{Mbit/s}$, $M = 3$. We further note that the corresponding curves for the throughput rate exhibit some performance fluctuations as the
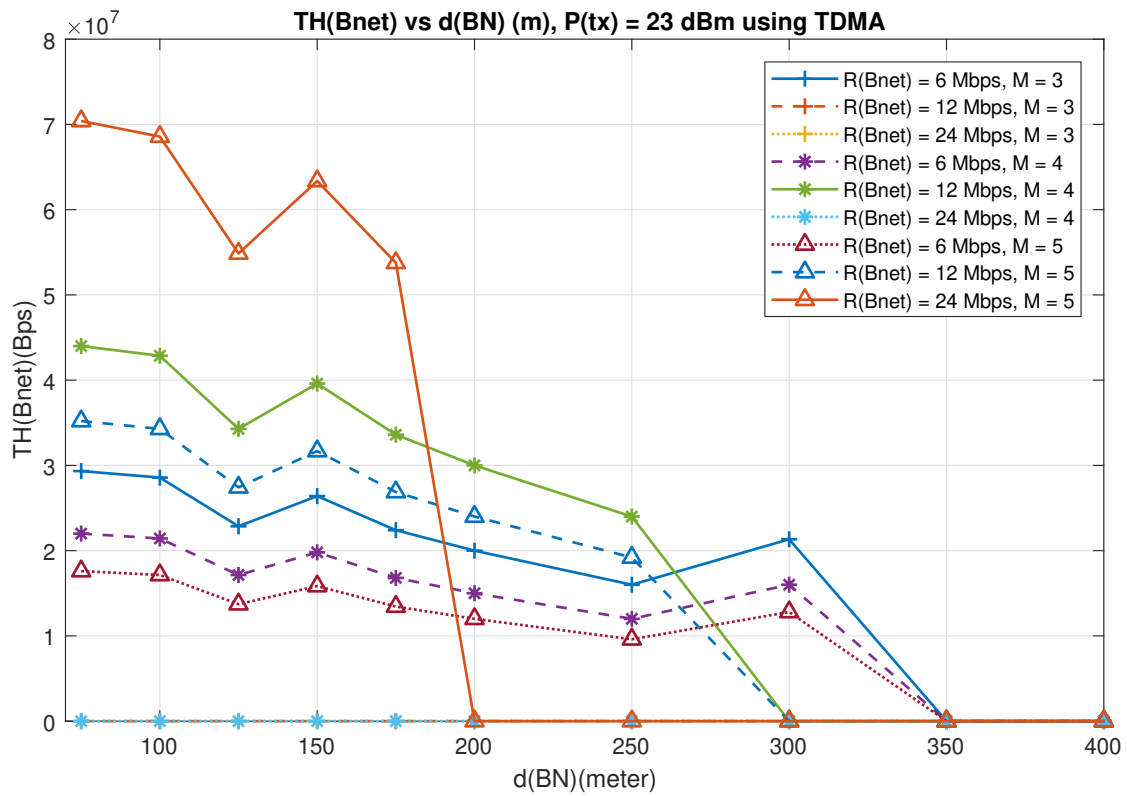
Figure 2.4: TH_{Bnet} (bit/s) vs d_{BN} (m) for $P_{\mathrm{tx}} = 23\,\mathrm{dBm}$

inter-Bnet range increase. These variations are explained by noting that as the inter-BN distance is raised, the number of dissemination hops traversed across the Bnet may decrease (showing quantization oriented fluctuations since the later number assumes integral values), serving to reduce the internal traffic produced across the Bnet links. In turn, the corresponding number of employed BNs also decreases causing reduction in the total bandwidth made available to support Bnet transmissions.

We also note that as the d_{BN} range is further increased, say to $300\,\mathrm{m}$, R_{Bnet} must be decreased to $6\,\mathrm{Mbit/s}$. This is caused by the ensuing decrease in the received power level, as the minimum received power level may then be reduced below the required receiver sensitivity value. To resolve such an issue, we have studied a system that uses an increased transmission power level, setting $P_{\mathrm{tx}} = 33\,\mathrm{dBm}$. We observed the increased transmit power system to not lead to increased throughput performance when setting shorter inter-BN range distances, such as $d_{\mathrm{BN}} = 100\,\mathrm{m}$ or $150\,\mathrm{m}$. However, an increase in the transmit power was noted by us to yield a significant throughput upgrade under longer inter-BN distances such as $d_{\mathrm{BN}} = 300\,\mathrm{m}$, under $R_{\mathrm{Bnet}} = 24\,\mathrm{Mbit/s}$, as it enabled the system to then meet the required minimum receiver sensitivity level. Also, using higher transmit power levels could also be useful when considering longer dissemination spans than those considered in our illustrative scenarios in this chapter. It is also noted that by increasing the Bnet data rate from $6\,\mathrm{Mbit/s}$ to $24\,\mathrm{Mbit/s}$, the resulting throughput rate increases in a less than proportional manner due to the ensuing increase in the reuse-M level.

In Figure 2.5, we show the variation of the optimum end-to-end combined Anet-Bnet throughput rate, $TH_{\mathrm{Anet,Bnet}}$, as a function of the configured inter-BN distance value. The performance is obtained from hybrid simulation and analytical evaluation, as expressed by the mathematical formula for $TH_{Anet,Bnet}$ presented in Section 2.6.1. We specify the targeted PDR to be at least 0.95, and the packet delay to be lower than $50\,\mathrm{ms}$ for $95\,\%$ of the served packets. The highest throughput rate is noted to be attained when setting $R_{\mathrm{Anet}} = 24\,\mathrm{Mbit/s}$, $k_{\mathrm{c}} = 3$, $R_{\mathrm{Bnet}} = 24\,\mathrm{Mbit/s}$, $M = 5$ at $d_{\mathrm{BN}} = 100\,\mathrm{m}$. As d_{BN} increases from $100\,\mathrm{m}$ to $150\,\mathrm{m}$, the system's throughput rate $TH_{\mathrm{Anet,Bnet}}$ is reduced due mainly to the lower number of employed
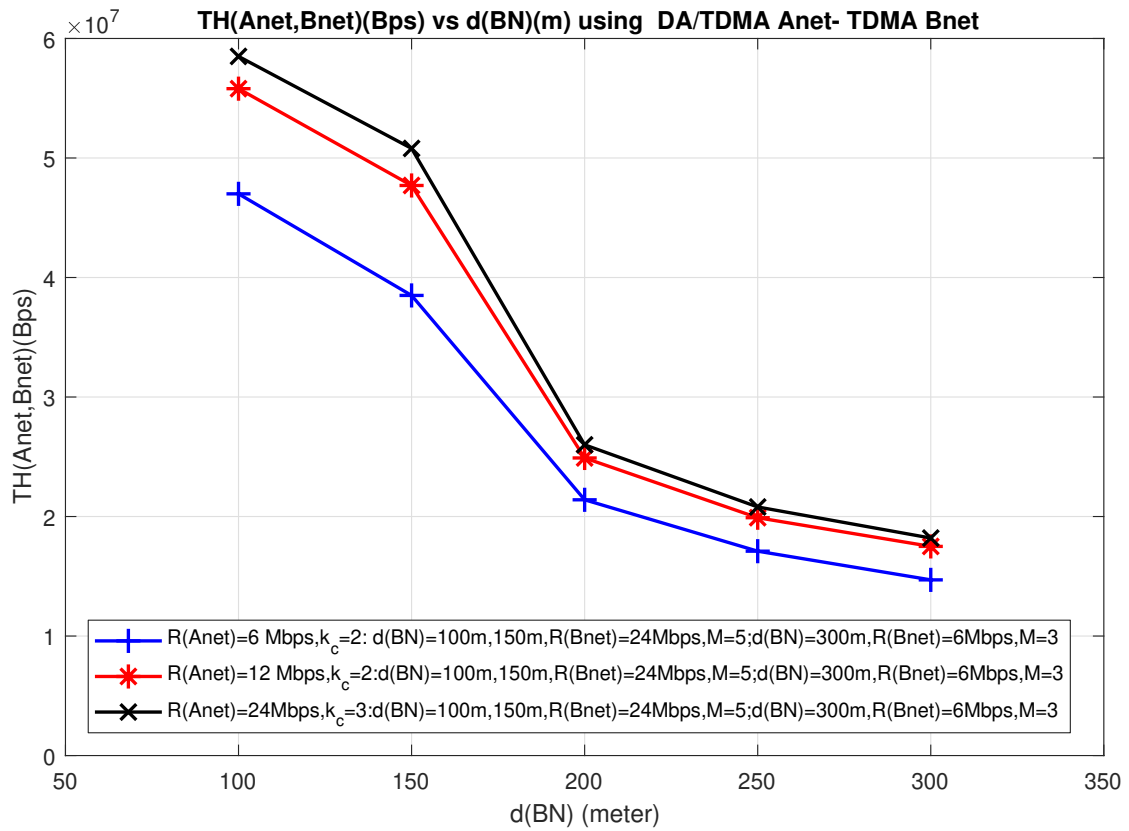
Figure 2.5: $TH_{\mathrm{Anet,Bnet}}(\mathrm{bit/s})$ vs d_{BN} (m) using DA/TDMA-TDMA with $P > 0.95$ $(D_{\mathrm{P}} < 50\,\mathrm{ms})$ and $PDR \geq 0.95$
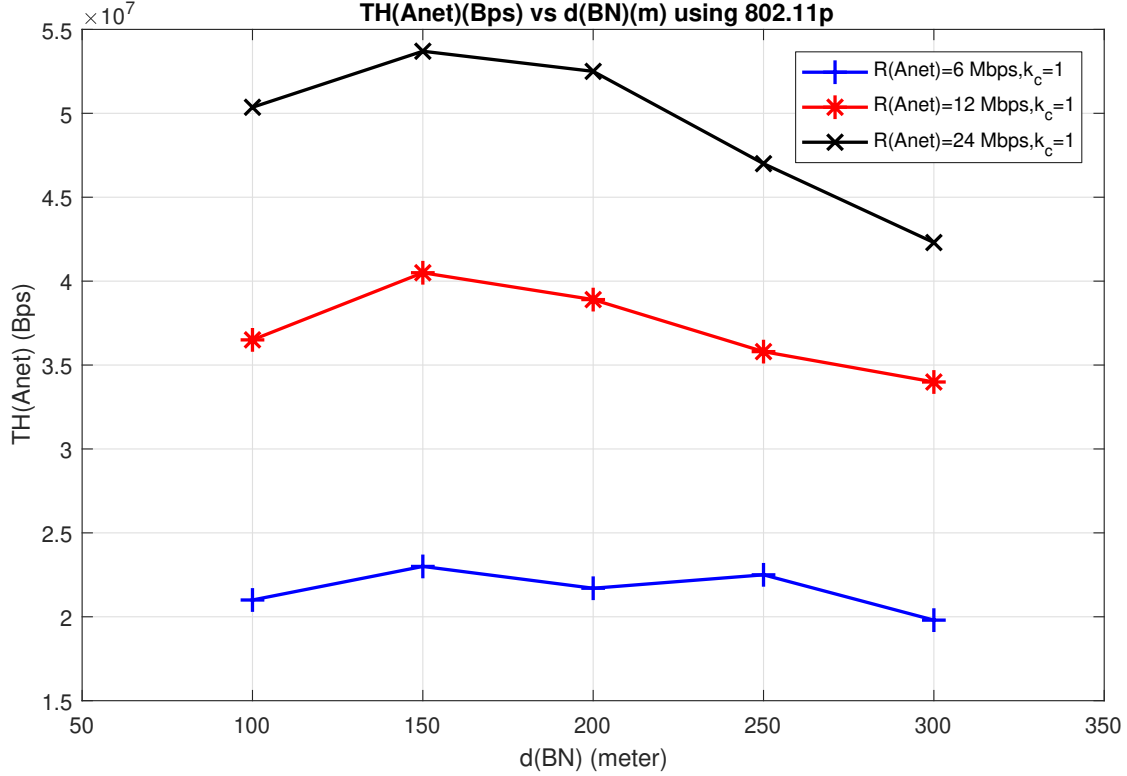
Figure 2.6: Maximum delay-capped TH_{Anet} (bit/s) and $PDR \geq 0.95$ vs d_{BN} (m) for IEEE 802.11p Anet

BNs. As d_{BN} is further increased to $300\,\text{m}$, a more significant throughput drop is observed, as now a lower $R_{\text{Bnet}} = 6\,\text{Mbit/s}$ must be used to meet the minimum SINR requirement at the targeted receiver. We have examined setting different Anet and Bnet data rates to determine the highest achievable system throughput rate. We note that for $d_{\text{BN}} = 100\,\text{m}$, setting $R_{\text{Anet}} = 6\,\text{Mbit/s}$ yields a lower throughput rate than that achieved when setting $R_{\text{Anet}} = 24\,\text{Mbit/s}$; yet, the difference is low as the performance when using $R_{\text{Anet}} = 6\,\text{Mbit/s}$ is then dominated by the setting of the same Bnet parameters, $R_{\text{Bnet}} = 24\,\text{Mbit/s}$, $M = 5$ and a lower Anet-coloring value $k_{\text{c}} = 2$.

2.7.2 TDMA Bnet and IEEE 802.11p Anet (MAC 2)

The attained maximum TH_{Anet} as calculated without imposing a packet delay limit is used to calculate the Anet and Bnet time periods configured within each frame. We have

noted a corresponding attained optimum throughput value of 65 Mbit/s at $d_{\mathrm{BN}} = 100$ m and $R_{\mathrm{Anet}} = 24$ Mbit/s. The delay constrained throughput performance is shown in Figure 2.6, which is obtained through a hybrid of NS-3 based simulation and analytical evaluation. In the simulation, the Anet client packet generation rate is increased, resulting in varied Anet throughput rate, or arrival rates of packets on the source BN from Anet clients, from which ρ_{BN} as explained in Section 2.6.2 can be analytically computed to aid computing end-to-end packet delay D_P. The Anet throughput for which D_P delay constraint is satisfied is TH_{Anet}, shown in Figure 2.6. As expected, a lower realized Anet throughput rate is attained. The maximum delay-capped TH_{Anet} value achievable for $R_{\mathrm{Anet}} = 24$ Mbit/s is equal to about 57 Mbit/s at $d_{\mathrm{BN}} = 100$ m. As d_{BN} increases to 300 m, the attainable TH_{Anet} values decrease, as higher signal interference levels are observed, particularly for mobiles that reside close to the Anet boundary. Such mobile transmissions tend then to become more sensitive to simultaneous transmissions taking place outside its carrier sensing range d_{CS}, which is equal to about 346 m when $P_{\mathrm{tx}} = 23$ dBm. As d_{BN} increases, the ratio of power received from an intended transmitter to the power received from interference decreases.

The Bnet throughput TH_{Bnet} performance behavior for this scheme is the same as that exhibited above under the DA/TDMA Anet - TDMA Bnet scheme, shown in Figure 2.4. We have studied the setting of possibly different Anet and Bnet data rate values in aiming to achieve the highest system throughput rate.

The $TH_{\mathrm{Anet,Bnet}}$ is as shown in Figure 2.7, which is obtained from the mathematical formula presented in Section 2.6.2, which consists of parameters evaluated using hybrid NS-3 based simulation for the Anet and analytical expression for the Bnet. As shown in Figure 2.7, the setting of $d_{\mathrm{BN}} = 100$ m, $R_{\mathrm{Anet}} = 24$ Mbit/s, $R_{\mathrm{Bnet}} = 24$ Mbit/s, $M = 5$, yields the highest delay-capped system throughput $TH_{\mathrm{Anet,Bnet}}$ value. It is followed by the setting of $d_{\mathrm{BN}} = 150$ m and then $d_{\mathrm{BN}} = 300$ m. The $TH_{\mathrm{Anet,Bnet}}$ value is not sensitive to changes in d_{BN} when d_{BN} is small; however, a significant drop is noticed at longer d_{BN} ranges such as 300 m. The $TH_{\mathrm{Anet,Bnet}}$ values are insensitive when increasing d_{BN} slightly from $d_{\mathrm{BN}} = 100$ m to $d_{\mathrm{BN}} = 150$ m as inducing a slight $TH_{\mathrm{Anet,Bnet}}$ decrease from 36 Mbit/s to 35 Mbit/s, although
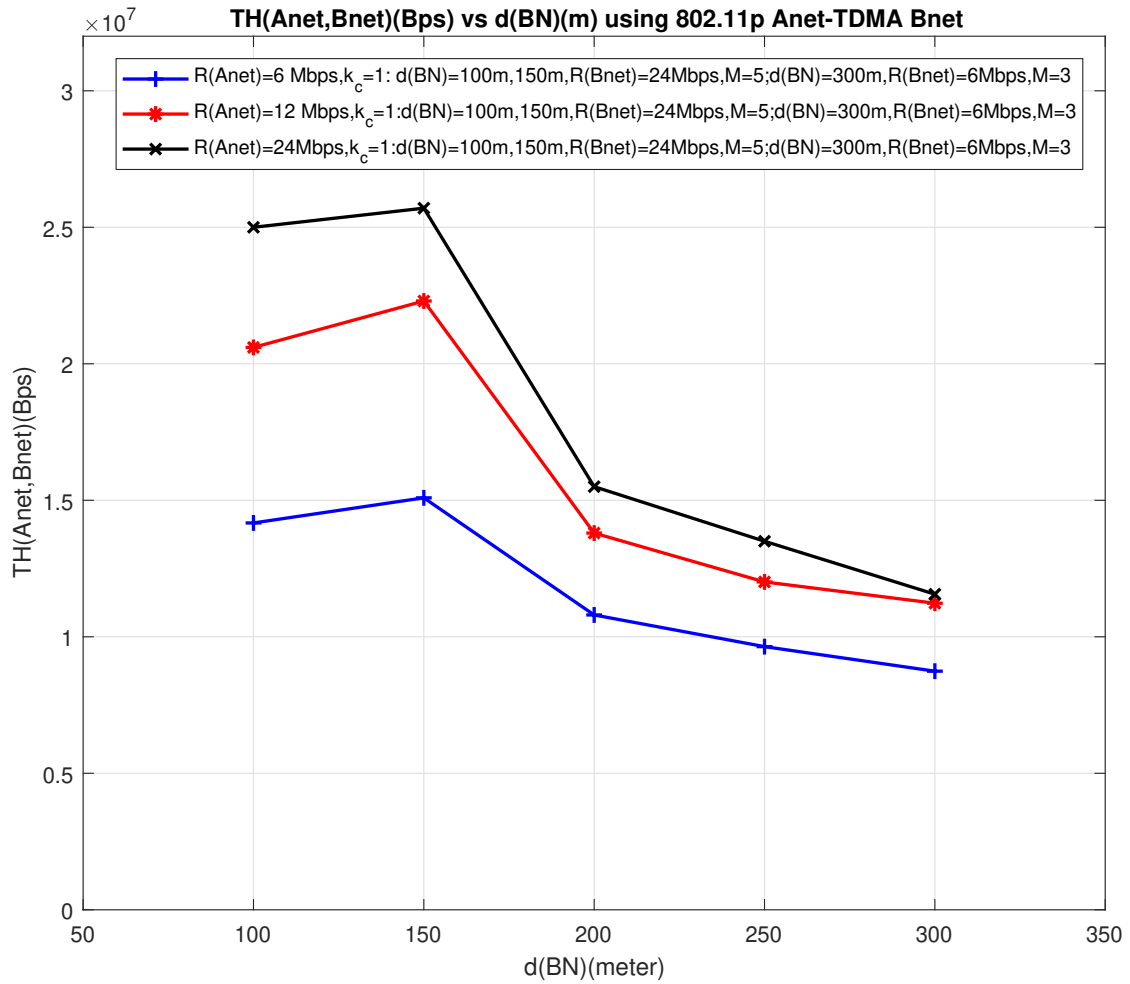
Figure 2.7: Delay-capped $TH_{\mathrm{Anet,Bnet}}$ (bit/s) vs d_{BN} (m) for IEEE 802.11p Anet-TDMA Bnet

the number of hops is reduced by 1. To explain, we note that low d_{BN} values such as 100 m and 150 m are within the d_{CS} range, resulting in an overall lower number of packet collisions. In turn, as d_{BN} is increased from 100 m to 150 m, the SINR level recorded at the receiver may assume a lower value because the receiver may be located closer to interference originated by sources outside d_{CS}. We also note that at higher inter-BN ranges, each Anet would need to support a higher number of client mobiles, leading to a higher collision rate. The performance results depicted in Figure 2.7 show that the setting of $R_{\mathrm{Anet}} = 24$ Mbit/s leads to a higher delay-capped system throughput $TH_{\mathrm{Anet,Bnet}}$ values.

A significant drop in the throughput rate is observed as d_{BN} increases from 150 m to 300 m under $R_{\mathrm{Anet}} = 24$ Mbit/s. This behavior is mainly due to the corresponding Anet performance behavior, as shown by Figure 2.6. At $d_{\mathrm{BN}} = 300$ m, we note this range to be close to the carrier sensing range, d_{CS}, and we also note that the SINR becomes very low, becoming close to the minimum SINR requirement for operation at $R_{\mathrm{Anet}} = 24$ Mbit/s, resulting in a low PDR. The $TH_{\mathrm{Anet,Bnet}}$ value for non-delay capped throughput has been determined by us (not shown) to be 20–50 % higher than the corresponding delay-capped throughput.

Our performance evaluation results show that the attained throughput values are insensitive to variations in the number n_{clients} of Anet clients. A higher number of such clients does not lead to a significant increase in the packet collision rate, due in a large extent to the impact of the carrier sensing range. We have also noted that the maximum delay-capped TH_{Anet} throughput level does not vary much as the number of Anet clients increases, provided the overall loading rate per Anet is controlled (so that the maximal allowed total offered loading rate is regulated).

2.7.3 IEEE 802.11p Bnet and IEEE 802.11p Anet (MAC 3)

In Figure 2.8, we show the variation of the system throughput rate under IEEE 802.11p Anet and Bnet MAC schemes vs. the setting of the inter-BN range. The performance results are based on running Monte Carlo simulations using NS-3 based simulation. We focus on the performance realized by Class 2 messages, assuming Class 1 message delay and PDR
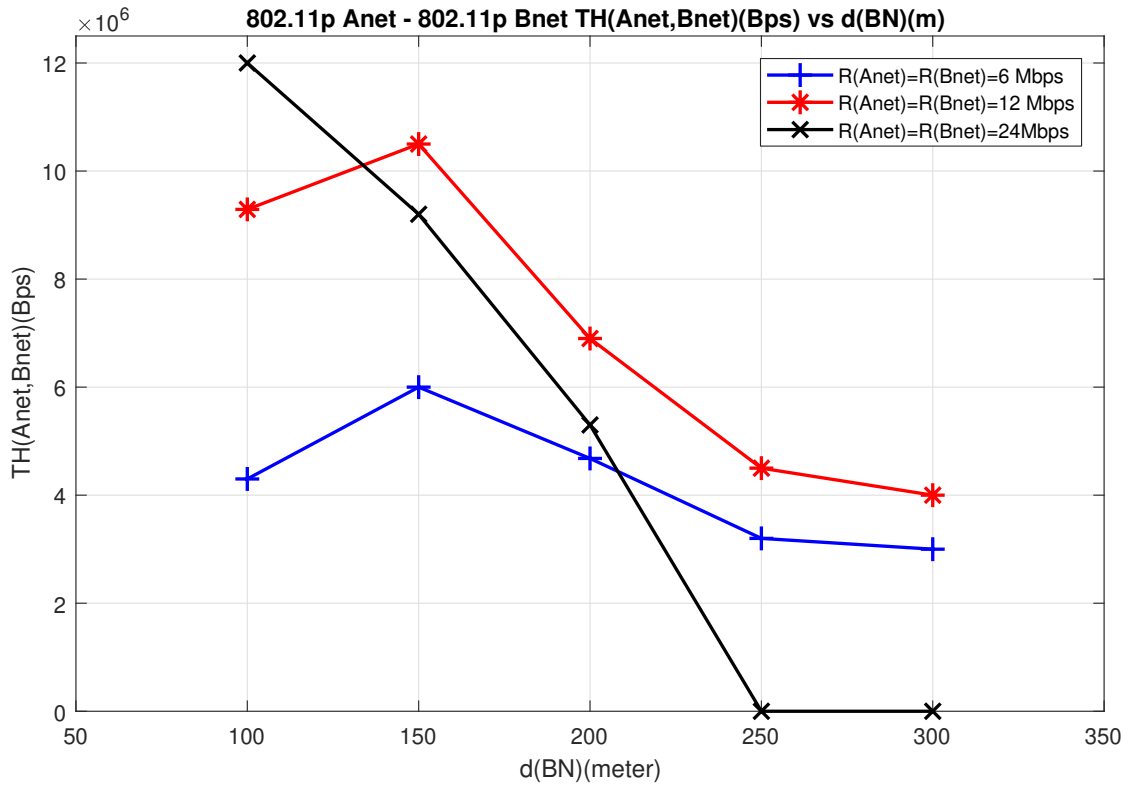
Figure 2.8: $TH_{\text{Anet,Bnet}}$ (bit/s) vs d_{BN} (m) at various R (Mbit/s), with $P > 0.95$ ($D_{\text{P}} < 50\,\text{ms}$) and $PDR \geq 0.95$ for IEEE 802.11p Anet - IEEE 802.11p Bnet scheme (MAC 3)

requirements to have been met, assuming a single lane loading of $N = 250$. The setting of a (Anet and Bnet) data rate $R = 24\,\text{Mbit/s}$ and $d_{\text{BN}} = 100\,\text{m}$ is shown to yield the maximum throughput rate. Under this high data rate, the throughput rate experiences significant degradation as the the inter-BN distance is increased. In turn, we observe the attained throughput values under $R = 12\,\text{Mbit/s}$ to be less sensitive to changes in d_{BN} due to its lower minimum SINR requirement.

The observed performance result is insensitive to variation of d_{BN} from $100\,\text{m}$ to $150\,\text{m}$ level, for $R_{\text{Anet}} = R_{\text{Bnet}} = 6$ and $12\,\text{Mbit/s}$. Although the average number of hops decreases from 3.5 hops to 2.5 hops, longer d_{BN} value means that an intended transmission by some Anet clients will become more sensitive to signal interference caused by simultaneous transmissions occurring due to sources outside the d_{CS} range. Hence, the gain in throughput attributed to the employed smaller number of hops is partly reduced by the lower SINR induced by the latter interference process.

2.7.4 Comparison Between the MAC Schemes

In Figure 2.9, we compare the delay-capped highest aggregate system throughput rate performance attained under the three MAC schemes combinations under consideration. We note that the TDMA Anet-TDMA Bnet scheme yields the highest throughput rate (which is equal to about $50\,\text{Mbit/s}$), followed by the Bnet TDMA-Anet IEEE 802.11p scheme (achieving a corresponding throughput rate of about $30\,\text{Mbit/s}$) and then by the joint-IEEE 802.11p scheme (producing a corresponding throughput rate of about $10\,\text{Mbit/s}$). The highest throughput rate is attained by the TDMA-Anet/TDMA-Bnet scheme when configured at $R_{\text{Anet}} = 24\,\text{Mbit/s}$, $R_{\text{Bnet}} = 24\,\text{Mbit/s}$, $M = 5$, $d_{\text{BN}} = 100\,\text{m}$, $k_{\text{c}} = 3$. When examining the sensitivity of the highest attainable throughput rate to variation in the setting of the inter-BN distance, we conclude that the TDMA/TDMA scheme generally yields the best performance when d_{BN} is set lower than $300\,\text{m}$.

By examining the delay capped throughput performance results exhibited in Figures 2.5, 2.7 and 2.8, we note the following. The highest throughput rate is attained by setting $d_{\text{BN}} = 100\,\text{m}$,
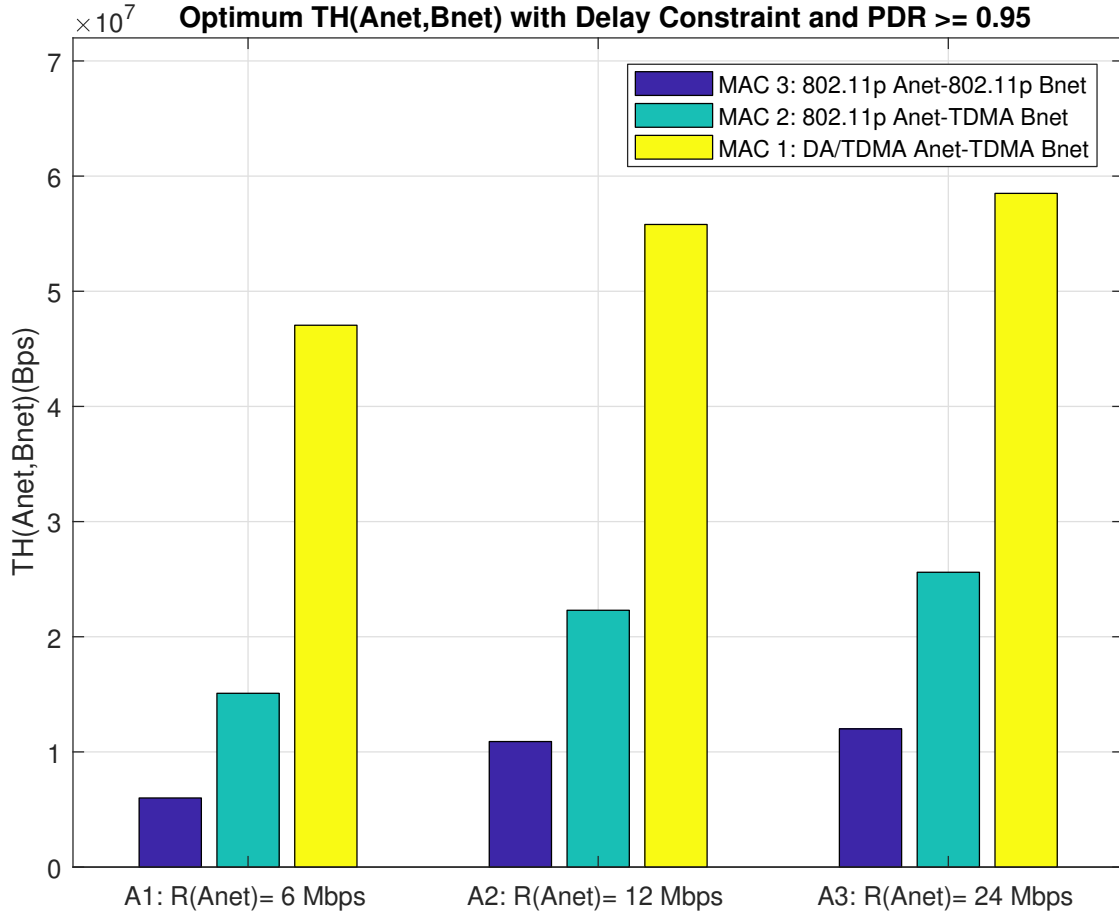
Figure 2.9: Comparison Delay-capped $TH_{\mathrm{Bnet,Anet}}$ (Mbit/s) vs R_{Anet} (Mbit/s) for $N = 250$. Bar explanation: (A1/A2/A3,MAC 3):$R_{\mathrm{Anet}} = R_{\mathrm{Bnet}}$; (A1/A2/A3,MAC 2): $R_{\mathrm{Bnet}} = 24\,\mathrm{Mbit/s}$, $M = 5$, $d_{\mathrm{BN}} = 100\,\mathrm{m}$; (A1/A2,MAC 1): $k_c = 2$, $R_{\mathrm{Bnet}} = 24\,\mathrm{Mbit/s}$, $M = 5$, $d_{\mathrm{BN}} = 100\,\mathrm{m}$; (A3,MAC 1): $k_{\mathrm{c}} = 3$, $R_{\mathrm{Bnet}} = 24\,\mathrm{Mbit/s}$, $M = 5$, $d_{\mathrm{BN}} = 100\,\mathrm{m}$

$R_{\text{Anet}} = 24\,\text{Mbit/s}$, $R_{\text{Bnet}} = 24\,\text{Mbit/s}$, $M = 5$, $k_c = 3$, $n_{\text{active}} \leq 10$, yielding a throughput rate that is equal to $47\,\text{Mbit/s}$, under the Anet TDMA - Bnet TDMA scheme. The next highest throughput, using the Anet TDMA - Bnet TDMA scheme, yielding $TH_{\text{Anet,Bnet}} = 41\,\text{Mbit/s}$, is attained by setting $d_{\text{BN}} = 150\,\text{m}$, in using the following configuration: $R_{\text{Anet}} = 24\,\text{Mbit/s}$, $R_{\text{Bnet}} = 24\,\text{Mbit/s}$, $M = 5$, $k_c = 3$, $n_{\text{active}} \leq 13$. The third highest attained throughput rate is $TH_{\text{Anet,Bnet}} = 25\,\text{Mbit/s}$, achieved by using the 802.11p Anet/TDMA Bnet scheme and setting $d_{\text{BN}} = 100\,\text{m}$, $R_{\text{Anet}} = 24\,\text{Mbit/s}$, $R_{\text{Bnet}} = 24\,\text{Mbit/s}$, $M = 5$.

2.8 Integrated System Design under Joint Networking Performance and Traffic Management Objectives

The results presented in the traffic management sections of [25] point to the configuration options available to the designer when aiming to achieve high vehicular flow rates under vehicular delay limits. The results presented in Section 2.7 identify the dependence of the system message communications throughput rate on the system's traffic parameter settings. In this section, we demonstrate how these results are combined to deduce an integrated system design that jointly meets prescribed vehicular and message communications performance objectives. For illustrative purposes, we consider a single lane highway segment of length $l = 5\,\text{km}$ while using the specific parameter values used in the highway traffic management design presented in [25]. As shown by [25], for $n = 2$ to $n = 10$, one should set the optimal speed to about $60\,\text{km/h}$. The corresponding vehicular flow rate that results varies from $1800\,\text{veh/h}$ to $3250\,\text{veh/h}$, and the d_{PL} ranges vary from $60\,\text{m}$ to $175\,\text{m}$. The optimal speed should be configured to about $60\,\text{km/h}$ when $n = 10$ and $d_{\text{PL}} = 175\,\text{m}$, yielding a vehicular throughput (flow rate) of $3250\,\text{veh/h}$.

To illustrate, assume the system manager aims to configure a system that achieves a vehicular throughput flow rate level that assumes values in a range which includes a high $3000\,\text{veh/h}$ level and a medium $2000\,\text{veh/h}$ level. At the same time, the system manager aims to attain a sufficiently high delay-capped packet communications throughput performance.
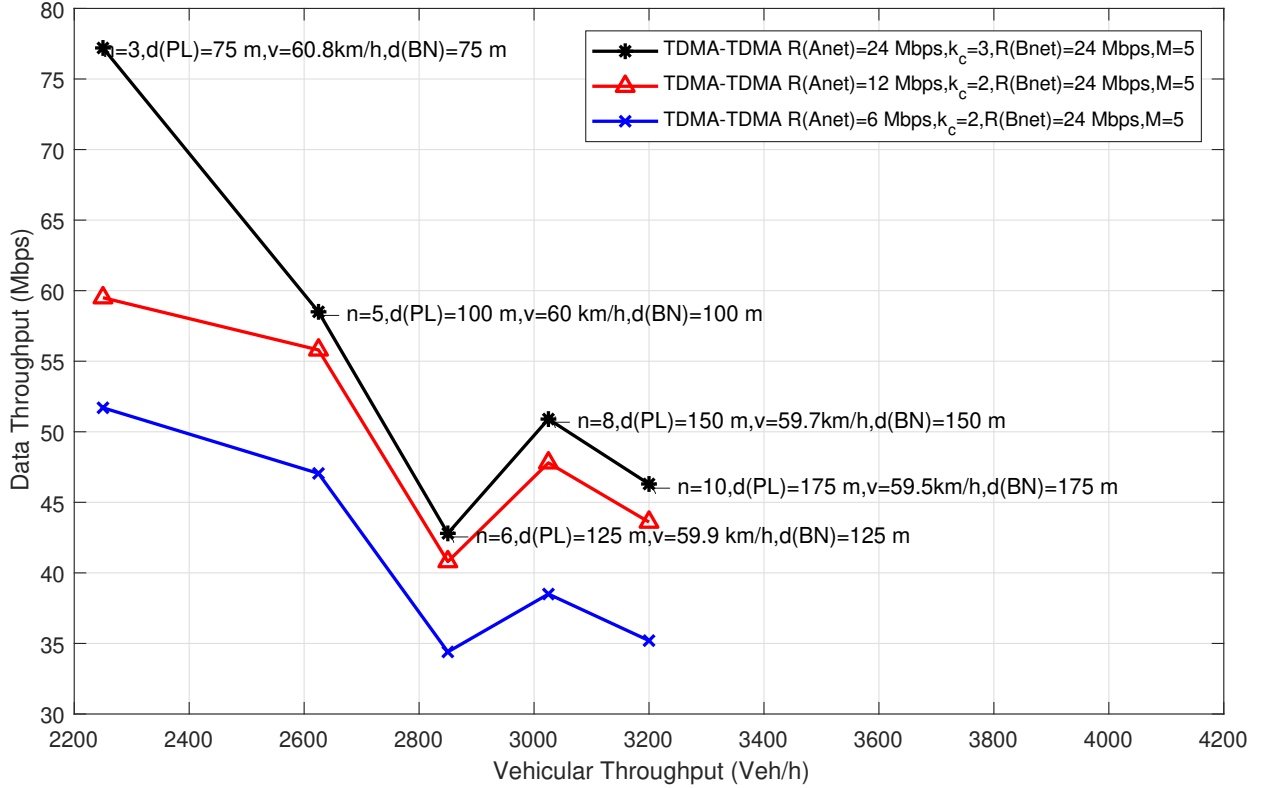
Figure 2.10: Data Throughput (Mbit/s) vs Vehicular Throughput (veh/h)

This throughput performance accounts for the dissemination of Class 2 messages, assuming that Class 1 messages are guaranteed a high PDR, $PDR \geq 0.95$, and an average delay that is not higher than 50 ms for successfully disseminated messages.

In Figure 2.10, we illustrate the tradeoffs available to the system designer as we observe that different design settings yield different combined (vehicular throughput, communications throughput) operational points. The performance points identified in the figure as we traverse each design combination (involving specified system parameters) by varying the d_{PL} values over the set 75, 100, 125, 150 and 175 m. For each case, we use the parameter values attained as the result of the optimization process carried out for the DA/TDMA Anet-TDMA Bnet (MAC 1) scheme.

To illustrate the underlying performance tradeoff available to the designer, assume first that it is of interest to achieve a high vehicular throughput level, equal to 3000 veh/h. It is

attained, as shown in [25], by setting $d_{PL} = 150\,m$ and $n = 8$. Under these parameter settings, we aim to maximize the data communications throughput performance in disseminating Class 2 message flows, while also meeting Class 1 message communications requirement. Assuming that d_{BN} is selected from the set 100, 150 and 300 m, we determine that the values $d_{BN} = 150\,m$ and $d_{BN} = 300\,m$ are feasible as they satisfy $d_{BN} \geq d_{PL}$. Accordingly, we determine the setting $d_{BN} = 150\,m$, $R_{Anet} = 24\,Mbit/s$, $R_{Bnet} = 24\,Mbit/s$, $M = 5$, $k_c = 3$ to yield a higher data throughput performance (when compared with the setting $d_{BN} = 300\,m$, $R_{Anet} = 24\,Mbit/s$, $R_{Bnet} = 6\,Mbit/s$, $M = 3$, $k_c = 3$). In consequently configuring $d_{BN} = d_{PL} = 150\,m$, the communication networking function requires a setting for which we have $n_{served} \leq 13$ in considering Anet clients which become active. Hence, all the platoon members can be served by the BN. The joint traffic management and networking parameters are therefore set as follows. The traffic management parameters are set to: $d_{PL} = 150\,m$ ($v = 60\,km/h$) and $n = 8$. The optimal networking configuration that is synthesized to achieve a high vehicular throughput implements the settings: $d_{BN} = 150\,m$, $R_{Anet} = 24\,Mbit/s$, $R_{Bnet} = 24\,Mbit/s$, $M = 5$, yielding an aggregate system throughput rate that is equal to $TH_{Anet,Bnet} = 41.6\,Mbit/s$.

In turn, when the system designer is willing to accommodate a medium vehicular throughput rate level of about 2750 veh/h, achievable by setting $n = 5$ at the optimal velocity level of $v = 60\,km/h$ and a d_{PL} range set to 100 m. The d_{BN} level should be selected such that the networking configuration satisfies $d_{BN} \geq d_{PL} = 100\,m$ (e.g. $d_{BN} = 100\,m$, or 300 m). Considering the latter values, we have determined that setting a TDMA/TDMA scheme at $d_{BN} = 100\,m$, $R_{Anet} = 24\,Mbit/s$, $R_{Bnet} = 24\,Mbit/s$, $M = 5$, $k_c = 3$, $n_{client} \leq 10$, would achieve (among the options considered in our analyses) the highest data throughput rate, yielding $TH_{Anet,Bnet} = 47.89\,Mbit/s$. Hence, the joint traffic management and data networking parameters are set as follows. The selected traffic management related parameters are: $d_{PL} = 100\,m$ ($v = 60\,km/h$) and $n = 5$. The related data networking parameters, selected to realize the networking configuration which achieves a high vehicular throughput rate, are given as: $d_{BN} = 100\,m$, $R_{Anet} = 24\,Mbit/s$, $R_{Bnet} = 24\,Mbit/s$,

$M = 5$. These setting yield an aggregate system data communications throughput rate that is equal to $TH_{\text{Anet,Bnet}} = 47.89\,\text{Mbit/s}$. As well demonstrated by these design settings, as we lower the targeted vehicular throughput requirement from $3000\,\text{veh/h}$ to $2750\,\text{veh/h}$, we are able to increase the data communications network throughput performance from $TH_{\text{Anet,Bnet}} = 41.6\,\text{Mbit/s}$ to $TH_{\text{Anet,Bnet}} = 47.89\,\text{Mbit/s}$.

It is interesting to note that as d_{PL} is increased from $100\,\text{m}$ to $125\,\text{m}$, the attained vehicular throughput is increased to $2850\,\text{veh/h}$, while the data communications throughput rate is reduced to $35\,\text{Mbit/s}$. However, if d_{PL} is further increased to $150\,\text{m}$, the system can sustain a higher vehicular throughput rate, of about $3000\,\text{veh/h}$, while also realizing a higher data throughput rate, which is equal to $42\,\text{Mbit/s}$. The joint performance is thus uniformly better than that attained when setting $d_{\text{PL}} = 125\,\text{m}$. The occurrence of such a performance spike has been explained when discussed in connection with the performance trends exhibited in discussing the results shown in Figures 2.3 and 2.4.

2.9   Concluding Remarks

We develop and study in this chapter data networking mechanisms for an autonomous transportation system. Vehicles that move in each lane are organized into platoons. A platoon leader is elected in each platoon and is used to manage, coordinate and synchronize platoon members. Using the platoon based formations, we develop a V2V wireless data communications networking protocol that is used to disseminate messages produced by highway vehicles and sent to other vehicles that travel within a specified range from the source vehicle. The hierarchical networking scheme that is presented and studied employs algorithms that are used to dynamically synthesize a mobile Backbone Network (Bnet). The latter consists of interconnected platoon leaders that are elected to serve as BNs. Each BN serves as an access point for its Access Network (Anet) mobile clients. We study the performance behavior of the network system and determine the optimal setting of its parameters, assuming both TDMA and IEEE 802.11p oriented wireless channel sharing (MAC) schemes for the Anet and Bnet subsystems. Packet delay limits are also imposed.

Integrating our mechanisms and schemes developed for the traffic management and for the data networking planes, we demonstrate the performance tradeoffs available to the system designer and to the transportation manager when aiming to assure a transportation system operation that achieves targeted vehicular flow rates and transit delays while also configuring the data communications network system to meet targeted message throughput and delay objectives. For example, we note that the use of a relatively short distance between elected BNs, jointly with the employment of higher transmission data rates across the Bnet and Anet systems, leads to higher delay-capped data throughput rates. In turn, to achieve a high vehicular flow rate, it is often necessary to structure platoons to have wider spans (inducing longer inter-BN ranges). Consequently, the system manager must select an operating point that is based on a compromise in terms of the ability to meet individual targeted traffic management and data networking performance metrics.

The approaches and mechanisms developed in this chapter can also be applied to the design of autonomous highway transportation systems whereby platoon formations are not imposed. For the hierarchical networking protocol, we note that the election of BNs, when coordinated by a regional manager or by a fully distributed algorithm, can be performed in a manner that does not depend on the existence of platoon formations and their identified and announced leaders. BNs (and consequently Anets and the Bnet) can be elected to meet advantageous access and coverage requirements, following analyses similar to those performed in this chapter, when not aided by the existence of platoon formations. Also, BNs can be elected, fully or partially, from a set of stationary RSUs, or access points, when they are (or become) available. When available, stationary (such as fiber optic based) RSU backbone networks, could be employed, or used to supplement the wireless V2V network over certain highway segments. Similarly, it is noted that our traffic management models, methods and results have wider applicability, including also non-platoon based vehicular mobility patterns. Yet, the platoon formation model is highly advantageous in serving to effectively offer tight coordination and rapid safety based reactive adaptations, when performed among vehicles that move as a group. It has thus been selected for the studies carried out in this chapter.

2.10 Credit

This chapter is partly based on I. Rubin, A. Baiocchi, Y. Sunyoto and I. Turcanu, "Traffic Management and Networking for Autonomous Vehicular Highway Systems", Ad Hoc Networks, Vol. 83, Pages 125–148, 2019, ©2019 Elsevier.

CHAPTER 3

Infrastructure Aided Networking for Autonomous Vehicle Highway Systems on the Sub-6 GHz Band

3.1 Introduction

As autonomous vehicle technologies advance rapidly and are becoming more widely used, advanced developments are also pursued for enhancing the communications and data networking performance of autonomous vehicle systems. A reliable, robust and delay-aware communications networking facility is essential for the support of safe and rapidly adaptive autonomous operation. The installation and control of a communications backbone infrastructure contribute in a significant manner to achieving these aims. In this study, we assume the use of such a backbone network. We assume this infrastructure to consist of roadside unit (RSU) stations that are placed along a highway segment. These RSUs are interconnected by a high capacity network, such as a fiber optic backbone. While we consider scenarios under which backbone nodes are placed at different density levels, we assume that each realized backbone topology is configured to provide direct communications coverage of all vehicles traveling along the highway segment. RSUs are equipped with wireless and point-to-point transceivers. The wireless radio is used by each RSU to transmit data packets downlink to vehicles covered by it, and to receive uplink data transmissions from such vehicles. The backbone system is used for the transmission of data packets among RSU stations. Vehicles are equipped with radios that are used for wireless communication with the infrastructure, enabling Vehicle-to-Infrastructure (V2I) and Infrastructure-to-Vehicle (I2V) transmissions.

We expect future systems to deploy a roadside infrastructure that will be used to critically

54

support vehicular communications and traffic management. A more dense installation of RSUs, acting as network and traffic base station management nodes results with a higher cost backbone system that may not offer sufficient commensurate performance advantages. It is therefore important to characterize the dependence of system's performance on the density level of the backbone system, as studied in this chapter. We characterize the performance behavior of the network system as a function of the backbone network density, and thus the inter-RSU distance, while simultaneously properly setting MAC and PHY layer system parameters, impacting the employed scheduling schemes, including configuring data rates, modulation/coding schemes (MCS) and transmit power levels. We develop and study TDMA-based and IEEE 802.11p-based protocols for the sharing of V2I and I2V wireless communication channels. The major contributions of this work are summarized as follows:

- A network architecture is synthesized and employed for the design of infrastructure-aided communication networking system.

- The network system must provide for timely dissemination of critical messages, while also supporting the dissemination of flows that often demand relatively high data throughput rates, such as status packet, sensor data and non-critical message flows. Therefore, we study in this chapter, as we vary the inter-RSU distance levels, the design of a infrastructure-aided autonomous vehicle system that achieves high data throughput rates, subject to specified bounds on the maximum allowable packet delay levels, while also prescribing a minimal acceptable value for the probability of successfully disseminating flow packets to all intended vehicular destinations (represented by the associated Packet Delivery Ratio (PDR)).

- For each configured inter-RSU distance level, we determine the desired joint cross-layer setting of involved network system parameters, such as the MCS, data rates and transmit power levels.

- For the IEEE 802.11p based scheduling scheme, we present an analytical approximation method that is used to compute the desired transmit power value when aiming to induce a high data throughput performance.

- We demonstrate the non linear dependence of the system's throughput performance on the density of the backbone system.

- We compare the data throughput performance attained by using the infrastructure aided communication system presented in this chapter with the performance attained by a pure V2V system that employs no infrastructure based backbone network, for both TDMA and 802.11p based schemes. There are several studies which discuss platoon-based V2V communications for autonomous vehicle systems, such as [8] and [25]. We use the V2V protocol and scheme presented in [25] for performance comparison to the infrastructure aided communication system presented in this chapter.

This chapter is organized as follows. In Section 3.2, we present an overview of related work. The network systems model, including the underlying network architecture, protocols and parameters, are presented in Section 3.3. In Sections 3.4 and 3.5, we respectively present the infrastructure-aided scheduling (MAC) schemes and the system's performance characteristics. Conclusions are drawn in Section 3.8.

3.2 Related Work

Several papers [33, 34, 35] study joint V2V and V2I dissemination mechanisms that are used when RSU stations are not able to fully cover the underlying highway. For such a hybrid environment, [33, 34] develop cooperative routing strategies, and [35] presents a RSU placement scheme which aims to bound the effective cost of implementation of the infrastructure while attaining acceptable performance. In contrast, our study focuses on the development of an approach that sets cross-layer PHY/MAC parameters in a manner that optimizes the targeted delay-throughput performance behavior, assuming that the installed infrastructure is capable of providing full coverage of the highway segment. The RSU backbone network density serves as a key factor in impacting the cost of the backbone system.

The authors in [36] study the downlink data throughput performance of a mmWave

infrastructure aided vehicular communication as a function of base station density (i.e. average inter base station distance). Beamforming is used for communication between a vehicle and a base station. The downlink data throughput performance is impacted by the stochastic occurrence of blockage scenarios. Some factors considered include resulting SINR between vehicle and base station, probability of coverage, and duration of maintaining connection during transmission. It considers transmission from each RSU to a single tracked vehicle. Unlike our study, [36] does not consider broadcasting packets from a source vehicle to all vehicles residing within a targeted geographical span, a scenario which is of critical importance for many classes of safety messages produced by vehicles traveling along the autonomous highway.

The authors in [37] and [38] consider backbone infrastructure systems that provide full highway coverage. In [37], inter-RSU distances are adapted to ensure a higher degree of seamless coverage. The authors in [38] propose a handover coordination method under which a vehicle selects the RSU which provides the best means of communications. In contrast with our study, the latter papers, while utilizing a backbone system, do not determine the desired setting of the underlying cross-layer (MAC/PHY) parameters, in aiming to attain high dissemination throughput rates under prescribed packet delay bounds, and as a function of the density of coverage by the infrastructure system.

Among the studies that present TDMA-based RSU aided vehicular communication schemes, we have the following related studies.

The study by [39] uses fractional frequency reuse (which is a hybrid of spatial reuse and frequency reuse) to mitigate interference among downlink transmissions by LTE base stations. However, the topological layout of the cellular base stations is non linear, impacting accordingly the interference signals that are produced. Several studies consider TDMA (or FDMA) oriented MAC schemes that are used to support vehicular system applications, including RSU-based scheduling schemes [40, 41, 42, 43], and ad hoc scheduling methods [44]. They often present methods for slot allocation for the purpose of accommodating contention free data transmissions by considering various performance objectives, including

metrics that involve throughput maximization [40] and message delay bounds [40, 41]. Several models also accommodate the transmission of high priority packets [40, 41]. The scheme presented in [40] attaches higher weights for the support of vehicles that are associated with higher channel quality conditions, while also considering the position of vehicles for service fairness purposes. The paper uses demand assigned TDMA schemes, whereby the duration of a random access reservation period is adapted to ensure low collision rate levels for the transmission of reservation request messages. Both [40] and [41] allocate time slots based on EDCA (AC) factor, as is employed by IEEE 802.11e based systems, by attaching higher priority indicators to critical messages. Consequently, several of these studies also evaluate the performance efficiency of the TDMA MAC schemes during the contention free transmission period. However, [40, 41] use TDMA scheduling within the neighborhood of a single RSU, and the slot scheduling scheme is tailored to yield performance efficiency within the RSU's region of coverage. Whereas, our study presents TDMA-based scheduling schemes which coordinate the scheduling of multiple RSUs jointly with the adaptive configuration of the employed data rate, MCS and spatial-reuse levels. Such an operation allows for interference mitigation, leading to system-wide throughput optimization.

In contrast, the authors in [42, 43, 44] propose a TDMA/FDMA based scheduling mechanisms that involve multiple RSUs. In [42], the authors propose a centralized RSU-centric TDMA time slots allocation scheme, in serving vehicles that reside within its coverage. The study assumes the use of two different frequency bands employed by adjacent RSUs, such that no signal interference is induced among transmissions executed in neighboring cells. The study [43] proposes installation of large number of base stations which are interconnected to a controller by optical fiber. Each base station covers a cell. The base stations are categorized into several groups, each forming a virtual cellular zone (VCZ), which consists of several base stations operating in the same frequency range. Only one base station can be active at a time to transmit downlink within a VCZ to prevent interference within a VCZ. Base stations transmissions within a VCZ are scheduled in a TDMA fashion. Adjacent VCZs also use disjoint frequency ranges. The study proposes a demand-assigned TDMA scheme within

each VCZ. The authors in [44] propose a combination of using SDMA, OFDMA and TDMA. In using SDMA, the highway is divided into cells, whereby each cell is allocated different sets of subcarriers from adjacent cells. Within each cell, the subcarriers are shared in a TDMA fashion. It also specifies that there should be four minimum different frequencies used for adjacent cells to avoid time slots oriented overlap collisions. The setting in [42, 44] however does not employ an optimized number of frequency bands for optimizing the spatial-reuse (coloring) configuration. Similarly, the scheme presented in [43] does not study methods for the optimization of the number of simultaneously active base stations employed within a VCZ. It also does not determine the best selection of the number of frequency bands that should be used at adjacent VCZs, as used to enhance throughput by mitigating signal interference. More TDMA protocols are discussed in [45]. In contrast with the setting of the joint uplink/downlink TDMA schemes employed by us in this chapter, above noted papers which use TDMA MAC schemes tend to not provide for joint uplink / downlink scheduling, whereby the aim is to maximize the data throughput rate for the dissemination of packets flows over a targeted span.

The authors in [46, 47] study the impact of RSU antenna designs and mounting on data throughput performance. In [37], a study of RSU-aided data networking performance is presented when considering several channel propagation models. Inter-RSU distances are adapted to ensure a higher degree of seamless coverage. These studies however do not consider MAC scheduling schemes that are employed for disseminating packet flows over specified spans, coupled with the effective setting of network parameters as performed in this chapter.

Among the studies that present 802.11p-based RSU aided vehicular communication schemes, we have the following related studies. Compared to studies on TDMA-based MAC V2I schemes, such as those presented in [45, 48], IEEE 802.11p-based schemes require a much simpler management and control system. They do not require time slot resource allocations, but rather allow for dynamic sharing of channel resources in autonomously adapting to traffic conditions. This is especially valuable when considering high priority data message applications that require low packet delays, while subjected to flow control regulations that

59

limit channel loading rates to the values derived in this study.

In [49] and [50], the authors present a mathematical model that can be used to calculate the probability that a packet transmission is successfully executed over a single hop broadcast communications channel that is shared by using IEEE 802.11p. These papers however do not provide models to be used for the cross-layer setting of transmit power (which in turn impacts the induced carrier sensing range) and data rate parameters, as presented in this chapter.

The authors in [51] present experimental results obtained for infrastructure-aided IEEE 802.11p communications. They account for data rate and transmit power parameter values as factors affecting V2I communications performance. The authors in [52, 53] present congestion control schemes, performing flow regulation by either adjusting the transmit power level or the beacon generation rate used for IEEE 802.11p-based V2V dissemination. The paper evaluates the ensuing message delivery ratio. An iterative transmit power adjustment scheme is presented, involving observed channel congestion levels and the distance to be incurred in forwarding a message by a node to the next forwarding node. However, these studies do not determine the effective transmit power level as a function of different employed data rates and inter-RSU distances to achieve a high PDR and to maximize aggregate data throughput.

We have identified no studies that examine the best cross layer setting and performance behavior of networking schemes such as those analyzed in this chapter. We determine here the joint setting of data networking parameters for an autonomous vehicle highway communication system that employs an infrastructure backbone network that provides full coverage of highway segment vehicles, whereby the MAC scheduling structure and parameters are optimally configured and message flows that are disseminated over specified spans. We aim to achieve high throughput rates, while meeting specified targeted packet delay and reception rate levels.
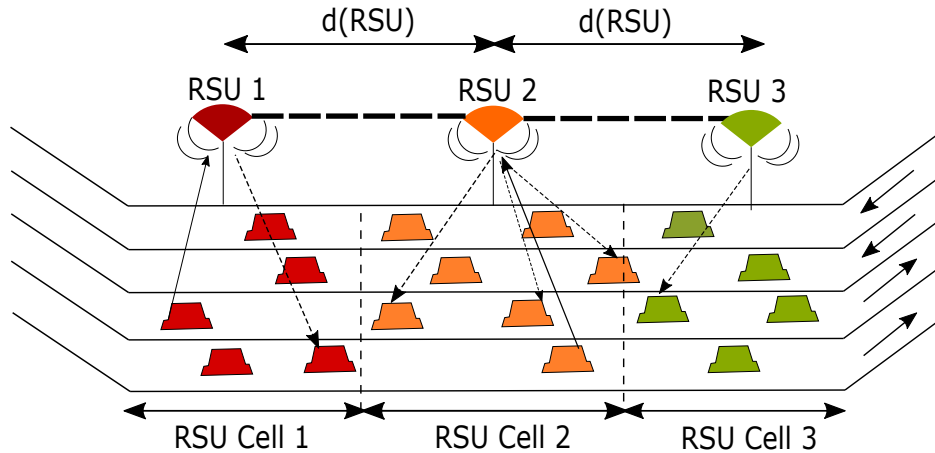
Figure 3.1: Highway Transportation Aided by Roadside Infrastructure

3.3 Network Systems Model

3.3.1 Network Parameters

RSUs are placed along the side of a linear multi-lane highway of length L with inter-RSU distance of d_{RSU}, forming a RSU backbone network. The RSU nodes are interconnected by high speed point-to-point (e.g., fiber optic) links. This infrastructure is used to facilitate communications networking along the vehicular highway system. Figure 4.1 illustrates the network system studied in this chapter. Vehicles are assumed to be distributed along the highway in either a random fashion or organized into platoons, which are often used in each lane of the autonomous highway. In carrying out network performance evaluations in this chapter, we assume, at no loss in generality, vehicles to be uniformly distributed along each lane.

To illustrate the performance tradeoffs available to the designer under various network configuration options, our performance evaluations employ the following parameter values. We consider d_{RSU} to range from $100\,\mathrm{m}$ to $1000\,\mathrm{m}$. The number of vehicles (N) admitted to a lane segment of length $L = 5$ km is varied between 100 and 500, which are commonly employed values when considering different highway congestion levels. For performance behavior discussion purposes, we set N to be equal to 250. To attenuate the impact of edge

effects, we evaluate the system's performance by considering the middle section of a longer road. We have found out that results presented for a single-lane well reflect the performance behavior of a multi-lane highway. Hence, we discuss here the system's performance by considering a single lane highway segment. To illustrate, we use wireless communications radios that employ the 5.9 GHz band (i.e., $f_c = 5.9$ GHz), as often used for testing autonomous vehicle system technologies such as DSRC and C-V2X [23] [24].

Our networking schemes make use of subdivision of the spectrum into distinct communication channels, including a control channel (CCH) and multiple service channels (SCH). The CCH is used in a manner that is similar to that employed by the WAVE system [17] and by other architectures. It is used by station entities to broadcast status and control messages [20] periodically (e.g., every 100 ms). This process allows RSUs and vehicles to exchange essential up-to-date status information such as vehicular location coordinates, speeds, destination objectives, channel quality indices, radio states, available processing rates and transmit power resource capabilities, which are then used for the synthesis of our network architecture.

A service channel (SCH) is used in our scheme for the transmission of data packet flows produced by a multitude of applications. To simplify, packet flows are categorized into two classes. Class 1 packets include critical (e.g., safety) messages and are granted higher priority. The throughput rate of such event-induced packet flows is relatively low. However, such packets should be disseminated across their spans to achieve a PDR that is equal to at least 0.95. Furthermore, successfully delivered packets should complete their dissemination within a 95-percentile time delay requirement of $D_{P,max} = 50$ ms. Class 2 message flows are of lower priority but often impose high throughput rate requirements. We assume in this study that packet flows can be generated by multiple source vehicles, and that each packet must be disseminated over a targeted dissemination span of d_{span}, reaching vehicles travelling behind the source vehicle within such distance.

We aim to configure the communications network to achieve high performance, realizing a high data throughput rate while satisfying prescribed message delay (95-percentile packet delay capped at $D_{P,max}$) levels and successful delivery rate (PDR ≥ 0.95) objectives. We carry

out our performance analysis and design evaluations under the assumption that vehicular nodes are highly loaded by packets that can either belong to Class 1 or Class 2. To illustrate, we assume $d_{\mathrm{span}} = 300\,\mathrm{m}$. Our protocols and basic models can readily be extended to scenarios whereby the dissemination span is applied bi-directionally to cover vehicles that move behind and ahead of each source vehicle.

We aim to determine the best configuration of uplink and downlink MAC scheduling schemes and their associated parameter values, uplink and downlink MCS configurations and their ensuing data rates, the spatial-reuse (coloring) levels, and the transmit power levels used by radio modules at the vehicles and at the RSUs, under varying d_{RSU} range values. Noting that packet transmissions across the infrastructure are carried out along the fiber optic based backbone links, we consider the wireless communications channels that are used for respective uplink and downlink transmissions to be shared according to one of the following MAC protocols: Demand-assigned (DA) TDMA uplink - TDMA downlink (MAC A), IEEE 802.11p uplink - IEEE 802.11p downlink (MAC B) and IEEE 802.11p uplink - TDMA downlink (MAC C). To carry out performance analyses of the TDMA-based MAC schemes, we combine the use of analytical models and simulation evaluations. Whereas, the performance modeling and analyses when using IEEE 802.11p-based MAC schemes combine the use of analytical models and of NS-3 (version 3.26) based simulation evaluations.

For illustrative performance analyses, we assume data rates to be selected among 3 Mbps, 6 Mbps, 12 Mbps; noting that each corresponding MCS employs a rate 1/2 coding scheme. These data rates are recommended as mandatory by [27] for use in the 10 MHz channels of IEEE 802.11p. Accounting for the code rate, using these data rates equivalently corresponds to transmission rate values R of 6 Mbps, 12 Mbps and 24 Mbps respectively. We subsequently express the data throughput performance behavior as a function of the latter transmission rate levels. We denote the transmission rates employed across the uplink and downlink channels as R_{ul} and R_{dl}, respectively. The transmit power levels P_{tx} used by vehicles and RSUs are denoted as $P_{\mathrm{tx,v}}$ and $P_{\mathrm{tx,r}}$, respectively. We use transmit power values that range from 5 dBm to 40 dBm. To simplify the presentation of results, we focus on 23 dBm and 33 dBm [23]. We

Parameter	Value	Parameter	Value
L	5 km	$P_{\text{tx,v}}, P_{\text{tx,r}}$	5–40 dBm
k_{ul}, k_{dl}	1,2,3,4	P_{noise}	-104 dBm
d_{RSU}	100–1000 m	CS_t	-85 dBm [27]
R_{ul}, R_{dl}	6, 12, 24 Mbps [27]	d_{span}	300 m [8]
$SINR_t$	7, 11, 20 dB [28, 29]	d_0, d_c	10, 80 m [26]
rv_t	-85, -82, -77 dBm [27]	γ_1, γ_2	1.9, 3.8 [26]
PDR	≥ 0.95	$D_{P,\max}$	50 ms [8]
P	3024 bits	f_c	5.9 GHz

assume a commonly employed dual-slope path loss model [26, 54, 3]. The model parameters that we employ, including λ, d_0, d_c, γ_1, γ_2, are defined in [26]. For illustration purposes, we configure the model's associated parameter values to be the same as those used by [26]. We assume vehicles and RSUs to use omni-directional antennas. RSU antennas are mounted at a height of at least d_0 from the ground (e.g., 10 m). The average noise power measured at a receiving node is assumed to be equal to $P_n = -104$ dBm. The average signal power level received at either a vehicle node or a RSU node, when transmitted by another node that is located at a distance that is equal to d, is denoted as $P_{\text{rx}}(d)$, is calculated as follows:

$$P_{\text{rx}}(d) = \begin{cases} P_{tx}\left(\frac{\lambda^2}{16\pi^2 d_0^2}\right)\left(\frac{d_0}{d}\right)^{\gamma_1}, \text{ if } d_0 \leq d \leq d_{\text{c}} \\ P_{tx}\left(\frac{\lambda^2}{16\pi^2 d_0^2}\right)\left(\frac{d_0}{d_c}\right)^{\gamma_1}\left(\frac{d_c}{d}\right)^{\gamma_2}, \text{ if } d > d_{\text{c}} \end{cases} \tag{3.1}$$

For a given data rate and MCS, to assure an acceptably high PDR, a link-level packet transmission is considered to be successful only if a minimum receiver SINR threshold $SINR_t$ and a minimum receiver sensitivity (i.e. minimum received power) rv_t levels are satisfied. For example, when $R = 24$ Mbps, we have $SINR_t = 20$ dB [28, 29] and $rv_t = -77$ dBm[27]. The network parameters that we use in our system evaluations are summarized in Table 3.1. Other relevant parameters are defined in Sections 3.3.4 and 3.4.

3.3.2   Performance Metrics

We characterize the data throughput performance in terms of sole aggregate uplink throughput $TH_{\text{ul,I}}$, sole aggregate downlink throughput $TH_{\text{dl,I}}$ and joint aggregate data throughput of the system $TH_{\text{ul,dl}}$.

The aggregate throughput rate of data packets supported across an uplink channel when assuming that all system bandwidth is allocated for uplink operations (thus isolating its performance from that induced by downlink operations) is denoted as $TH_{\text{ul,I}}$. Similarly, assuming all system bandwidth to be used for downlink operations, the aggregate downlink data throughput is denoted as $TH_{\text{dl,I}}$.

The aggregate joint system throughput $TH_{\text{ul,dl}}$ represents the total supported data rate of uplink packet flows originating from source vehicles. Included are only messages that are successfully disseminated to vehicles within d_{span} from their source vehicles. A flow of such packets is considered to be successfully disseminated if its packets are correctly received by at least 90% - 95 % of vehicles residing within d_{span} (i.e., PDR of at least between 0.90 and 0.95), while incurring a packet delay level that is lower than $D_{\text{P,max}} = 50$ ms [8] for at least 90 %-95 % of the packets. To illustrate, the packet length (P) is set to 3024 bits [30]. The aggregate data throughput metric is scaled by a factor that is proportional to the number of RSUs placed along the highway segment, N_{RSU}.

3.3.3   Network Architecture

In the network architecture that is formed, we assume that the number of RSUs forming the backbone network is sufficient to allow these RSUs to provide full communications coverage of all vehicles traveling along the underlying highway segment. Packet dissemination flows are thus carried out without resorting to the use of V2V communications. As a vehicle travels along the highway, it proceeds to associate with the RSU from which it receives the highest quality radio signals. The vehicle is then deemed to become a member of the selected RSU's cell. For analytical simplification, we assume RSU cell regions to be disjoint, as illustrated

in Figure 4.1, though our approach and protocols readily apply to practical scenarios under which cell areas well overlap. Each RSU station manages a RSU cell, which is normally set to extend over a highway region whose boundary envelopes a range of $d_{RSU}/2$ from the RSU station covering vehicles travelling in both directions.

A HSM is employed. It exchanges status information with the RSUs, which includes vehicular status vectors, obtained from status message exchanges across the CCH. The HSM also communicates with the RSUs to set system-wide data networking parameters, which are then announced by the RSUs to their mobiles.

3.3.4 Networking Protocol

During any period of time, packets are generated by certain vehicles that happen to be stochastically engaged in the origination of packet flows. The packets produced by each source vehicle must be disseminated to all vehicles located within d_{span} from the source, assuming here the dissemination to proceed in a direction that is opposite to the travel direction of the source vehicle. For this purpose, a source vehicle transmits its packets uplink to its associated RSU. The RSU may then forward the received packets across the backbone network to other RSUs so that the RSUs, including that which is associated to the source vehicle, then transmit these packets downlink across their cells to reach all vehicles which are located within a range of d_{span} from the source vehicle. We denote by n_{span} the number of RSUs, which are used to multicast these packets across their downlink channels. The average value of n_{span} is expressed as $E[n_{\mathrm{span}}] = 1 + \frac{d_{span}}{d_{RSU}}$.

At times the selection of RSUs to forward packets may induce packet reception by vehicles that reside beyond the targeted span. Depending on the underlying application, such excess receptions may be acceptable (e.g., for safety messages). Otherwise, the receiving mobile may filter unwanted messages by using location or other identifiers.

| Tp_{rsv} | $Tp_{ul,1}$ | $Tp_{ul,2}$ | $Tp_{dl,1}$ | $Tp_{dl,2}$ |

T_f
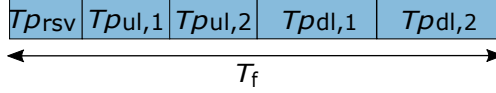
Figure 3.2: Illustrative time slot formation in a time frame of MAC A with $k_{ul} = 2$ and $k_{dl} = 2$. $Tp_{ul,1}$ and $Tp_{dl,1}$ denote uplink and downlink periods used by RSU cells of index 2n-1. $Tp_{ul,2}$ and $Tp_{dl,2}$ denote uplink and downlink periods used by RSU cells of index 2n $(n \geq 1)$.

3.4 Infrastructure-aided Medium Access Control (MAC) Schemes

Packet transmissions between RSUs are executed across a high-capacity backbone network at a data rate that is much higher than that used across the system's uplink and downlink channels. Hence, packets received across a wireless uplink at a RSU are effectively instantly transported to the other RSUs that need to receive such packets for dissemination to vehicles through their scheduling for downlink tnsmissions. The ensuing packet delays incurred across the backbone are therefore relatively negligible.

3.4.1 DA/TDMA Uplink - TDMA Downlink MAC Scheme (MAC A)

We assume that RSUs acquire time synchronization from a regional network manager. The RSUs transmit periodically beacons that provide time stamp information, which allows regional vehicles traveling along the underlying highway segment to be time synchronized, enabling the implementation of a TDMA mechanism across the system uplinks and downlinks. A Demand Assigned TDMA (DA/TDMA) scheme is used to allocate uplink access resources. Each time frame, denoted as T_f, contains periods used by mobiles to send reservation packets, as well as time periods used by mobiles and by RSUs to transmit uplink and dowlink packets. We denote the duration of the per-frame reservation period as Tp_{rsv}, the duration of the per-frame uplink data transmission period as Tp_{ul} and the duration of the per-frame downlink data transmission period as Tp_{dl} (see Figure 3.2). Hence $T_f = Tp_{rsv} + Tp_{ul} + Tp_{dl}$.

Only a single vehicle member of a RSU cell is assigned to execute uplink transmission while

using a given time slot. To reduce the impact of interference signals induced by simultaneous uplink transmissions by mobiles that reside in neighboring RSU cells, an uplink coloring factor (i.e., spatial-reuse index) k_{ul} is employed. During a Tp_{ul} period, active vehicles that are members of a certain RSU cell are set to transmit for a fraction of time that is equal to $\frac{1}{k_{ul}}Tp_{ul}$, so that during such a period only 1 out of k_{ul} consecutive RSU cells is scheduled to allow uplink transmissions. Each corresponding time slot assumes the duration $Ts_{ul} = \frac{P}{R_{ul}}$ for the transmission of a packet.

Through performance analyses, we determine the value for k_{ul} in aiming to mitigate inter-RSU cell interference signals, serving to assure a high uplink PDR level, PDR_{ul}, of at least 0.95, while attaining the highest feasible uplink throughput level. The coloring value to be properly configured depends on the employed R_{ul}. The value of k_{ul} is determined by using Monte Carlo simulation of uplink transmissions. For design purposes, we assume a conservative case whereby all RSU cells are assumed to be always active (i.e., vehicles are kept highly loaded with packets that they wish to disseminate) such that all RSU cells are kept busy during the entire Tp_{ul} and Tp_{dl} periods. When a higher R_{ul} is used, a higher reuse k_{ul} level is typically required due to the higher SINR threshold that is required at the intended receiver. For example, we have determined that, for the underlying scenario, under $R_{ul} = 6$ Mbps and $R_{ul} = 12$ Mbps, an optimal reuse level of $k_{ul} = 2$ should be employed. In turn, under $R_{ul} = 24$ Mbps, one should set an optimal reuse level of $k_{ul} = 3$. Similarly, we can determine optimal k_{dl} value, which depends on the employed R_{dl} by the RSUs. Overall, optimal coloring values k_{ul} and k_{dl} must be selected to ensure that at least 90 % of the packets meet the corresponding required minimum SINR levels, and guarantee reception of packets across for both uplink and downlink channels at high success rates to reach their intended destination mobiles. For example, to simplify system design, we note that by guaranteeing $PDR_{ul} > 0.95$ and $PDR_{dl} > 0.95$, we assure a PDR level that is equal to a high value, which is often equal to at least 90.25 %.

We coordinate the joint allocation of uplink and downlink bandwidth resources, noting that each RSU node must be able to process and transmit (downlink) the traffic that it

receives (across its uplink) from vehicles in its RSU cell and from other RSU nodes (across the fiber-optic links), provided it is located within the traffic's backbone dissemination path. Included are packets received from $E[n_{span}] - 1$ neighboring RSU nodes. Hence, the corresponding time periods Tp_{ul} and Tp_{dl} allocated in each frame are set to satisfy the following ratio:

$$\frac{Tp_{\text{ul}}}{Tp_{\text{dl}}} = \frac{R_{\text{dl}} PDR_{dl} k_{ul}}{E[n_{\text{span}}] R_{\text{ul}} PDR_{ul} k_{dl}} \tag{3.2}$$

Noting that our throughput analysis has been performed by assuming vehicles to be highly loaded in the production of packet flows, and hence inducing highly loaded RSU nodes, we deduce that the aggregate uplink throughput can be expressed as $TH_{\text{ul,I}} = N_{\text{RSU}} \frac{R_{\text{ul}} PDR_{\text{ul}}}{k_{ul}}$. The aggregate system throughput is expressed as follows (noting that all traffic flows are generated by mobiles):

$$TH_{\text{ul,dl}} = TH_{\text{ul,I}} \frac{Tp_{\text{ul}}}{T_{\text{f}}} \tag{3.3}$$

To assess the packet delay components, we note the following. The Frame Latency (FL) delay component represents the time elapsed between the arrival (or production) time of a packet at the source vehicle and the time instant at which the vehicle transmits its reservation packet. FL is incurred only by the first packet of a packet flow (or 'stream'); the underlying scheme can use the first data packet to include (piggyback) a reservation request. Subsequent flow packets will not experience such FL delays, as we assume that the flow is allocated slots at a rate that matches its requested rate. To state an upper bound on incurred packet delay level, we set a worst case frame latency to assume the value $FL = T_{\text{f}}$. The MAC A scheme is especially suitable for the scheduling of stream-oriented packet flows, which are characterized by periodic generation process at an application specific rate.

High priority Class 1 messages may use periods allocated within the CCH to assure a very high success rate in the transmission of short critical data packets and/or reservation packets to reserve TDMA time slots. Various other reservation schemes can be employed (for example the discussion in [45]). Clearly, a longer reservation period allocated within a SCH time-frame results in a lower residual capacity available to support the transmissions of

data packets. In our performance analyses, we assume there that the targeted reservation latencies are met with the use of reservation schemes which adapt to the underlying traffic rate to ensure high probability of success.

To achieve a bounded delay level performance for admitted packets, we employ the following flow regulation and control scheme at each RSU node. All packets that reach a RSU node during a time frame period, either from its uplink channel or from its neighboring RSUs, are targeted by the RSU node for complete downlink transmission during the current time frame downlink period. Since the uplink and downlink time period setting uses an averaged n_{span} parameter, $E[n_{span}]$, to regulate the loading on each RSU under conditions whereby different flows may require dissemination along a different number of RSUs, we configure the system would to employ a flow control mechanism that serves to block the admission of flows which induce overloading of the downlink queue at RSU nodes. In this manner, one can assure an end-to-end packet delay of the order of $D_p \leq FL + T_f \leq 2T_f$ (supplemented by an ensuing reservation delay when applicable, normalized in relation to the average flow duration as only the first packet of the flow incurs the latter delay component).

A MAC A type scheme can be applied in a similar manner when resources are assigned in the joint time/frequency (TDMA/FDMA) two-dimensional domain, as often performed by 4G cellular systems.

3.4.1.1 DA/TDMA Uplink - TDMA Downlink (MAC A) under Adaptive Uplink Transmission Rate Selection

A mobile position-based adaptive uplink rate selection scheme can be implemented as follows. A vehicle adjusts its uplink data transmission rate R_{ul} in accordance with its current distance from the associated RSU. A corresponding higher R_{ul} value is set by a vehicle when it is located around the center of a cell, while a lower R_{ul} level is used by a vehicle that is located closer to the cell's boundary. An uplink coloring index k_{ul} is jointly configured in relation to the employed uplink rate R_{ul}, following the design method described above in Section 3.4.1. The aggregate uplink throughput $TH_{ul,I}$ determined for the adaptive uplink rate scheme is

obtained by first averaging the attainable uplink data rate R_{ul} by assuming mobiles to be uniformly distributed over a single RSU cell area. We then scale the results by considering the totality of system RSU cells. For analytical simplicity in deriving an approximate expression for the system's throughput efficiency when using adaptive uplink rate, the Tp_{ul} and Tp_{dl} durations are apportioned by using the average values obtained for the system's R_{ul} and k_{ul} parameters. Note that due to the multicast nature of the message dissemination process, the downlink transmission rate R_{dl} values are configured to provide for reception by all vehicles residing within the RSU cell, regardless of their position. Hence, the values determined for the R_{dl} and k_{dl} parameters are selected in a fashion that is similar to that used when considering the non-adaptive rate scheme, as explained above in Section 3.4.1.

We note that such an adaptive uplink rate scheme can improve data throughput performance. An optimal selection of distance thresholds that are used to adapt the uplink transmission rate is yet to be investigated.

3.4.2   IEEE 802.11p Uplink - IEEE 802.11p Downlink MAC Scheme (MAC B)

We assume the system to employ an IEEE 802.11p protocol to coordinate the sharing of the wireless channel. Such a mechanism is simple to implement, fully distributed and does not involve complex control, network management and resource allocation schemes. It is especially suitable to support data flows that require rapid dissemination and do not induce high channel loading, as is often the case for many safety oriented packets. An entity (a vehicle or a RSU) attempting to send packets and gain channel access must contend for wireless transmission resources with currently active nodes, including active RSU and vehicular nodes that reside within its carrier sensing range, d_{CS}. The latter is determined by the configured value of the carrier sensing threshold CS_t [27]. It is noted that active nodes that are located even further away from a transmitting node, and thus do not have their carrier sense indication activated, may still interfere with the reception of the intended signal if they contribute to a total interference level at the latter receiver that leads to an unacceptable SINR level. We assume that the same transmission rate R level to be used by all vehicles and RSU nodes (so

that $R_{ul} = R_{dl}$). The d_{CS} value is calculated using (3.1), by setting the power level received from a transmitter located at this distance away from the receiver, and operating at a given transmit power level, to be equal to CS_t.

The interference distance d_I is calculated as the farthest distance at which a dominant interfering node would be located away from the intended receiver, while inducing an interference power level $P_{rx}(d_I)$ at the intended receiver, and consequently a SINR level at the intended receiving node that is just too low (or barely sufficient) to permit successful reception at the employed data rate R. For its calculation, in considering a conservative system design approach, we assume the transmission distance of the intended signal to be equal to the longest of any intended transmission distance within a cell, setting it therefore to $0.5d_{RSU}$. Hence, $P_{rx}(d_I) = \frac{P_{rx}(0.5d_{RSU})}{SINR_t} - P_n$. The corresponding d_I is then computed by using (3.1).

We employ the following approach to determine a design that induces an effective value for the transmit power level, P_{tx}^*. We note that if the transmit power level is set to a too low value, so that $d_{CS} < d_I + 0.5d_{RSU}$, the carrier sensing range then assumes a too short value, leading to a situation whereby an interfering node may be located too close to the receiver, inducing a low SINR level at the intended receiver. In turn, under a higher transmit power level, when $d_{CS} > d_I + 0.5d_{RSU}$, the resulting carrier sensing range tends to be longer than that required to effectively keep away interfering nodes, which tends to prevent the simultaneous activation of other transmitters and thus to reduce the realized spatial-reuse factor. In the latter case, the effective number of simultaneously active successful transmissions would be reduced, leading to a reduced throughput rate. Accordingly, we use the following observation to derive an approximate P_{tx}^* formula:

$$d_{CS} = d_I + 0.5d_{RSU} \tag{3.4}$$

Using (3.1) and (3.4), we express P_{tx}^* by considering: (3.5a) $d_0 \leq d_I \leq d_{CS} \leq d_c$, $d_0 \leq 0.5d_{RSU} \leq d_c$, (3.5b) $d_0 \leq d_I \leq d_c$, $d_{CS} > d_c$, $d_0 \leq 0.5d_{RSU} \leq d_c$, (3.5c) $d_{CS} > d_I > d_c$, $d_0 \leq 0.5d_{RSU} \leq d_c$, (3.5d) $d_{CS} > d_I > d_c$, $0.5d_{RSU} > d_c$.

$$P_{tx}^* = \begin{cases} \dfrac{CS_t(SINR_t^{\frac{1}{\gamma_1}}+1)^{\gamma_1}(0.5d_{RSU})^{\gamma_1}}{d_0^{\gamma_1}\lambda^2/(16\pi^2 d_0^2)} & \text{(3.5a)} \\[2em] \dfrac{CS_t(SINR_t^{\frac{1}{\gamma_1}}+1)^{\gamma_2}(0.5d_{RSU})^{\gamma_2}}{d_c^{\gamma_2-\gamma_1}d_0^{\gamma_1}\lambda^2/(16\pi^2 d_0^2)} & \text{(3.5b)} \\[2em] \dfrac{CS_t(SINR_t^{\frac{1}{\gamma_2}}(d_c/(0.5d_{RSU}))^{1-\frac{\gamma_1}{\gamma_2}}+1)^{\gamma_2}(0.5d_{RSU})^{\gamma_2}}{d_c^{\gamma_2-\gamma_1}d_0^{\gamma_1}\lambda^2/(16\pi^2 d_0^2)} & \text{(3.5c)} \\[2em] \dfrac{CS_t(SINR_t^{\frac{1}{\gamma_2}}+1)^{\gamma_2}(0.5d_{RSU})^{\gamma_2}}{d_c^{\gamma_2-\gamma_1}d_0^{\gamma_1}\lambda^2/(16\pi^2 d_0^2)} & \text{(3.5d)} \end{cases} \qquad (3.5)$$

Assuming that the system implements a flow control mechanism that is used to regulate the offered packet flow rate activity so that the collision rate is kept at a sufficiently low level, P_{tx}^* is used to calculate the desired d_{CS} value. We note that due to the conservative assumption made in relation to assuming a receiver that is located at the RSU cell's edge, the approximated desired transmit power value tends to be often somewhat higher than the level required in actual simulation implementations.

3.4.2.1 Adaptive Uplink Transmission Rate Selection by Using MAC B

A mobile position based adaptive uplink transmission rate selection scheme can be implemented as follows. A vehicle adjusts its uplink transmit data rate based on its current distance from the associated RSU. A corresponding higher uplink data rate is set by a vehicle when it is located around the center of a cell, while a lower uplink data rate is used by a vehicle that is located closer to the cell's boundary. Note that due to the multicast nature of message dissemination, the downlink transmission rates are configured to provide for reception by all vehicles within the RSU cell, regardless of their position. Hence, the latter rates are set in a manner that is similar to that used by the non-adaptive rate scheme, as explained above in Section 3.4.2. We note that such an adaptive uplink rate scheme can enhance data throughput performance. The optimal setting of the uplink data rate for such an adaptive scheme is not part of the investigation performed in this chapter.

3.4.3 IEEE 802.11p Uplink - TDMA Downlink (MAC C)

In this section, we discuss the performance features of a system that employs an IEEE 802.11p type CSMA/CA MAC scheme for vehicles to transmit uplink to their corresponding RSUs and a TDMA scheme to share the RSU downlink communication resources.

We assume that RSUs acquire time synchronization from a regional network manager. The RSUs transmit periodically beacons that provide time stamp information. These transmissions are used by vehicles traveling along the underlying highway segment to maintain time synchronization. A IEEE 802.11p based scheme is used by vehicles to share uplink access resources, and a TDMA scheme is used by each RSU to transmit packets downlink. Each time frame, whose duration is denoted as T_f, contains periods used by vehicle mobiles and by RSUs to transmit uplink and dowlink packets, respectively. We denote the duration of the per-frame uplink data transmission period as Tp_{ul} and the duration of the per-frame downlink data transmission period as Tp_{dl}. Hence, $T_f = Tp_{ul} + Tp_{dl}$.

For uplink transmission, for a given vehicle transmit power $P_{tx,v}$, we assume the carrier sensing range to be at d_{CS}, which may extend beyond a single RSU cell coverage. A higher transmission power induces a longer d_{CS} for a fixed carrier sensing threshold, CS_t. A mobile that is currently in the process of transmitting its message, prevents other mobiles that are within d_{CS} from it from initiating new transmissions. The carrier sensing induced by a transmit power value helps reduce interference signals caused by simultaneous transmissions by vehicles in other RSUs but on the other hand can also reduce spatial reuse along the highway. The design considerations for the IEEE 802.11p based scheme associated with the setting of the parameter d_{CS} and its impact on the realized spatial reuse factor, as the transmit power levels are varied, are explained in detail when discussing the MAC B scheme. For downlink transmission, each RSU is configured to use R_{dl} and a properly configured TDMA based downlink coloring of k_{dl}, which is configured to attain sufficiently high SINR and receiver sensitivity levels, while achieving high throughput rates. The corresponding periods are sized such that the infrastructure's RSUs can accommodate the packets which are transmitted uplink by vehicles to their associated RSUs and are then disseminated for

downlink transmission by the RSU and $E[n_{span}] - 1$ neighboring RSUs.

Accordingly, we set the durations of the corresponding periods to satisfy the following relationship:

$$\frac{Tp_{\text{ul}}}{Tp_{\text{dl}}} = \frac{N_{\text{RSU}} R_{\text{dl}}}{TH_{\text{ul,I,max}} E[n_{\text{span}}] k_{dl}} \tag{3.6}$$

The explanation of the time bandwidth apportioning is similar to that outlined for MAC A, except that data traffic arrival rate at each RSU under MAC C is attributed to uplink transmissions which employ the IEEE 802.11p based MAC scheme. To simplify the implementation of the access scheme, $Tp_{\text{ul,I}}$ and $Tp_{\text{dl,I}}$ are allocated on a fixed ratio basis, which is calculated based on $TH_{\text{ul,I,max}}$, which represents the highest attainable aggregate uplink throughput rate over the loading range under consideration when the uplink system is operated separately from the downlink operation. The allocation is set to guarantee that the average data rate which is received by a RSU from the vehicles within its RSU cell , $TH_{\text{ul,I,max}}/N_{\text{RSU}}$, supplemented by the data rate for packets received from neighboring RSU, is equal to the average rate at which data can be served (i.e., transmitted downlink) by a RSU.

For a given R_{ul}, as the data load produced by vehicles in a RSU cell is increased, $TH_{\text{ul,I}}$ increases accordingly until it is measured to reach its maximum value, denoted as $TH_{\text{ul,I,max}}$. This throughput performance is impacted by the stochastic occurrence of collisions and re-transmissions across the IEEE 802.11p-channel. It is further noted that packets that are re-transmitted four times are subsequently discarded and assumed to not be successfully delivered. A flow control mechanism is employed to guarantee that the average packet rate received at each RSU (from its clients within RSU cells and from other RSUs) is lower than the effective service rate (i.e., packet transmission rate) that can be executed by the RSU. To evaluate the performance of the MAC C scheme, we carry out Monte Carlo simulations for the IEEE 802.11p-based uplink system in isolation from downlink. We obtain the delay throughput performance evaluation of the separate IEEE 802.11p-based uplink system by using a NS-3 based simulation.

We set mobiles that belong to distinct RSU cells to be simultaneously active to account

for the impact of inter-RSU cell uplink interference signals. The performance of the TDMA based downlink transmission by RSU in isolation is carried out by using the mathematical expressions presented in Section 3.4.1. The resulting performance metrics are then used to calculate the uplink and downlink per-time-frame periods Tp_{ul} and Tp_{dl} by using the mathematical relationship stated above.

The data traffic loading each RSU consists of data packets received from the vehicles in RSU cell associated with this RSU and of data packets that are received from neighboring RSUs. Hence, the aggregate data packet arrival rate at a RSU is equal to $\lambda_{\mathrm{RSU}} = E[n_{\mathrm{span}}]\frac{TH_{\mathrm{ul,I}}}{N_{\mathrm{RSU}}}\frac{Tp_{\mathrm{ul}}}{T_{\mathrm{f}}}\frac{1}{P}$ (packets/sec). It is noted that the packet arrival rate at each RSU depends on the number of RSUs involved in the dissemination of a flow to cover d_{span}, on the coloring factor k_{ul} and on the employed uplink transmission rate R_{ul}, through the realized $TH_{\mathrm{ul,I}}$, and the per-frame period allocated for uplink transmissions. The service rate provided by a RSU for downlink transmission, μ_{RSU}, is expressed as $\mu_{\mathrm{RSU}} = \frac{R_{\mathrm{dl}}Tp_{\mathrm{dl}}}{k_{dl}(T_{\mathrm{f}})}\frac{1}{P}$ (packets/sec). It is noted that μ_{RSU} depends on the proportion of time allocated for downlink transmissions within the time frame, on the k_{dl} factor used by the TDMA downlink mechanism, and on the employed RSU downlink transmission rate R_{dl}.

The time delay incurred by a packet while traversing the uplink, denoted as D_{ul}, is measured from the instant of its generation at the source vehicle to the instant that it is successfully transmitted to the associated RSU (given that its flow has been admitted). We have evaluated this delay component by performing Monte Carlo simulations. An approximation of the total delay time incurred by a packet at each RSU node while waiting and while being transported for downlink transmission, denoted as D_{dl}, has been calculated by using an analytical approach.

The targeted end-to-end packet delay, D_P, is then calculated as the sum of the FL delay, the delay time incurred across uplink IEEE 802.11p-channel D_{ul}, the delay time experienced by packet transmissions across the point-to-point backbone infrastructure and the delay time incurred for downlink transmissions D_{dl}. D_{dl} is obtained from the sum of downlink waiting time, denoted as W_{RSU}, incurred by packet at the RSU and the RSU downlink

76

packet transmission time $\frac{P}{R_{\text{dl}}}$. Assuming that the value of the packet delay time incurred for performing packet transmission across the backbone infrastructure is much smaller than other delay components, the end-to-end packet delay can be expressed as $D_P = FL + D_{\text{ul}} + D_{\text{dl}}$.

The waiting time incurred by a packet at each RSU, W_{RSU}, has been evaluated by approximating the RSU downlink queue as M/M/1 queueing system. Packets arrive at each RSU from its vehicle clients and from neighboring RSUs in a stochastic manner that is induced by the random times at which successful transmissions occur across the IEEE 802.11p based channel sharing scheme. Consequently, RSU forwards the packet to adjacent RSU at much higher data rate than processing by RSU for downlink transmission. As a result, packets from neighboring RSUs also come to a given RSU in a stochastic manner as well.

In our simulations runs, we examine varying level of data traffic load generated by vehicles, which induce various $TH_{\text{ul,I}}$ levels. For each traffic load, we calculate the 95-percentile delay incurred by a packet for downlink transmission D_{dl}. By subtracting this delay value from the specified end-to-end level, we obtain a value that is used as the targeted 95-percentile delay to be incurred by packets transmitted across the uplink channel by vehicles in the RSU cell (D_{ul}). It is noted that, as an approximation, when D_{ul} and D_{dl} are assumed to be independent random variables, the attained D_P is then guaranteed to hold for at least 90 % of the packets. The realized combined system throughput rate is then given by $TH_{\text{ul,dl}} = TH_{\text{ul,I}} \frac{Tp_{\text{ul}}}{T_{\text{f}}}$. For illustrative purpose, we assume to size one time frame T_f to accommodate k_{dl} downlink slots. This serves to reduce the *FL* induced latency component.

This MAC scheme is suitable for packet with sporadic generation rate. Hence, there is no need for reservation channel for uplink transmission.

3.5 Performance Behavior

3.5.1 DA/TDMA Uplink - TDMA Downlink (MAC A)

In Figure 3.3, we show the variation of the aggregate system throughput rate, $TH_{\text{ul,dl}}$, as a function of the configured d_{RSU}. The $TH_{\text{ul,dl}}$ performance is obtained by using the

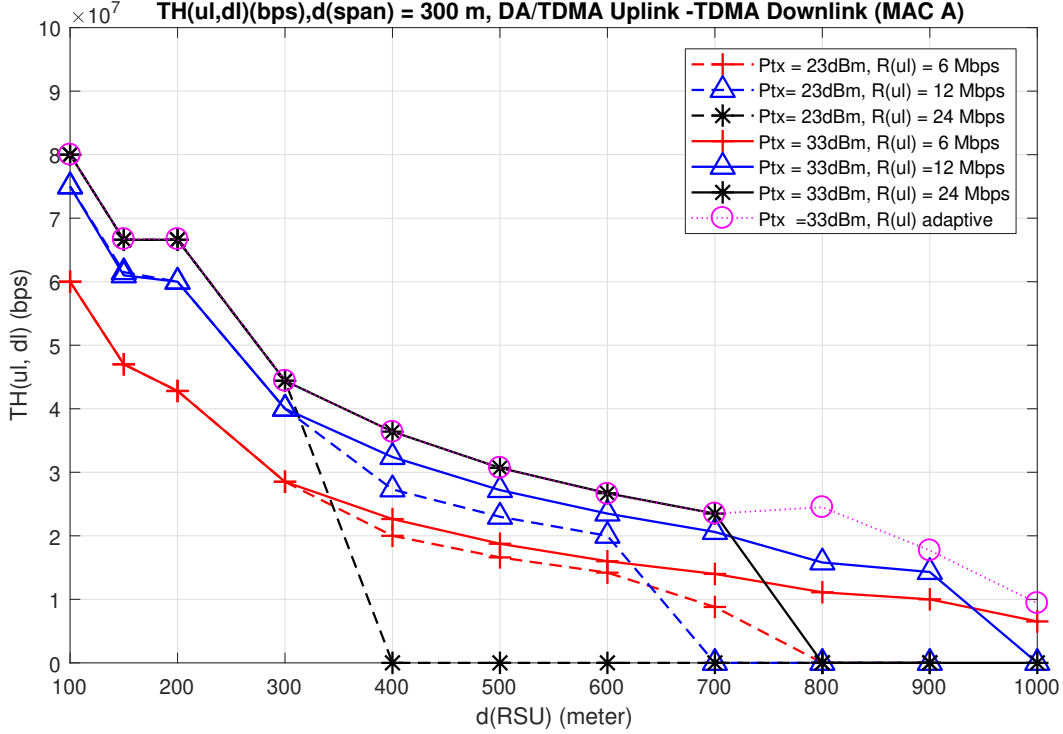Figure 3.3: $TH_{\text{ul,dl}}$ (bps) vs d_{RSU} (m) using MAC A

mathematical model presented in Section 3.4.1. We specify the targeted overall PDR to be higher than 0.90 and the packet delay to be lower than $50\,\text{ms}$. For a given uplink rate R_{ul}, the downlink rate and coloring factor parameters, R_{dl} and k_{dl}, are selected such that the aggregate data throughput rate is maximized. For example, when vehicles and RSUs use a transmit power level $P_{tx,v} = P_{tx,r} = 23$ dBm at $d_{RSU} = 100$ m, and vehicles use $R_{ul} = 6$ Mbps, these values are paired with $R_{dl} = 24$ Mbps and $k_{dl} = 3$.

The highest throughput rate is noted to be attained when setting $R_{ul} = 24$ Mbps, $k_{ul} = 3$, $R_{dl} = 24$ Mbps, $k_{dl} = 3$ at $d_{\text{RSU}} = 100\,\text{m}$. As d_{RSU} increases from $100\,\text{m}$ to $800\,\text{m}$, n_{span} is reduced, which on its own serves to enhance throughput performance. However, we find that the global throughput $TH_{\text{ul,dl}}$ rate is actually reduced. This is attributed to the lower number of RSUs that are installed leading to an overall reduction in the aggregate spectral resources available and thus to the reduced level of available uplink and downlink transmission rate capacity. It is also noted that by increasing the uplink rate from 6 Mbps to 24 Mbps, the resulting throughput rate increases in a lower than proportional manner due to the ensuing

increase in k_{ul}. In order to evaluate the performance of different coloring factors k_{ul} and k_{dl} for the uplink and downlink operation, we have carried out a Matlab-based Monte Carlo simulation. We note that as the d_{RSU} is further increased, say from 100 m to 400 m, R_{ul} and R_{dl} must be decreased to 12 Mbps. This is caused by the decrease in the received power level, which may then be reduced below the required receiver sensitivity value, especially for vehicles located at the edge of the RSU cell. To resolve such an issue, we have studied a system that uses an increased transmission power level. We have set $P_{\mathrm{tx,r}} = P_{\mathrm{tx,v}} = 33\,\mathrm{dBm}$. We observed the increased transmit power to not lead to increased throughput rate performance when setting shorter inter-RSU range distances, such as $d_{\mathrm{RSU}} = 100\,\mathrm{m}$ to $300\,\mathrm{m}$. However, an increase in the transmit power level yields a significant throughput upgrade under longer inter-RSU distances such as $d_{\mathrm{RSU}} \geq 400$ m, as it enabled the system to meet the required minimum receiver sensitivity level of using high transmit rate $R_{ul} = 24$ Mbps and $R_{dl} = 24$ Mbps.

3.5.1.1 DA/TDMA Uplink - TDMA Downlink (MAC A) under Adaptive Uplink Rate Selection Scheme

As discussed in Section 3.4.1.1, an adaptive scheme can be used to command a vehicle to adjust its uplink transmission data rate and associated parameters in accordance with is location within a cell and its distance from the associated RSU.

Observing the results presented in Figure 3.3, we conclude that when $P_{tx,r} = P_{tx,v} = 33$ dBm and vehicles adopt non-adaptive uplink rate selection, for $d_{RSU} < 800$ m , we should set $R_{ul} = 24$ Mbps. As the d_{RSU} range increases to $800 \leq d_{RSU} < 1000$ m, we set $R_{ul} = 12$ Mbps, and under $d_{RSU} \geq 1000$, we configure $R_{ul} = 6$ Mbps. Using these results, we have implemented a corresponding adaptive uplink rate setting scheme. A corresponding higher data rate is set by a vehicle when it is located around the center of a cell, while a lower uplink data rate is used by a vehicle that is located closer to the cell boundary. Accordingly, to illustrate, vehicles which are located in a distance from the RSU that is lower than 365 m, use the highest uplink transmission rate, $R_{ul} = 24$ Mbps; those are located at a corresponding

distance that is in the range 365 m - 450 m, use $R_{ul} = 12$ Mbps, while vehicles located farther than 450 m away from their RSU nodes, use the lowest uplink transmission rate, $R_{ul} = 6$ Mbps.

Using this illustrative adaptive uplink rate scheme, we aim to enhance the data throughput performance of the scheduling scheme. In Figure 3.3, we demonstrate that when using adaptive uplink transmission rate scheme, under the setting of $d_{RSU} = 800$ m, the aggregate data throughput $TH_{ul,dl}$ increases from 15.7 Mbps (attainable under a fixed uplink rate scheme) to 24 Mbps, thus resulting in a 52% increase in performance. For a more dense backbone, under $d_{RSU} = 100$ m to 700 m, all vehicles use uplink rate of $R_{ul} = 24$ Mbps and coloring of $k_{ul} = 3$, under the adaptive scheme, as well as under the non-adaptive scheme, so that there is no improvement attained under the use of the underlying adaptation mechanism.

3.5.2 IEEE 802.11p Uplink - IEEE 802.11p Downlink (MAC B)

The results presented in Figure 3.5 and Figure 3.6 have been obtained by performing Monte Carlo simulations using the NS-3 simulation program, version 3.26. For presentation and analytical simplification, we assume that the vehicles and the RSU nodes use the same transmit power values P_{tx} and transmit rate values R.

The results presented in Figure 3.5 demonstrate the effect of setting different transmit power values on the aggregate data throughput performance, under distinct d_{RSU} and R values. We note that under a short d_{RSU}, such as 100 m, the desired transmit power P_{tx} values are equal to about 17 dBm and 12 dBm for R values of 24 Mbps and 12 Mbps, respectively. When using longer d_{RSU}, such as 300 m, the corresponding desired P_{tx} values are equal to about 31 dBm and 26 dBm for R values of 24 Mbps and 12 Mbps, respectively. When comparing the desired transmit power values obtained by these simulations with the analytical calculations based on the formula derived in Section 3.4.2, we have confirmed the precision of the latter formula. For example, for $d_{RSU} = 100$ m, $R = 24$ Mbps, the desired transmit power values obtained by simulation and analysis are equal to 17 dBm and 19.6 dBm, respectively. For other configurations, the analytical value has been determined to
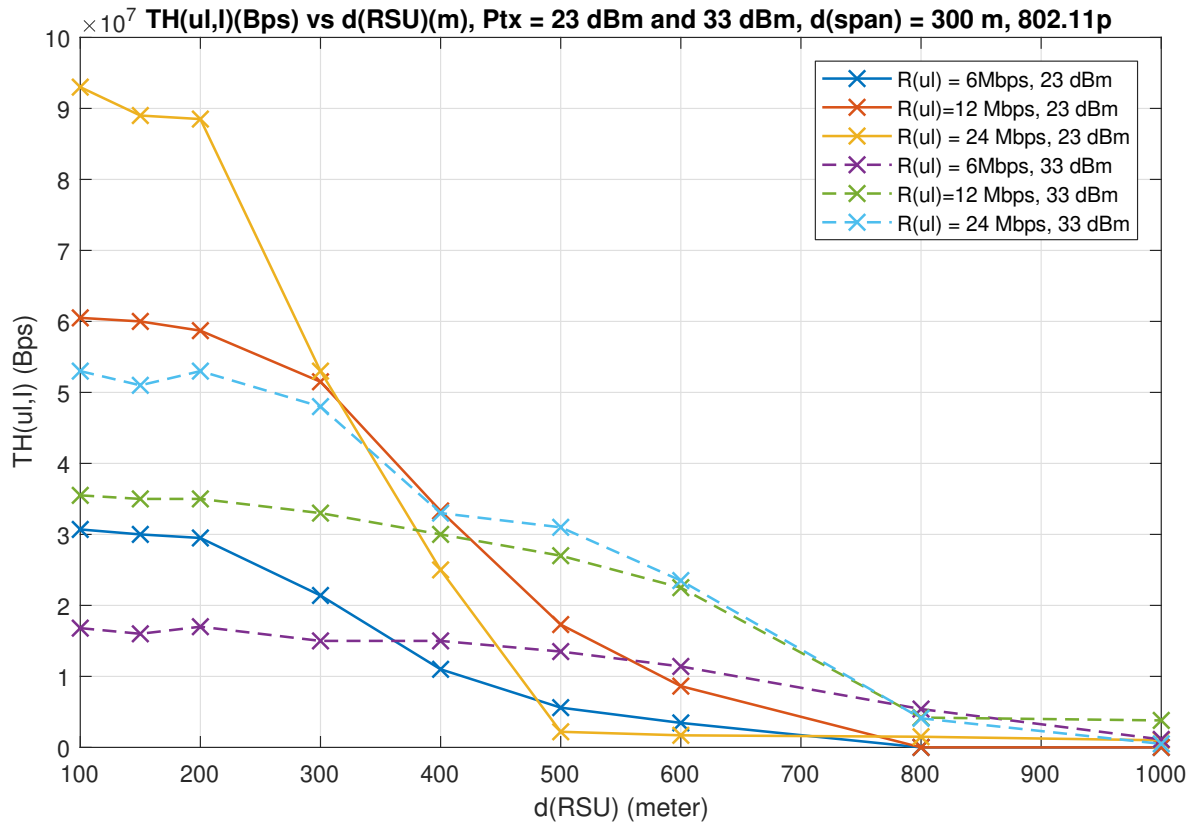
Figure 3.4: Maximum delay-capped TH_{ul} (bps) and $PDR \geq 0.95$ vs d_{BN} (m) for IEEE 802.11p uplink.

be higher than the simulation one by no more than 3 dBm. This difference is due to the conservative assumption made in deriving the formula by focusing on communications with nodes that are located farther away from their RSUs than is the situation in the average case.

To explain the desired transmit power value at $d_{RSU} = 100$ m by setting $R =24$ Mbps, we note the following. As shown in Figure 3.5, as we increase P_{tx} from 12 dBm to 17 dBm, the data throughput increases. Under the latter transmit power values, we have $d_{CS} < d_I + 0.5d_{RSU}$, so that the carrier sensing distance is shorter than the value required to satisfy the SINR threshold level. As the transmit power level is increased within the latter range, a longer d_{CS} is induced. Though the signal power of other transmissions also increases, the longer d_{CS} results in an overall higher SINR because the closest interferer tends to be located farther away from the receiver, leading to a net increase in the aggregate throughput level $TH_{ul,dl}$, as in this range the corresponding decrease in the spatial-reuse level does not dominate. For example, when $P_{tx} = 12$ dBm, we have $d_{CS} = 165$ m and $d_I = 214.36$ m. As we increase P_{tx} to 17 dBm, we obtain $d_{CS} = 224$ m and $d_I = 213$ m, which more closely satisfies the formula used by us to derive the analytical calculation of the preferred setting, $d_{CS} = d_I + 0.5d_{RSU}$. As the transmit power is further increased (e.g., from 17 dBm to 23 dBm), we observe that $d_{CS} > d_I + 0.5d_{RSU}$, where $d_{CS} = 322$ m and $d_I = 212.6$ m at transmit power level of 23 dBm. In this range, the resulting longer d_{CS} becomes a dominating factor, leading to a decreased spatial reuse value, while providing no enhanced SINR level at the intended receiver. Consequently, active nodes are provided less frequent medium access opportunities, leading to higher access contentions, higher packet delays and a lower net throughput rate.

We also note in Figure 3.5 that under a prescribed d_{RSU} level, the desired P_{tx} to be used under a lower R value, such as 12 Mbps, is lower than that to be used under a higher R, such as 24 Mbps. This is to be expected as the corresponding longer d_{CS} induced by higher P_{tx} contributes to the attainment of the required higher SINR level to provide for a higher data rate. The impact of the longer d_{CS} is essential here as the following is noted. Given an interfering node that resides at a given location, the SINR measured at an intended receiver
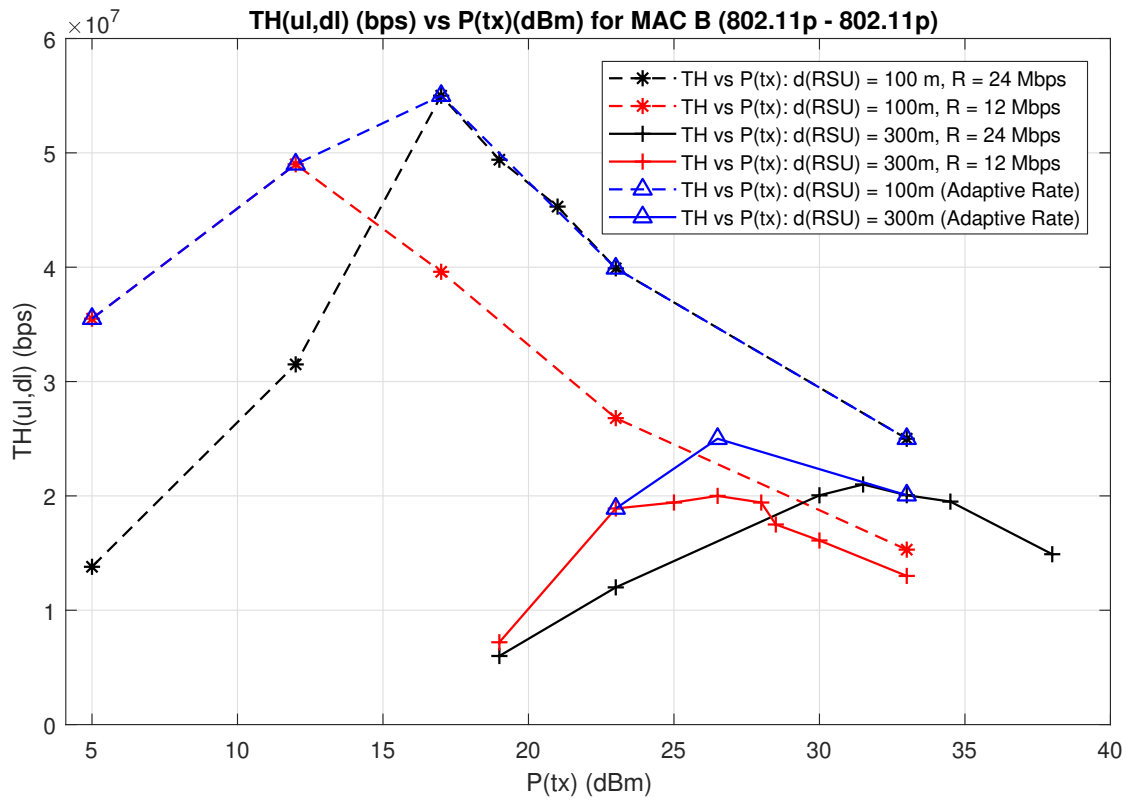
Figure 3.5: Delay-capped $TH_{\mathrm{ul,dl}}$ (bps) vs P_{tx} (dBm) of MAC B

as the transmit power levels of the sending and interfering nodes are proportionally increased remains effectively unchanged when operating in an interference dominating mode (i.e., the intended receiver experiences higher interference power than ambient noise power level). In this range, to attain higher SINR levels, it is thus essential to induce a longer d_{CS}, so that interfering nodes are forced to generally be located farther away from the intended receiver.

We also note that under a prescribed data rate value, the desired transmit power level that should be configured under a longer d_{RSU}, such as 300 m, must clearly be higher than that used under a shorter d_{RSU}, such as 100 m. When wider RSU cells are formed, setting a higher transmit power level induces longer d_{CS}, as required to assure many receiving nodes (particularly those that are located closer to the cell boundary) with acceptable SINR levels.

In Figure 3.6, we show the system's data throughput performance behavior as a function of d_{RSU}. We focus on the throughput performance behavior realized when prescribed delay and PDR requirements are met, and when P_{tx} is set to either 23 dBm or 33 dBm. The highest $TH_{ul,dl}$ value is obtained when d_{RSU}=100 m by setting $R = 24$ Mbps and $P_{tx} = 23$ dBm. Under a fixed transmit power level such as 23 dBm, and assuming a fixed CS_t level, different d_{RSU} values induce different desirable R values. Under a shorter d_{RSU} range, the desired transmission rate is set to a high value, $R = 24$ Mbps, while under a longer d_{RSU}, we set the desired transmission rate to a lower value, $R = 6$ Mbps. This is explained by noting that under a wider RSU cell span, vehicles that are located closer to the cell boundary tend to experience lower SINR values, requiring the use of a lower data rate.

We observe that under a given joint setting of data rate and transmit power levels, $TH_{ul,dl}$ experiences significant degradation as d_{RSU} is increased while operating at a high transmit rate R. In turn, we observe that the throughput values achieved under the use of lower R values are less sensitive to changes in the inter-RSU d_{RSU} range, due to the lower minimum SINR level that is now required. To illustrate, we note that the performance behavior exhibited under $P_{tx} = 23$ dBm is insensitive to variation in d_{RSU} from 100 m to 300 m, when using the lower transmission rate $R = 6$ Mbps, yielding a decrease in $TH_{ul,dl}$ from 13.5 Mbps to 10 Mbps. On the other hand, when using a higher transmission rate, $R = 24$ Mbps, $TH_{ul,dl}$
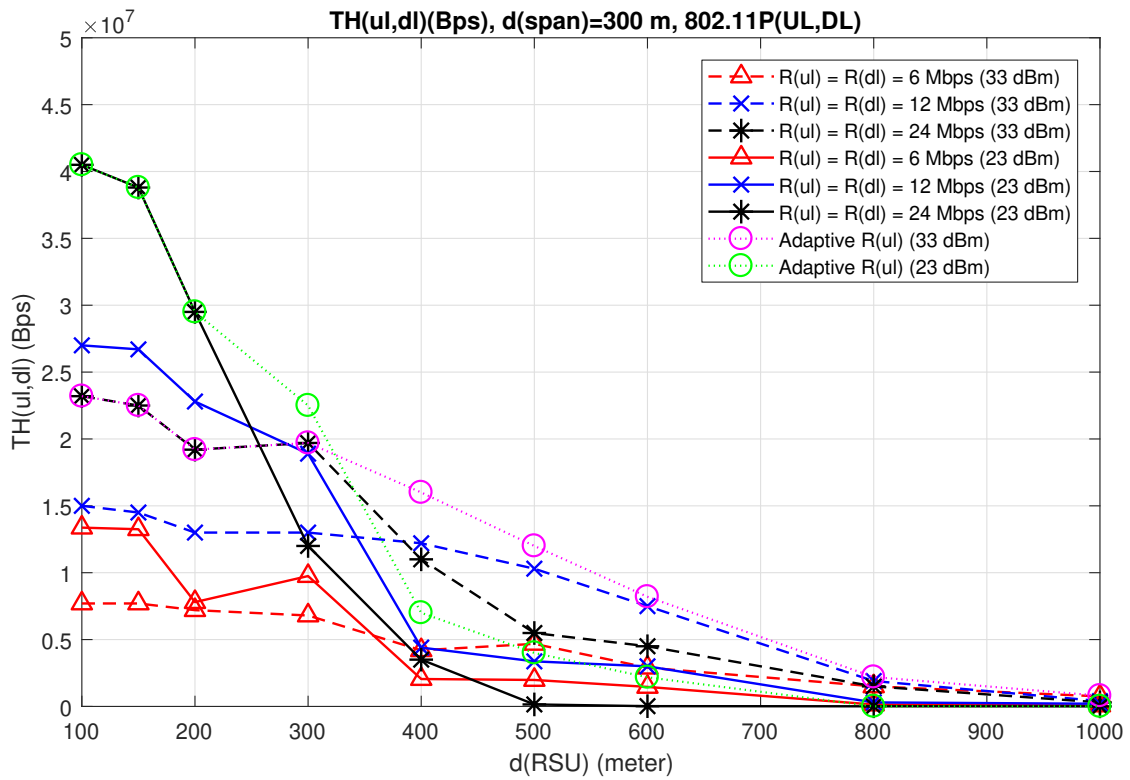
Figure 3.6: $TH_{\text{ul,dl}}$ (bps) vs d_{RSU} (m)

decreases significantly, from 40 Mbps to 12 Mbps. When using a less dense infrastructure, and thus a longer d_{RSU} value, for the underlying illustrative case, $E[n_{span}]$ decreases from 4 to 2, leading to reduced internal network loading. On the other hand, the system's RSU cells encompass wider spans. Consequently, intended packet receptions tend to become more sensitive to signal interference effects, noting that the underlying employed d_{CS} level is now less effective in reducing interfering signals.

When setting $R =24$ Mbps, under a short d_{RSU} level, such as 100 m, we observe the following. A higher data throughput is realized when P_{tx} is set to 23 dBm than when it is set to 33 dBm. Both transmit power values satisfy $d_{CS} > d_I + 0.5d_{RSU}$. Under this condition, the increase in throughput performance by using lower transmit power is dominated by increase in spatial reuse. Under a longer d_{RSU} value, such as 300 m, both transmit power levels satisfy $d_{CS} < d_I + 0.5d_{RSU}$, so that when transmit power level is increased the system's performance behavior is dominated by higher SINR levels at the intended receivers, which consequently leads to enhanced throughput performance. Furthermore, the intended and interfering signal power levels tend to be relatively low under $P_{tx} = 23$ dBm, so that the system then tends to operate in a noise dominated mode. The throughput rate is therefore enhanced by using a higher transmit power level, such as 33 dBm.

Our performance analyses indicate that the system's performance behavior is relatively insensitive to the number N of admitted vehicles. As N increases, only a modest decrease in the aggregate throughput rate is observed, noting the impact of the carrier sensing based operation.

3.5.2.1 IEEE 802.11p Uplink - IEEE 802.11p Downlink (MAC B) under Adaptive Uplink Rate Selection Scheme

Observing Figure 3.6, we conclude that when $P_{tx} = 23$ dBm and $d_{RSU} < 300$ m, we should set $R_{ul} = 24$ Mbps. As d_{RSU} increases to $300 \leq d_{RSU} < 900$ m, we should set $R_{ul} = 12$ Mbps; when $d_{RSU} \geq 900$, we should configure $R_{ul} = 6$ Mbps. Using these results, we have implemented a corresponding adaptive uplink rate adaptation scheme, as discussed in Section

3.4.2. For an illustrative case, the adaptation process employs the following scheme. Vehicles that are located at a distance from their RSUs that is lower than 175 m use $R_{ul} = 24$ Mbps, those in the range 175 m - 450 m use $R_{ul} = 12$ Mbps, and those farther away than 450 m use $R_{ul} = 6$ Mbps. In Figure 3.6, we demonstrate that when using this uplink rate adaptation scheme, under the setting of $d_{RSU} = 400$ m, $TH_{ul,dl}$ is enhanced by about 28 % (i.e., from 12.5 Mbps to 16 Mbps). For a more dense backbone system, when $d_{RSU} < 200$ m, we observe that that use of the adaptation scheme is not needed as it is preferable then to use the highest uplink data rate level for all vehicles, even for vehicles that are located near the periphery of the cell. For $d_{RSU} > 800$ m, we observe that a high proportion of the vehicles would have to employ the lowest data rate (to achieve their targeted SINR levels) so that the use of the adaptation scheme also leads to no performance gains. Thus, for the system under consideration, we find the uplink rate adaptation scheme to be advantageous when 200 m $\leq d_{RSU} \leq 800$ m.

3.5.3   IEEE 802.11p Uplink -TDMA Downlink (MAC C)

The attained maximum $TH_{\text{ul,I}}$ as calculated without imposing a packet delay limit, $TH_{\text{ul,I,max}}$, is used to calculate the uplink and downlink time periods configured within each frame. We have noted a corresponding attained optimum throughput value of $TH_{ul,I,max} = 104\,\text{Mbit/s}$ with the use of $R_{ul} = 24\,\text{Mbit/s}$ and $P_{tx,v} = 23$ dBm at $d_{\text{RSU}} = 100\,\text{m}$.

    The delay constrained aggregate uplink throughput $TH_{ul,I}$ performance behavior is shown on Figure 3.4. Results have been obtained through the execution of a NS-3 based simulation coupled with analytical evaluations. Under the Monte-Carlo simulation process, the uplink packet generation rate is gradually increased, leading to variations in the resulting uplink throughput rate $TH_{ul,I}$. The latter induces the packet arrival rate levels loading the RSU, as generated by the vehicles within RSU cell, from which the traffic intensity parameter ρ_{RSU} presented in Section 3.4.3 is analytically calculated. It is subsequently used to compute the ensuing end-to-end packet delay D_P. The realized uplink throughput rates $TH_{ul,I}$ under which the prescribed delay level is satisfied is shown in Figure 3.4. As expected, for this case, $TH_{ul,I}$

levels are less than their corresponding $TH_{ul,I,max}$ levels when delay and PDR constraints are imposed. The maximum delay-capped $TH_{ul,I}$ value achievable for $R_{ul} = 24\,\mathrm{Mbit/s}$ is equal to about $85\,\mathrm{Mbit/s}$ at $d_{\mathrm{RSU}} = 100\,\mathrm{m}$. A key factor impacting D_P is noted to be contributed mostly by the waiting time value incurred at the downlink queue at the RSU for downlink, and secondly by the delay incurred across the IEEE 802.11p-channel for uplink tranmsission, D_{ul}, and lastly by the latency values associated with packet transmission downlink. Under high traffic load, such as the load at which maximum throughput is realized, $TH_{ul,I,max}$, the downlink queueing delay and delay incurred for uplink operation are similar. As we increase d_{RSU} from 100 m to $150\,\mathrm{m}$, the rate of transit packet flows loading a RSU queueing system is noted to be reduced due to smaller $E[n_{span}]$. Hence, packets arriving to a RSU from its RSU cell are served at a higher rate. Consequently, the waiting time incurred by such packets at the RSU is improved. The throughput rate supported across each RSU cell uplink can consequently be allowed to increase (as packets can then be allowed to incur higher uplink delays). However, since the number of RSU cells, N_{RSU}, is reduced, the attained aggregate throughput rate is not expected to change in a noticeable manner, as confirmed by the depicted simulation results. Hence, the net delay gain achieved by the reduced $E[n_{span}]$ is not significant, while just a slight increase in the $TH_{ul,I}$ level is attained. As d_{RSU} is increased to $300\,\mathrm{m}$, the attainable $TH_{ul,I}$ values decrease, as lower SINR levels due to higher signal interference levels are observed, particularly for vehicles that reside close to the RSU cell boundary. Such mobile transmissions tend then to become more sensitive to simultaneous transmissions taking place outside its carrier sensing range d_{CS}, which is equal to about $346\,\mathrm{m}$ when $P_{\mathrm{tx}} = 23\,\mathrm{dBm}$, because the ratio of power received from an intended transmitter to the power received from interference decreases, in particular for vehicles which are located at the edge of RSU cell. The downlink throughput $TH_{dl,I}$ performance behavior for this scheme is similar to that of MAC A scheme.

The $TH_{ul,dl}$ performance behavior is shown in Figure 3.7. We have studied the setting of optimal pair of downlink data rate R_{dl} for each uplink R_{ul} and values in aiming to achieve the highest system throughput rate. These results have been obtained by using the
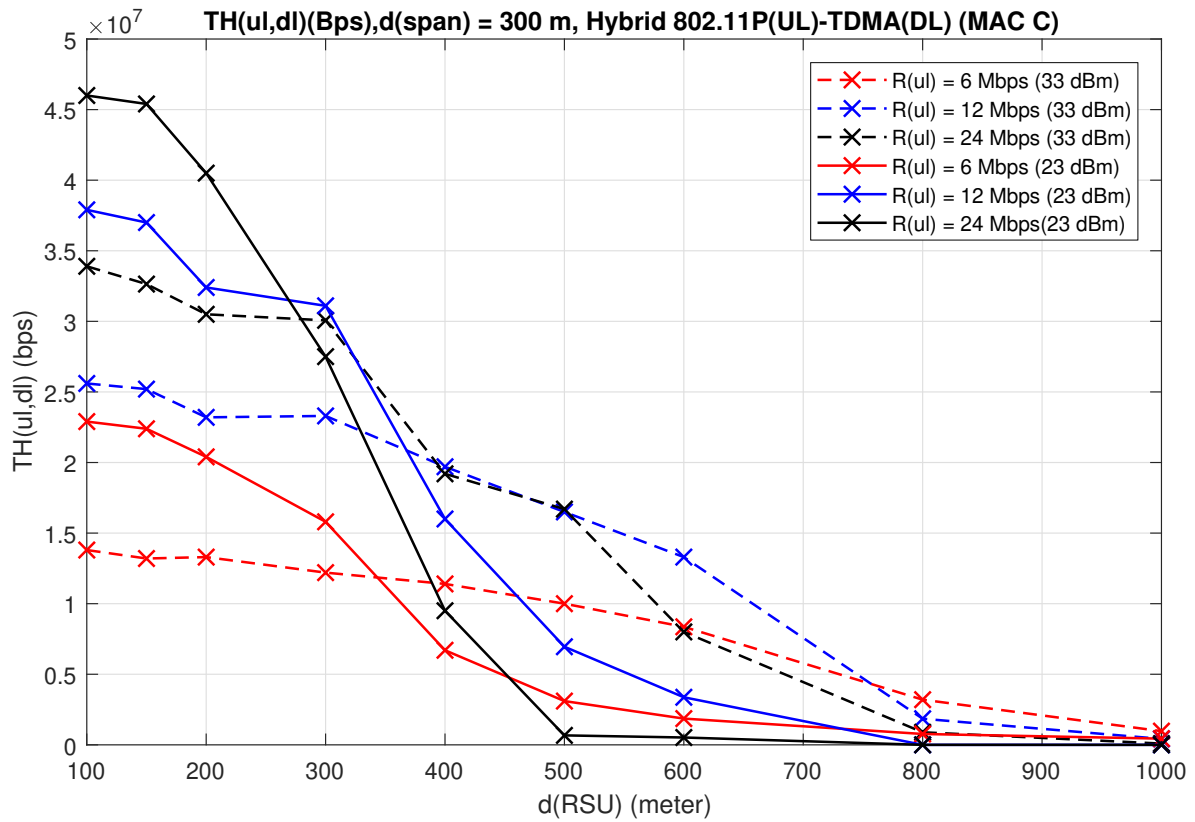
Figure 3.7: Delay-capped $TH_{\mathrm{ul,dl}}$ (bps) vs d_{RSU} (m) for MAC C

mathematical formula presented in Section 3.4.3, which includes parameters evaluated by using the NS-3 based simulation process for the isolated uplink transmissions coupled with the use of analytical calculations for the downlink system. As shown in Figure 3.7, the setting of $d_{\text{RSU}} = 100\,\text{m}$, $R_{\text{ul}} = 24\,\text{Mbit/s}$, $R_{\text{dl}} = 24\,\text{Mbit/s}$, $k_{dl} = 3$, and $P_{tx,r} = P_{tx,v} = 23$ dBm yields the highest delay-capped system throughput $TH_{\text{ul,dl}}$ value. The $TH_{\text{ul,dl}}$ value is not sensitive to changes in d_{RSU} when d_{RSU} is small (e.g. 100 m to 150 m); however, a significant drop is noticed at longer d_{RSU} ranges such as 300 m. The $TH_{\text{ul,dl}}$ values are insensitive when increasing d_{RSU} slightly from 100 m to 150 m as inducing a slight $TH_{\text{ul,dl}}$ decrease from 46 Mbit/s to 44 Mbit/s. The increase in d_{RSU} results in lower $E[n_{span}]$ by 1, implying the number of uplink load which can be served by each RSU increases. We note that low d_{RSU} values such as 100 m and 150 m have all vehicles within the range $d_{\text{CS}} < d_I + 0.5 d_{RSU}$ range. As explained in Section 3.4.2, this range indicates relatively high SINR levels at the edge of cell, when also considering low level of collisions within the carrier sensing range. However, the throughput gain is attenuated by the following reasons. The system spatial reuse for uplink transmissions is affected by d_{CS}, which is in the order of 340 m for $P_{tx,v} = 23$ dBm. Furthermore, we also note that at longer d_{RSU} ranges, N_{RSU} decreases and each RSU cell would need to support a higher number vehicles, leading to a higher collision level transmissions per RSU cell. As for downlink transmission, the setting of $d_{RSU} = 150$ m has lower $E[n_{span}]$ value by 1 than that of $d_{RSU} = 100$ m. In turn, setting $d_{RSU} = 150$ m yields an N_{RSU} value that is lower than that calculated for $d_{RSU} = 100$ m, which leads to lower aggregate data throughput and thus lessens the gain induced by the reduction in the $E[n_{span}]$ value.

A significant drop in the throughput rate is observed as d_{RSU} increases from 150 m to 300 m under $R_{ul} = 24\,\text{Mbit/s}$. This behavior is mainly due to the uplink performance using IEEE 802.11p. At $d_{\text{RSU}} = 300$ m, as explained in Section 3.4.2 , we find that $d_{CS} < d_I + 0.5 d_{RSU}$ and note that d_{CS} is insufficient to ensure support higher SINR requirement for operation at $R_{ul} = 24\,\text{Mbit/s}$.

The data throughput performance when using $P_{tx,v} = P_{tx,r} = 23$ dBm is higher than

using 33 dBm when d_{RSU} is short. For example, when $d_{RSU} = 100$ m and $R_{ul} = 24$ Mbps, both transmit power levels satisfy $d_{CS} > d_I + 0.5d_{RSU}$ (explained in Section 3.4.2), inducing carrier sensing range which is sufficiently long to satisfy minimum SINR requirements of R_{ul}. On the other hand, transmit power level of 23 dBm induces a shorter d_{CS}, which allows higher spatial reuse. However, when d_{RSU} is longer such as 300 m, using $P_{tx} = 33$ dBm yields higher data throughput than using 23 dBm. Using $P_{tx} = 33$dBm satisfies $d_{CS} > d_I + 0.5d_{RSU}$, while using $P_{tx} = 23$dBm induces carrier sensing which is too short ($d_{CS} < d_I + 0.5d_{RSU}$) to satisfy minimum SINR levels especially for vehicles nearing to the cell edge. More detailed trade-off between jointly setting R_{ul}, d_{RSU} and transmit power values in affecting throughput performance is demonstrated in Section 3.5.2 when discussing MAC B's performance behavior when using IEEE 802.11p.

Our performance evaluation results show that the attained maximum aggregate throughput values, for a given d_{RSU} are insensitive to variations in the number of active vehicles on the highway, provided the overall loading rate by vehicles in a RSU cell is controlled (so that the maximal allowed total offered loading rate is regulated) and mostly limited by the carrier sensing and random backoff mechanisms when the channel is highly busy.

3.6   Performance Comparison among the MAC Schemes

In Figure 3.8, we present the variation of the aggregate data throughput $TH_{ul,dl}$ attained by using the three MAC schemes, under delay and PDR constraints, as a function of the underlying inter-RSU distance d_{RSU}. Under each prescribed d_{RSU} value, for each scheme, we have set optimal values for the attained data rates and the respective coloring value to yield the best aggregate throughput performance for each scheme.

Under specified transmit power values, the MAC A scheme is noted to yield the highest throughput rate, under all d_{RSU} distance levels. It is followed by the MAC C scheme. The lowest throughput rates are attained when using the MAC B scheme. The highest throughput rate is attained by MAC A when configured at $R_{ul} = 24$ Mbps, $k_{ul} = 3$, $R_{dl} = 24$ Mbps,
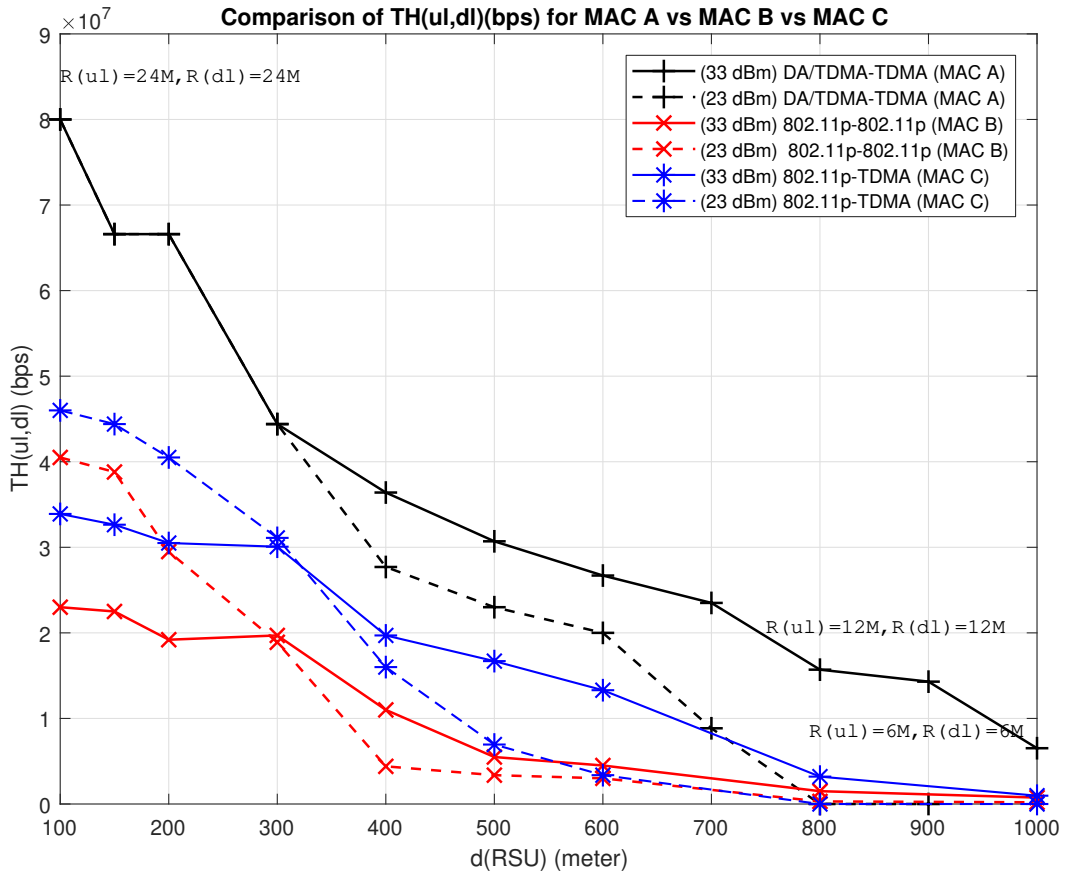
Figure 3.8: Comparison between MAC A, MAC B, MAC C : $TH_{\text{ul,dl}}$ (bps) vs d_{RSU} (m)

$k_{dl} = 3$ at $d_{\mathrm{RSU}} = 100\,\mathrm{m}$, which is equal to about 80 Mbps). While generally MAC C achieves higher data throughput than MAC B, the throughput differential is lower than that attained when comparing the throughput advantage realized by using MAC A. For all the MAC schemes, we note the corresponding increase in system throughput that is realized as the number of installed RSU nodes is increased. Yet, the throughput variation depends in a non linear manner on the prescribed d_{RSU} level. As an example, we note that MAC A's exhibited $TH_{ul,dl}$ values experience rapid degradation at shorter d_{RSU} ranges (i.e., shorter than 300 m) when compared with those incurred when longer d_{RSU} ranges are used (i.e., longer than 300 m). Especially, the use of a MAC A scheme is noted to be highly effective when implementing a high density backbone network whose density is incrementally increased (e.g., when the d_{RSU} is reduced from 300 m to 100 m).

3.7 Performance Comparison of Infrastructure-aided V2I and V2V Systems

Two different communication networking architectural modes are considered in this section. On one hand, we consider the system studied above, which employs a backbone of RSUs that provide full coverage of vehicles traveling along the highway segment. The system uses V2I and I2V wireless transmissions as well as the underlying fiber-optic backbone network to disseminate packet flows. It is labeled here as the "V2I" system. In contrast, we consider a system that employs no infrastructure, using vehicle-to-vehicle communications for disseminating packet flows, which is labeled here as the "V2V" system. We assume that for the "V2V" system vehicles are admitted into each lane to form platoons. Platoons move along the autonomous highway at prescribed speeds and inter-vehicular distances. Each platoon is managed by a Platoon Leader (PL) that serves to control and synchronize its platoon members. Under the architecture developed in [25], an algorithm is used to elect certain PLs to act as Backbone Nodes (BNs).

The BNs form a vehicular backbone network (Bnet), whereby the inter-BN distance is

denoted as d_{BN}. Vehicles associate with the nearest BN, or the one from which they receive the best signal, and are then identified as the clients of the latter BN. The client vehicles of a BN form the access network (Anet) of this BN. Packets produced by each vehicle are disseminated across this "V2V" network by first being transmitted across the corresponding Anet to its associated BN. Subsequently, packets are transmitted across the wireless Bnet to other BNs that reside in their dissemination span, and are simultaneously broadcasted for reception also by vehicles located in the corresponding Anets. The system forms a two layer hierarchical network that consists of a Bnet and several Anets. However, the architectural topology is not fixed; as vehicles travel along, enter or exit the highway, Anet and Bnet formations are dynamically re-synthesized.

We compare the performance behavior of the two architectures as a function of the following parameters. For the "V2I" network, we vary the infrastructure's d_{RSU} distance levels as well as the uplink and downlink transmission rates, R_{ul} and R_{dl} (and the corresponding coloring values, k_{ul} and k_{dl}, when applicable for MAC A and MAC C). For the "V2V" system, we vary the inter-BN distance d_{BN}, and the transmission rates across the Anet and Bnet sub-networks, R_{Anet} and R_{Bnet} respectively.

3.7.1 Performance Comparison of Infrastructure-aided V2I and V2V Systems Using TDMA

In Figure 3.9, we present the aggregate data throughput performance attained when using TDMA-based MAC schemes under "V2I" (DA/TDMA Uplink-TDMA Downlink) and "V2V" (DA/TDMA Anet-TDMA Bnet) modes, as d_{RSU} and d_{BN} are varied respectively. We set a higher transmit power level at the RSU nodes, $P_{tx,r} = 33$ dBm, while the transmit power by a vehicular node is lower, $P_{tx,v} = 23$ dBm.

We observe that generally the "V2I" system exhibits uniformly better performance behavior than that attained by the "V2V" system, under various d_{RSU} and d_{BN} distance ranges. The "V2I" system is noted to achieve aggregate data throughput values that are about 30%- 40% higher than those achieved by the "V2V" system, when setting for $d_{RSU} = d_{BN}$, assuming
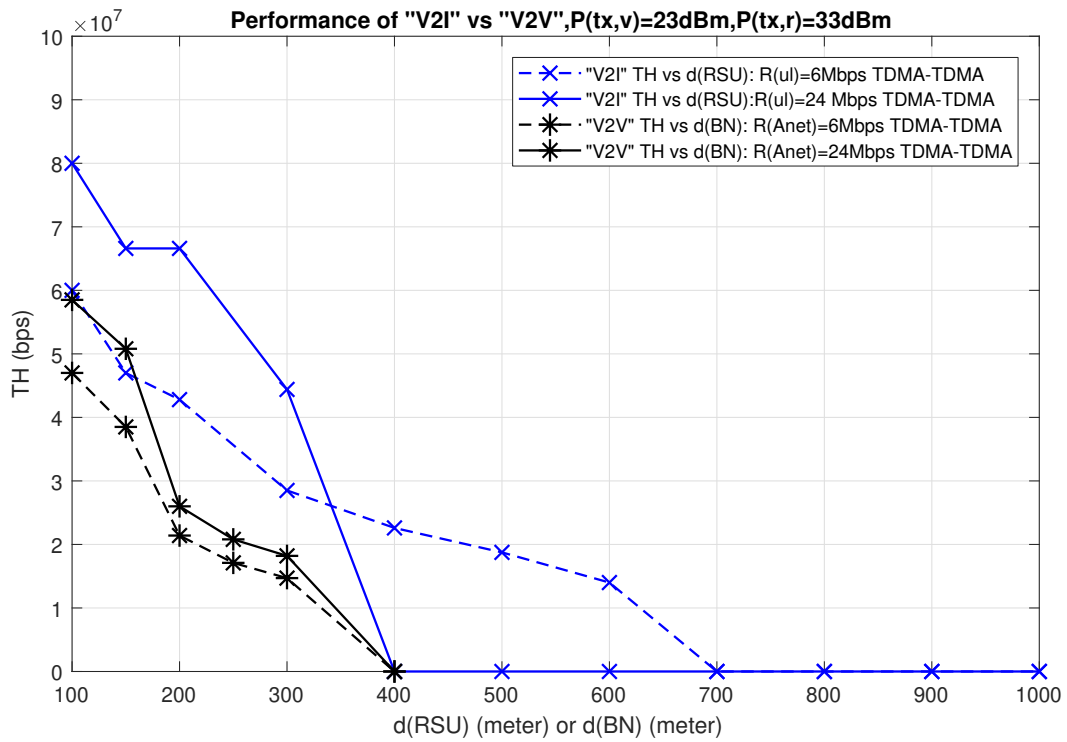
Figure 3.9: Data Throughput TH (bps) vs d_{RSU} for "V2I" (m) or d_{BN} for "V2V", using TDMA MAC schemes

the inter-RSU distances to be configured to values in the 100 m - 300 m range. For longer inter-RSU ranges, it is much more advantageous to employ a "V2I" system.

In aiming for a medium level data throughput of, say, 30 Mbps, when d_{RSU} is low, such as $d_{RSU} < 400$ m, such a data throughput level can be achieved by using the "V2I" system, by setting $R_{ul}=R_{dl}=24$ Mbps. In turn, under a sparse RSU infrastructure with $d_{RSU} \geq 400$ m, the designer can institute a "V2V" operation by grouping vehicles into vehicular formations (or platoons) such that $d_{BN} < 200$ m. This can be readily realized when the highway segment is quite loaded by vehicular traffic. Yet, under such conditions, if the backbone network is expanded so that one can place RSUs at relatively short inter-RSU distances, a much enhanced operation is realized, as we capitalize on the high data rate capacity of the backbone network and on the availability of RSU nodes that are placed at fixed known locations.

A higher data throughput level, no lower than 75 Mbps, assuming the underlying scenario and parameter levels, can be achieved only by using the "V2I" system, with RSU nodes set to fully cover the highway segment at $d_{RSU} < 150$ m. Under the considered "V2V" system, when the d_{BN} range assumes widely different values in a range of 100 m to 1000 m, the system is noted to achieve a data throughput rate that is no higher than 60 Mbps.

3.7.2 Performance Comparison of Infrastructure-aided V2I and V2V Systems Using IEEE 802.11p

The performance results comparison of the two systems are presented in Figure 3.10. We observe that in general the "V2I" systems exhibit uniformly better data throughput performance when compared with that obtained under the "V2V" system, when examining the throughput rate attained by each (under strict packet delay and PDR target levels) under prescribed $d_{RSU} = d_{BN}$ ranges. The "V2I" system is noted to achieve aggregate data throughput values that can be higher by up to 200% when a dense infrastructure backbone system is configured.
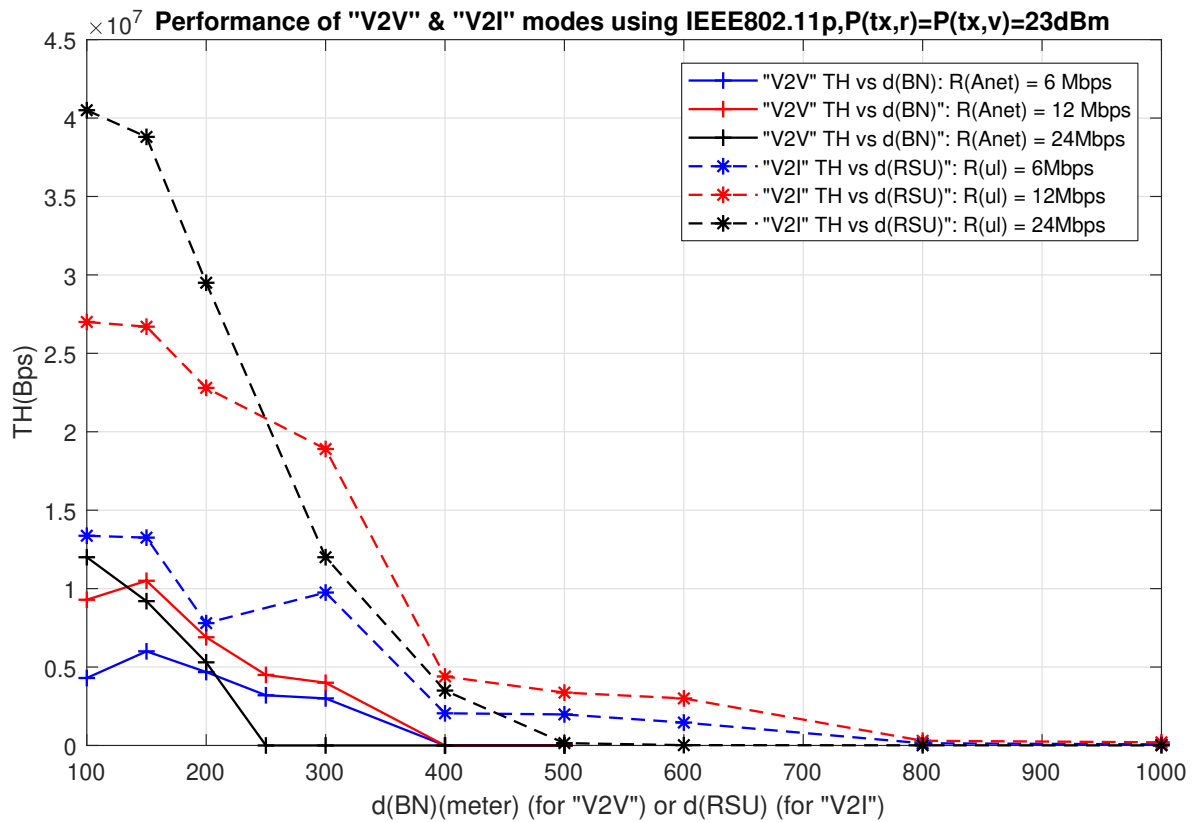
Figure 3.10: Data Throughput TH (bps) vs d_{RSU} for "V2I" (m) or d_{BN} for "V2V", using IEEE 802.11p

3.8 Concluding Remarks

In this study, we develop data networking schemes that are used to disseminate packet flows to and from highway vehicles. To aid in the dissemination process, a roadside backbone infrastructure is employed. It consists of RSUs that are interconnected through high speed point-to-point communication links. The infrastructure system provides communication coverage of all vehicles traveling along the underlying highway segment. We study the data throughput performance behavior of such an infrastructure aided network system, under prescribed packet delay and packet delivery ratio requirements, as a function of the density level of coverage provided by the infrastructure system. We study the data throughput performance behavior of the infrastructure aided network system as a function of inter-RSU distance levels. We determine the optimal setting of the network system parameters, including the values set for the uplink and downlink data rates, configuration of the MAC scheduling schemes for the uplink and downlink wireless channels, spatial-reuse factor values and transmit power levels. In evaluating the ensuing data throughput performance behavior, we require the dissemination and scheduling scheme to meet prescribed limits for packet delay and packet success reception rates.

When using TDMA-based MAC schemes for uplink and downlink channels (MAC A), we find that the system yields higher aggregate data throughput rates when shorter inter-RSU distance levels are employed, within limits. Yet, we demonstrate the corresponding dependence to exhibit a nonlinear functional behavior. When using IEEE 802.11p-based MAC schemes (MAC B and MAC C), it is interesting to note that when the infrastructure density is high, and when the transmit power range level is higher than a certain identified value, a higher throughput rate is achieved by setting a lower, rather than a higher, transmit power level. For example, when the inter-RSU distance is equal to 100 meters, a reduction in the transmit power level from 33 dBm to 23 dBm yields a 60% increase in the realized throughput rate level. In addition to presenting results that are based on simulation-based evaluations, we also develop an analytical approximation to calculate the effective setting of the transmit power level.

We have carried out performance comparisons between the different infrastructure-aided MAC schemes. Though we impose there 90-percentile packet delay and PDR limits for the TDMA schemes, we have shown the latter schemes to induce lower statistical variations than the IEEE 802.11p schemes, and thus exhibit throughput performance that is similar to that incurred under 95-percentile PDR and delay limit requirements. We note that while the use of controllers to assign uplink and downlink TDMA slots leads to enhanced throughput performance, it requires the design and operation of an extensive management subsystem. In turn, employing an IEEE 802.11p scheme allows the use of a less complex and dynamically auto-adaptive distributed system implementation, while generally inducing a lower throughput performance behavior.

We also compare the performance of the underlying infrastructure aided V2I system with that of a V2V based vehicular backbone network. The enhanced performance extent achieved by the V2I system is exhibited and characterized. Such an advantage is realized when a sufficient number of RSU nodes are placed along the highway segment. Otherwise, V2I communications can be integrated with V2V operation, as the latter is employed over highway portions that do not provide for communications with RSU nodes. For highway segments that are not fully covered by RSU nodes, a hybrid system that employs both V2V and V2I networking components can be used. The cross layer design of such a system, as well as of a system that jointly supports autonomous and non-autonomous vehicle nodes, are topics of ongoing studies.

3.9   Acknowledgment

This work was supported in part by a research grant provided by the UCLA Institute of Transportation Studies under the support of California SB1.

3.10   Credits

The contents of this chapter are partially based on the following articles:

- I. Rubin and Y. Sunyoto, "Infrastructure-aided Networking for Autonomous Vehicular Systems" In: Arai K., Bhatia R., Kapoor S. (eds) Proceedings of the Future Technologies Conference (FTC) 2019. FTC 2019. Advances in Intelligent Systems and Computing, Vol. 1070. ©Springer Nature Switzerland AG 2020

- Y. Sunyoto and I. Rubin, "Infrastructure-based Networking for Autonomous Transportation Systems Using IEEE 802.11p", 2019 IEEE Vehicular Networking Conference (VNC) (IEEE VNC 2019), December 2019, ©2020 IEEE

CHAPTER 4

Millimeter Wave Data Networking for Autonomous Vehicle Highway Systems

4.1   Introduction

As autonomous vehicle technologies rapidly progress, advanced developments are pursued for enhancing the communications and data networking performance of autonomous vehicle systems. An ultra reliable, robust and low-latency communications networking facility is essential for the support of safe and rapidly adaptive autonomous operations. This is of critical importance for the dissemination of safety messages and for the maintenance of platoon based vehicle formations. In turn, the availability of high data throughput rates is essential for maintaining the dissemination of sensor data and non-critical message applications. Using the mmWave band for both low latency and high throughput objectives is attractive as it offers wide spectral resources that are needed to support ensuing high data rates. Yet, mmWave signal propagation characteristics induce high blockage and related high attenuation levels. To enhance communications, directional antennas are employed, noting that smaller antenna array structures are implemented. In turn, high propagation attenuation levels coupled with the use of directional transmission links offer the opportunity to use scheduling schemes that employ more effective spatial reuse factors. It is noted, however, that the use of directional communications links tends to increase the underlying traffic loading rates when multicast data packet dissemination flows are considered. In this chapter of the dissertation, in considering data multicast disseminations of critical messages over mmWave bands, we present and study two networking algorithms: a RSU-aided multicast

101

dissemination protocol (RAMDA), and (for comparison purposes) a V2V based mmWave multicast dissemination protocol (V2VDA). RAMDA uses joint V2V and V2I mmWave data links, which carry data transmissions between adjacent vehicles on the same lane (identified as intralane transmissions), transmissions between vehicles on adjacent lanes (identified as interlane transmissions), uplink and downlink transmissions between vehicles and their associated RSUs, as well as RSU-to-RSU transmissions across the infrastructure backbone. In turn, communications links employed under the V2VDA scheme are used for V2V intralane and interlane transmissions. The major contributions of this work are as follows:

1. We evaluate the performance of RAMDA and V2VDA by considering several parameters, namely the inter-RSU distance, inter-vehicular distance, underlying modulation/coding scheme (MCS) and associated link data rate, the transmit power level and the antenna beamwidths used by RSUs and vehicles, as well as FDMA / TDMA based resource allocation medium access control (MAC) schemes and the employed and spatial reuse factors (SRFs).

2. We evaluate the delay-throughput performance of the system under the use of both algorithms. We aim to design a system operation that attains high throughput capacity in disseminating data packets over specified ranges, while meeting a Packet Delivery Ratio (PDR) of at least 95% and a 95-percentile packet latency requirement of 1 ms.

3. Our analyses show that when the RSU density is higher than an identified threshold level, the RAMDA scheme yields significantly better delay performance than that attained under the V2VDA protocol, while attaining comparable throughput capacity level. Using a RSU backbone network allows for significant reduction in the number of transmission hops experienced by a packet flow which is disseminated over wide ranging distance that can span multiple RSU-managed cell areas.

The chapter is organized as follows. In Section 4.2, we present an overview of related work. The network architecture, networking algorithms and system parameters, are presented in Section 4.3. In Sections 4.4 and 4.5, we present the involved scheduling and networking schemes and the results for our studies, displaying their performance characteristics. Conclusions are

drawn in Section 4.6.

4.2 Related Work

The authors in [55] have presented studies that evaluate beam matching of vehicles communicating on the highway, aiming to minimize the total packet delay. Data rates and beamwidths are used as parameters. The paper, however, does not assume geocast oriented dissemination, and does not employ a utility function that is based on the system's achievable throughput rate, while imposing a strict packet delay requirement, as done in this chapter. The authors in [25, 56, 57] study multicast/broadcast schemes using V2V dissemination protocols for linearly arranged vehicles. In [25], a vehicular backbone network is configured and used in aiding in the packet geocast dissemination. In contrast with the current chapter, multicast dissemination is attained by using non-directional data links in the sub-6 GHz band. In [56], the delay throughput performance of a mmWave broadcast TDMA based scheduling scheme is evaluated. In [57], the authors study IEEE 802.11ad-scheduled V2V transmissions for a two dimensional platoon, aiming to minimize the total transmission delay. When involving V2V flows, none of the above papers consider the setting of a proper scheduling spatial reuse factor and the use of a RSU infrastructure to aid in the packet dissemination process, as studied in this chapter.

The authors in [36, 58] study infrastructure-based mmWave data networking schemes, and their downlink/uplink data throughput performance behavior. The parameters considered include data rate, vehicular mobility, antenna beamwidths and alignment overhead. The authors in [36] also consider the base station (BS) density as a system parameter. However, both studies do not account for the multicast dissemination of vehicular data flows that employ joint V2I / I2V, V2V and RSU-to-RSU transmissions, as performed in our study. The authors in [48, 59] discuss multicast schemes which utilize both V2I and RSU-to-RSU transmissions, using TDMA and 802.11p based scheduling schemes, respectively. However, these studies assume the use of a sub-6 GHz band. The authors in [60] study a mmWave TDMA based scheduling scheme for Device-to-Device (D2D) or indirect D2D transmissions. The latter are
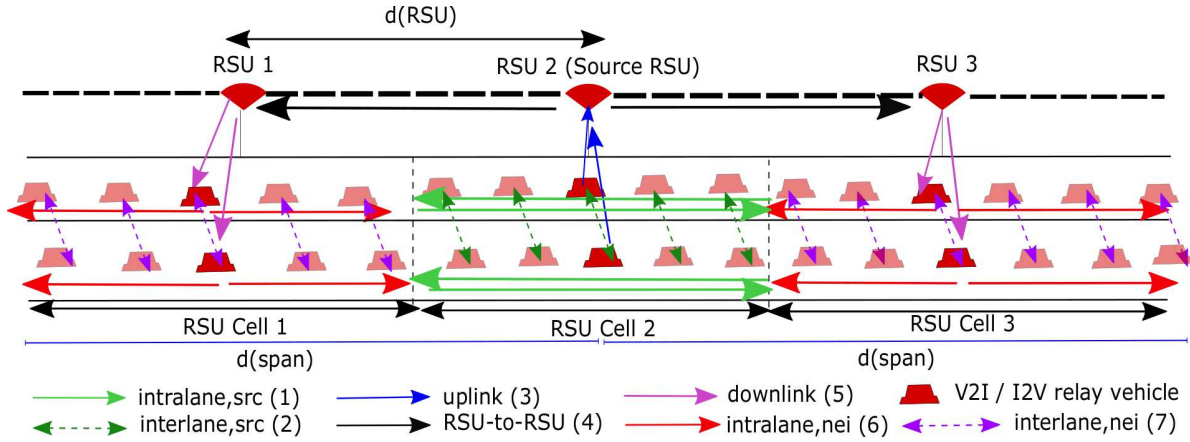
Figure 4.1: Infrastructure-aided Data Communications (RAMDA)

performed by using Device-to-Base Station (D2B) and BS-to-BS (B2B) links. However, it does not evaluate the delay vs. throughput system performance that can be realized when used to multicast data flows across a vehicular highway. The authors in [61] propose to use combined V2V and V2I / I2V for mmWave geocast. Directional mmWave V2V transmissions are used when the corresponding V2V link is not blocked. Otherwise, a RSU is used as a relay to transmit data packets to the next intended vehicular recipient. The study does not compare the delay-throughput performance behavior of such a RSU aided system with that of a V2V aided algorithm, when line-of-sight V2V links can be realized. Furthermore, the study does not incorporate RSU-to-RSU networking mechanism. In our study, the RSU backbone's density is a key system design parameter. We have identified no published studies that examine the setting of the system's PHY/MAC cross-layer configuration, when used for geocast data networking across mmWave links, aiming to achieve enhanced delay-throughput performance, as undertaken in this chapter of the dissertation.

4.3 Network Systems Model

4.3.1 Network Parameters

To illustrate the performance tradeoffs available to the designer under various network configuration options, our performance evaluations employ the following parameter values. RSUs are placed along the side of a linear two-lane highway segment of length L, forming a RSU backbone network. We denote the number of lanes as n_{lanes}. We assume an inter-RSU distance of d_{RSU}. The RSU nodes are interconnected by high-speed point-to-point (P2P) (e.g., fiber optic) links. Vehicles are assumed to be uniformly distributed along each lane at a distance D_v from one another. The number of vehicles admitted to each lane across the highway segment is denoted as N, where $N = \frac{L}{D_v}$. Vehicular speed is assumed to be equal to $v = 25$ m/s. The lane width is equal to 5 m. Our data networking algorithms employ a mmWave frequency of $f_c = 60$ GHz , assuming the overall bandwidth allocated for the underlying data networking system to be equal to $BW_{total} = 1$ GHz. Our networking schemes make use of spectral and/or temporal subdivisions of BW_{total} into distinct communication channels. The latter are employed to carry different types of data transmissions, including data transmissions among vehicles traveling along the same lane (intralane flows) and such that are transported between adjacent lanes (interlane flows), as well as data transmissions across uplink and downlink channels from/to RSUs. Each RSU is equipped with two mmWave radios, one aimed at a vehicle traveling along Lane 1 and the other at a Lane 2 vehicle. Each vehicle is equipped with five mmWave radios: one mounted at the front bumper (to communicate with the vehicle in front of it), another one is installed at the rear bumper (to communicate with a vehicle traveling behind it), two are mounted on the two sides of a vehicle (used to communicate with vehicles traveling on an adjacent lane) and one is installed on the rooftop [62, 61] (and used for uplink / downlink communications with RSUs). We assume vehicles and RSUs to use Uniform Planar Array antennas[63, 36]. For simplicity, we use a sectorized antenna model [64], and assume the same main lobe beamwidth value, θ, for all data transmissions. The antenna main lobe gains for the transmitter, G_t, and the

105

receiver, G_r, are expressed as $G_t = G_r = \frac{4\pi}{\theta^2}$ [65]; the side lobe gains are approximately set as zero. The effective gain of a transmitter - receiver pair is denoted as $G_{t,r}$. RSU antennas and vehicular antennas used for V2V networking processes are placed at a height of $h_{bs} = 25$ m and $h_{ut} = 1.5$ m, respectively [63]. The beam alignment delay, τ, is computed as $\tau = \frac{\psi_t \psi_r}{\theta_t \theta_r} T_p$ [55, 66], where ψ is the sector level beam-width and T_p is the pilot transmission time. Other beam forming strategies are described in [67].Beam alignment is performed periodically, whereby the period duration is denoted as T_{total}. The latter consists of the data transmission period T_{data} supplemented by τ (i.e., $T_{total} = T_{data} + \tau$). We use ω to denote the fraction of time that a link is used for data transmission, $\omega = 1 - \frac{\tau}{T_{total}}$. For intralane, interlane, uplink and downlink transmissions, we use the notations ω_{intra}, ω_{inter}, ω_{ul}, ω_{dl}, respectively. For illustrative purposes, we assume for all data links $\psi = 90°$ [64] and $T_p = 20\mu s$ [66]. To ensure continuous connectivity, we also assume that $T_{data} = T_L = \frac{d_{beam,V2I}}{v}$, where T_L represents the time it takes a vehicle to lose beam coverage, as it relates to the V2I / I2V links associated with the corresponding induced shortest beam projection over a distance range of $d_{beam,V2I}$. We use the underlying geometry to calculate a lower bound on the corresponding beam alignment interval. These are conservative computations, as we note that intra-lane links are expected to often assume lower beam alignment overhead ratios due to the fixed relative positions of neighboring vehicles that may move in platoon formations. The average noise power measured at a receiver is equal to P_n, and is calculated based on the noise spectral density N_0. The path loss (PL) model and corresponding shadow factor (SF) for uplink/downlink (V2I) [68, 63] and V2V [69, 63] are shown on Table 4.2. Each data link j belongs to one of the following link types: intralane, interlane, uplink, or downlink. The configured data link j spectral efficiency and the bandwidth level allocated to this link is denoted as η_j and BW_j, respectively. The corresponding data rate value is computed as $R_j = BW_j \eta_j = BW_j \log_2(1 + SINR_j)$, where $\sum_j BW_j = BW_{total}$, and $SINR = \frac{G_{t,r} P_{tx}/PL(d)}{P_n + \sum_i G_{i,r} P_{tx}/PL(d_i)}$, where d is the distance between a receiver and its intended transmitter, d_i is the distance between a receiver and an interfering node i, P_{tx} is the transmit power level used by vehicular and RSU nodes. For illustrative simplicity, we assume $P_{tx} = 27$ dBm [63]. The network parameters are summarized in Table 4.1.

Table 4.1: Network Parameters

L	5 km	P_{tx}	$\leq$ 27 dBm	f_c	60 GHz
d_{RSU}	50–1000 m	N_0	-174 $\frac{\text{dBm}}{\text{Hz}}$	BW_{total}	1 GHz
θ	5°-90°	d_{span}	1000 m	D_v	10-100 m

Table 4.2: Millimeter Wave Path Loss Models

PL_{V2I}^{LOS}	$28 + 22\log_{10} d + 20\log_{10} f_c$, if $10 \leq d \leq d_{bp}$
	$28 + 40\log_{10} d + 20\log_{10} f_c - 9\log_{10} C$, $d \geq d_{bp}$
	SF = 4 dB , $d_{bp} = 2\pi h_{bs} h_{ut} f_c/(3 \cdot 10^8)$
	$C = (d_{bp}^2 + (h_{bs} - h_{ut})^2)$
PL_{V2V}^{LOS}	$32.4 + 20\log_{10}(f_c d)$, SF = 3 dB
PL_{V2V}^{NLOS}	$\text{PL}_{V2V}^{LOS} + 5 + \max(0, 15\log_{10}(d) - 41)$, SF = 4 dB

4.3.2 Performance Metrics

We carry out our performance analysis and design evaluations under the assumption that vehicular nodes produce message flows that can consist of a mix of critical and non-critical packets. The aggregate system throughput capacity metrics $TH_{C,system}$ and $TH_{C,v}$ represent the total supported rate of data packet flows generated by all source vehicles and by each vehicle, respectively, where each packet flow must be disseminated to all vehicles traveling within a targeted dissemination span of d_{span} along the vehicle's forward and backward directions (for a total dissemination span of $2d_{span}$) on both lanes. The aggregate system throughput, TH_{system}, identifies the throughput rate of admitted packets, accounting only for those packets that are correctly received by at least 95 % of the vehicles traveling within d_{span} (i.e., PDR $\geq$ 0.95). A fraction of this throughput rate can be employed for the support of packets that belong to specific packet classes for which we further impose a packet delay requirement. For example, for packets that belong to a critical packet class, which are granted higher priority, the imposed delay requirement is such that we limit the throughput rate of such packet flows to the maximal value that assures that such packets incur a delay level D_P that is not higher than $D_{P,max} = 1$ ms for at least 95 % of the (successfully end-to-end

disseminated) packets belonging to this class [70]. Non critical packets are accommodated at the highest feasible packet throughput rate that induces a less strict packet delay bound, or no delay constraint at all. All throughput metrics are normalized to a single lane. For illustrative purposes, we assume the packet length (P) to be equal to 5000 bits.

4.3.3 Network Architecture

A HSM is employed. It exchanges status information with the RSUs. The later gather system situational data about the highway segment's vehicles through continuous message exchanges that are carried out across the control channel. A control channel is used for RSUs and vehicles to exchange key up-to-date status data, such as vehicular location coordinates, speeds, destination objectives, channel quality indices, radio and channel states, available processing rates and transmit power resource capabilities. We assume that a sub-6 GHz band is used for the control channel, as well as for the transport of system management data [71, 67]. As a vehicle travels along the highway, it proceeds to associate with the RSU from which it receives mmWave radio signals at the highest quality. It then becomes a client of this RSU and a member of its corresponding cell. For analytical simplification, we assume RSU cells to be disjoint, as illustrated in Figure 4.1, though our approach and protocols readily apply to realistic scenarios under which cell areas tend to well overlap. Each RSU manages a RSU cell, whose boundary envelopes a range of $d_{RSU}/2$ from the RSU, which consists of $N_v = \frac{d_{RSU}}{D_v}$ vehicles. The HSM communicates its system management data (including spectral/temporal communications channel sharing, scheduling oriented resource allocations and traffic management and autonomous mobility commands) to the RSUs. The latter communicate these commands to their client vehicles. Such commands are also used to announce the election of vehicular relay nodes.

4.3.4 Networking Protocol

4.3.4.1 RSU-aided mmWave Networking Dissemination Algorithm (RAMDA)

RAMDA's networking protocol uses elected vehicular gateways nodes that act as relays that aid in the dissemination of packet flows. Across each lane, relative to each RSU node, a vehicle that is determined by the area manager to monitor the strongest mmWave uplink and downlink SINR levels in relation to communications to/from the associated RSU node, is commanded to act as a temporary V2I relay node and a I2V relay nodes, respectively.To simplify the description, we assume hereby channel reciprocity for uplink and downlink transmissions, so that the same vehicular node is elected to act as both the I2V and V2I relay node for its RSU managed cell. This relay is often the mobile that has the shortest distance from its RSU. For computational simplicity, we have assumed the latter case in the calculations carried out in this chapter. The key elements of this protocol are noted as follows, and are illustrated in Figure 4.1.

1. A source vehicle transports its packets to neighboring vehicles in both forward and backward directions (the number of directions, n_{dir}, is equal to 2), by transmitting its flow packets over N_v V2V hops, aiming to reach all vehicles within its RSU cell. We allow certain vehicles that are located in an adjacent cell to receive at times spillover packets.

2. Upon receiving such intra-lane packets, each vehicle either aggregates them and transmits the aggregate message, or immediately transmits every packet to a vehicle on the other lane that it determines (through signal monitoring) to have the highest communications quality reception from it, which is often the one that is closest to it. For illustrative purposes, we use the latter approach (i.e., no packet aggregation for data transmissions over any link). This enables information exchange / dissemination between vehicles on Lane 1 to Lane 2 and vice versa.

3. Within each cell, the elected V2I relay vehicle on each lane transmits uplink the data packets that have been disseminated (intra-lane) across its cell, including packets generated by source vehicles traveling along the same lane, to its associated RSU node. We have also

studied an alternative scheme under which each vehicle transmits such packets directly to its associated RSU, using distinct uplink frequency bands. Our performance analyses have shown that such an uplink operation tends to generally yield as good or somewhat better delay-throughput performance behavior. However, we note that the latter scheme involves the use of more complex beam alignment procedures.

4. An RSU node that receives a packet flow from a gateway V2I relay node located in its cell proceeds to disseminate these packets to neighboring (forwarding) RSUs across the RSU backbone on a multihop basis to cover the dissemination span. The number of involved neighboring RSUs is $n_{RSU} = 2\frac{d_{span}}{d_{RSU}} - 1$ (which follows by noting that each RSU does not transmit downlink packets which it has received from its cell or from adjacent RSU cell by V2V transmissions). At times, the selection of forwarding RSUs may induce packet receptions by vehicles that reside beyond d_{span}. Depending on the underlying application, the receiving mobile may filter unwanted messages by using location identifiers.

5. Upon receiving packets from n_{RSU} other RSU nodes, a RSU will transmit them downlink across its allocated I2V channel, aiming for reception by the elected I2V relay. The RSU transmits downlink to Lane 1 and to Lane 2 relays only those respective packets that have been received from Lane 1 and Lane 2 sources, respectively, when considering packets received at the RSU from neighboring RSU cells. As an alternative, we have also studied a scheme under which each RSU transmits downlink by using a wide beamwidth so that its packets are multicasted in a single transmission to all intended mobiles residing in its cell. Our analyses have shown that generally the use of narrow beam leads to better delay-throughput performance behavior.

6. The I2V relay located on each lane forwards only its lane-specific data messages, using multihop V2V intralane transmissions in aiming to reach all vehicles situated within the same cell along its forward and backward directions, traversing in each direction as many as $0.5N_v$ vehicles.

7. Upon receiving packets from the I2V relay through intralane multihop transmissions, each

vehicle then relays these packets to a corresponding vehicle (in a similar manner as in Step 2) located on an adjacent lane (interlane flows). Eventually, in this manner, packet flows are disseminated to all vehicles that reside within d_{span}.

4.3.4.2   V2V aided Networking Algorithm (V2VDA)

A source vehicle transmits its data packets, in both directions, if applicable, to its neighboring vehicles. The packets are then disseminated in a multihop V2V manner, covering $n_{hops,V2V} = \frac{d_{span}}{D_v}$ hops in each direction, without resorting to the use of any RSU oriented transmissions. Each vehicle along the dissemination route transmits the packets that it receives in this manner to a corresponding (typically, the nearest) vehicle traveling on another lane.

4.4   FDMA/TDMA based Medium Access Control (MAC) Scheduling and Resource Allocations

4.4.1   Scheduling for RAMDA

In this section, we present the scheduling method used by RAMDA and perform the ensuing resource allocations. Resources are allocated on a FDMA basis to uplink and downlink channels. Also, intra-lane (and similarly inter-lane) transmissions are performed by using distinct frequency bands for each direction of flow dissemination. In turn, other communications links involved in the flow dissemination process are shared on a TDM/spatial-TDMA basis. To achieve high throughput efficiency across the dissemination path, we allocate resources in a manner that enhances the bottleneck links induced across each path, leading to the following resource allocations.

1. For intralane transmissions within a source RSU cell, we assume that each V2V front and rear radio is simultaneously active in transmit and receive modes by using two corresponding distinct frequency bands (i.e., frequency division duplex), each having an allocated bandwidth of $BW_{intra,ori,1dir}$. For each intra-lane transmission direction (Section 4.3.4.1 Step 1),

111

scheduling is done by using a TDM/TDMA scheme and employing a spatial reuse factor (SRF) of M_{intra}, so that each link is shared on a TDM basis. Packets that belong to a given flow are transmitted simultaneously in time across different links on a reuse-M spatial TDMA basis. We assume that intralane transmissions executed on both lanes occur simultaneously in time in a highly directional manner so that no (or minor) inter-lane signal interference is induced.

2. Interlane links residing within the source RSU cell, with identified transmission direction (Section 4.3.4.1 Step 2) are each allocated a bandwidth of $BW_{inter,ori,1dir}$. Adjacent interlane links share resources on a TDMA basis, using a SRF of M_{inter} (Table 4.3 Item 2).

3. Adjacent uplink transmissions share resources on a TDMA basis using a SRF of M_{ul}. The V2I relay elected on each lane (Section 4.3.4.1 Step 3) is allocated an uplink bandwidth value of $\frac{BW_{ul}}{n_{lanes}}$, so that a total of BW_{ul} is allocated for uplink transmissions (Table 4.3 Item 3). For illustrative purposes, we assume a uniform traffic matrix. Hence, half of the intralane traffic arriving at the V2I relay node originates from vehicles located in adjacent RSU cells and is excluded from using the uplink.

4. RSU-to-RSU transmissions are carried out by using P2P links. They are assumed to have sufficient capacity and their bandwidth is not included in BW_{total}.

5. Each RSU downlink, per destination lane (Section 4.3.4.1 Step 5), is allocated a bandwidth level of $\frac{BW_{dl}}{n_{lanes}}$. Downlink transmissions by adjacent RSUs targeted to I2V relays situated on the same lane share resources on a TDMA basis with a SRF of M_{dl} (Table 4.3 Item 5).

6. To forward packets from the I2V relay (Section 4.3.4.1 Step 6), each intralane direction within forwarding RSU cells is allocated a shared bandwidth of $BW_{intra,nei}$. The TDMA SRF is set to M_{intra} (Table 4.3 Item 6).

7. Interlane transmissions within forwarding RSU cells (Section 4.3.4.1 Step 7) are assigned, for each inter-lane direction a bandwidth of $BW_{inter,nei,1dir}$, and configured a TDMA SRF of M_{inter} (Table 4.3 Item 7).

Table 4.3: Resource Allocation

(2)	$\dfrac{BW_{inter,ori,1dir}}{n_{dir}BW_{intra,ori,1dir}}$	$= \dfrac{\omega_{intra}\eta_{intra}/M_{intra}}{\omega_{inter}\eta_{inter}/M_{inter}}$
(3)	$\dfrac{BW_{ul}/n_{lanes}}{BW_{intra,ori,1dir}}$	$= \dfrac{0.5n_{dir}\omega_{intra}\eta_{intra}/M_{intra}}{\omega_{ul}\eta_{ul}/M_{ul}}$
(5)	$\dfrac{BW_{dl}/n_{lanes}}{BW_{ul}/n_{lanes}} = \dfrac{BW_{dl}}{BW_{ul}}$	$= n_{RSU}\dfrac{\omega_{ul}\eta_{ul}/M_{ul}}{\omega_{dl}\eta_{dl}/M_{dl}}$
(6)	$\dfrac{BW_{intra,nei}}{BW_{dl}/n_{lanes}}$	$= \dfrac{\omega_{dl}\eta_{dl}/M_{dl}}{\omega_{intra}\eta_{intra}/M_{intra}}$
(7)	$\dfrac{BW_{inter,nei,1dir}}{BW_{dl}/n_{lanes}}$	$= \dfrac{\omega_{dl}\eta_{dl}/M_{dl}}{\omega_{inter}\eta_{inter}/M_{inter}}$

We note that induced by the FDMA allocation applied to different transmission directions employed across intralane, interlane and V2I / I2V links, minimal interference is incurred between signals transmitted across distinct directions. Similar spatial reuse methods are described in [60]. Since each vehicle's front and rear radios operate the intralane transmissions as transmitting source vehicle and as forwarding vehicle as well as a receiver of packets, intralane transmissions bandwidth components are not shared. Hence, $BW_{intra} = n_{dir}(BW_{intra,ori,1dir}) + BW_{intra,nei}$. Similarly, each vehicle's side radio must transmit and receive lane packets (within source and non-source RSU cells, so that the corresponding interlane spectral resources are not reused; hence, $BW_{inter} = n_{lanes}(BW_{inter,ori,1dir} + BW_{inter,nei,1dir})$. Each RSU is assumed to use a single radio module to receive uplink packets and to transmit downlink ones, so that uplink and downlink frequency bands are not reused. The effective shared bandwidth level is set as :

$$BW_{total} = \max(BW_{intra}, BW_{inter}, BW_{ul} + BW_{dl}) \tag{4.1}$$

The resource allocation process can induce excess bandwidth levels that become available at times in a particular transmission direction, which can be be reserved for the improved dissemination of safety messages (e.g., critical status alarms). The aggregate throughput capacity $TH_{C,system}$ is calculated as follows :

$$TH_{C,system} = NTH_{C,v} = \frac{L}{D_v}\frac{\omega_{intra}\eta_{intra}BW_{intra,ori,1dir}}{M_{intra}N_v} \tag{4.2}$$

To provide guaranteed quality of service, we assume that the regional manager provides vehicles with flow control pacing-threshold levels. Source vehicles use these levels to implement

a flow control and admission control mechanism, which includes a pacing operation. The time intervals between subsequent packet transmissions are configured at each source vehicle to be not shorter than this specified threshold level. In this manner, the traffic loading process of the system is deterministically controlled. Incorporating the assumed flow control operation, we use an approximation approach for the computation of the packet delay metric. We calculate D_P to represent a conservative estimate of the 95-percentile end-to-end packet delay, expressing it as the sum of two components, $D_P = W_P + T_{tx}$. The first component is the 95-percentile waiting time incurred by a packet while being queued at its source vehicle prior to its transmission across the system. The second component, T_{tx}, is set equal to the maximum time latency that a packet incurs in traversing its dissemination route, measured from the instant that it is transmitted by its source vehicle (following its queueing delay) to the time that it is received by the farthest vehicle located along its dissemination path.

To illustrate the behavior of the queueing delay component, we calculate W_P by modeling the source mobile queueing process as that induced by a M/M/1 queueing system. Consequently, we have: $W_P = \max(0, \frac{\ln(\rho/0.05)}{\mu(1-\rho)})$. The packet arrival process at each source node from its underlying application layer is modeled with Poisson process. We denote the packet arrival rate to the system as λ [packets/unit time]. As explained above, the service rate provided by the flow controlled queueing system model to its packets, denoted as μ [packets/unit time], is set by the system manager to be equal to the peak rate at which the source vehicle is allowed to feed packets into the system ($\mu = \frac{TH_{C,v}}{P}$). The maximum packet load rate (per each packet class type) must then be limited so that accommodated packets experience a delay value that satisfies the prescribed level. The traffic intensity parameter ρ measures the ratio of the admitted packet arrival rate (λ) to the vehicle's service rate (μ). Using the calculated loading rate that induces acceptable packet delay level, we calculate the realized (maximal) traffic intensity level ρ. Assuming all active source vehicles to be loaded at the same level at the packet traffic admitted rate, we note the corresponding system throughput level to be equal to $TH_{system} = \rho TH_{C,system}$.

We can readily show that we have set the source pacing operation, allocated bandwidth

resources to the route links, and configured the links' scheduling schemes and spatial reuse factors in a manner that guarantees packets that traverse the network route (after transmission by their source vehicles) to experience deterministically bounded delays.

For conservative design, we consider a packet which is disseminated across a relatively long end-to-end route in a pipelining fashion with queueing delay experienced only at the source node. The latter route involves a source node that is located fathest from the I2V relay within the same lane and a destination node that is located on the farthest away lane and farthest away from the end-route RSU. Then, $T_{tx} = t_{intra,ori} + t_{inter,ori} + t_{ul} + t_{dl} + t_{intra,nei} + t_{inter,nei}$. In the following computation, all transmission time values include the associated worst case frame latencies. The transmission times incurred across each intralane and interlane link embedded within the source RSU's cell, $t_{intra,ori}$ and $t_{inter,ori}$, are equal to $\frac{(M_{intra}-1+N_v)P}{\omega_{intra}R_{intra}/n_{dir}}$ and $\frac{M_{inter}P}{\omega_{inter}R_{inter,ori,1dir}}$, respectively. The transmission times incurred across an uplink and a downlink, t_{ul} and t_{dl}, are equal to $\frac{M_{ul}P}{\omega_{ul}R_{ul}/n_{lanes}}$ and $\frac{M_{dl}P}{\omega_{dl}R_{dl}/n_{lanes}}$, respectively. The transmission time across each intralane and interlane link within a neighboring RSU cell are denoted as $t_{intra,nei} = \frac{(M_{intra}-1+N_v)P}{\omega_{intra}R_{intra}/n_{dir}}$ and $t_{inter,nei} = \frac{M_{inter}P}{\omega_{inter}R_{inter,nei,1dir}}$, respectively.

4.4.2 Scheduling for V2VDA

The ratio of allocated bandwidths for intralane and interlane transmissions is given as $\frac{BW_{inter,1dir}}{BW_{intra,1dir}} = \frac{n_{dir}\omega_{intra}\eta_{intra}/M_{intra}}{\omega_{inter}\eta_{inter}/M_{inter}}$. Frequency bands are re-used across intralane and interlane transmissions, so that $BW_{total} = \max(BW_{intra}, BW_{inter})$, where $BW_{intra} = n_{dir}BW_{intra,1dir}$ and $BW_{inter} = n_{dir}BW_{inter,1dir}$. We have $TH_{C,system} = \frac{L}{D_v}\omega_{intra}\frac{\eta_{intra}BW_{intra,1dir}}{n_{hops,V2V}M_{intra}}$. The computation of D_P is performed in a similar manner to that used under RAMDA.

4.5 Performance Behavior

To illustrate the system's performance behaviors, we use the following parameter values: $v = 25$ m/s, $D_v = 10$ m; d_{RSU} values that are equal to 50 m, 200 m, 300 m and 500 m; $L = 5$ km, and $d_{span} = 1000$ m. We assume $\theta = 10°$, which yields a 4 % alignment overhead. For

other design cases, when we use narrower and wider beamwidth values, such as $\theta = 5°$ and 20°, respectively, $TH_{C,system}$ is noted to attain significantly lower levels than that obtained when using $\theta = 10°$, when considering the underlying trade-off involving on one hand the attained data rate and on the other hand the corresponding beam alignment overhead. We select M_{intra} value by carrying out detailed analytical and simulation based performance evaluations of a system in isolation (from the remainder link types) that involves multihop intralane transmissions over d_{span}. A lower M_{intra} level induces higher interference signals at the intended receiving node but in turn yields a higher spatial reuse level. Our analyses have determined that the setting of $M_{intra} = 1$ yields the best data throughput performance, and will thus use this spatial reuse value for the setting of the systems that we discuss in the following. Under our system configuration assumptions, no interbeam interference is produced for adjacent directional interlane, uplink and downlink transmissions when using $\theta = 10°$. Our illustrative performance evaluations hence use $M_{inter} = 1$, $M_{ul} = 1$ and $M_{dl} = 1$.

In Figure 4.2, we exhibit the system's delay throughput (i.e., D_P vs. TH_{system}) performance behavior under the use of the RAMDA scheme, assuming as parameters several RSU density levels (which are inversely related to d_{RSU}), and that of V2VDA scheme. We have also conducted Monte Carlo simulations for the V2V segments executed under both schemes. Each curve in Figure 4.2 is produced by monotonically increasing the admitted packet flow rate, represented by the parameter λ, as included in our packet delay performance formulas. The admitted packet arrival rate is increased up to a point at which the induced system's throughput reaches the system's throughput capacity level ($\lambda < \frac{TH_{C,system}}{P}$).

In comparison with our analytical evaluations, we have noted that the realized throughput capacity values obtained through simulations to be lower by about 5%. In turn, when considering higher priority messages, which load the system at a rate that is typically lower than 50% of the system's capacity, we have noted our simulations to yield mean message delay results that are very close to those obtained via the mathematical model presented in this chapter. Simulation based 95-percentile message delay results have been noted to be lower than our corresponding conservative analytical results by less than a factor of 2.5 to 1.
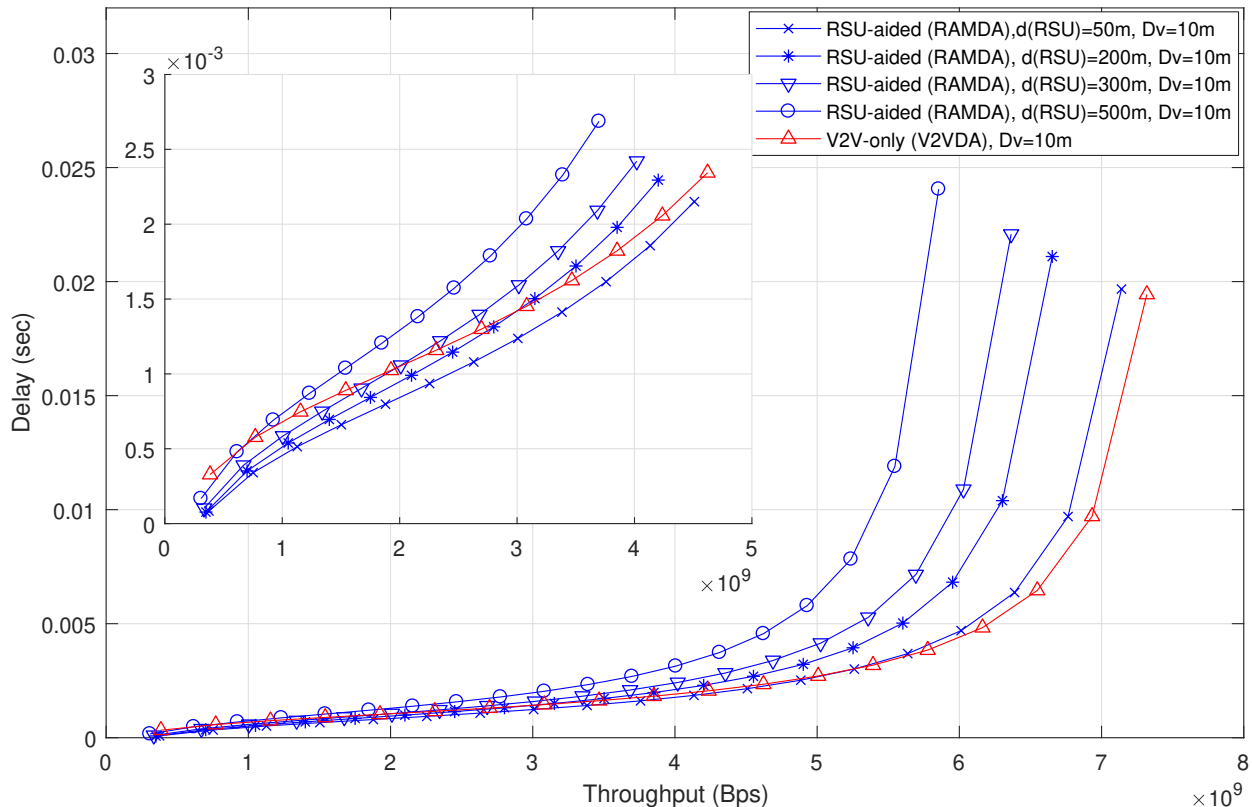
Figure 4.2: Delay (s) vs. Throughput (bps) for RAMDA and V2VDA

This confirms the analytical M/M/1 queueing model as serving to yield an upper bound on the packet delay performance.

Figure 4.2 shows that when we increase d_{RSU} from 50 m to 500 m, $TH_{C,system}$ of RAMDA, remains relatively unchanged. We find that according to Equation 4.1, when the d_{RSU} is relatively short such that the n_{RSU} term dominates, the d_{RSU} term effectively cancels out and thus the throughput performance is relatively insensitive to changes in the d_{RSU} values. This can be explained as follows. By setting $n_{lanes} = 2$ and $n_{dir} = 2$, under our illustrative parameter values, we obtain $BW_{total} = BW_{intra,ori,1dir} \max(n_{RSU} + 2, 2\frac{\omega_{intra}\eta'_{intra}}{\omega_{inter}\eta'_{inter}}(n_{RSU} + 2), 2\frac{\omega_{intra}\eta'_{intra}}{\omega_{ul}\eta'_{ul}} + 2n_{RSU}\frac{\omega_{intra}\eta'_{intra}}{\omega_{dl}\eta'_{dl}})$. We note that the intralane bandwidth BW_{intra} term is a dominant factor in determining the required value of BW_{total} (Equation (4.1)), due to the low spectral efficiency realized for intralane transmissions. The latter is induced by the presence of signal interference caused by transmission performed by nearby vehicles (noting

117

that $\eta_{intra} = 3.08$ bps/Hz, whereas $\eta_{inter} = 25$ bps/Hz, $\eta_{ul} = 20.8$ bps/Hz and $\eta_{dl} = 22.2$ bps/Hz). Thus, $BW_{total} = BW_{intra,ori,1dir}(n_{RSU} + 2)$.

The system throughput $TH_{C,system}$ is inversely proportional to $n_{RSU} + 2 = 2\frac{d_{span}}{d_{RSU}} + 1$, and is inversely proportional to $N_v = \frac{d_{RSU}}{D_v}$. When $\frac{d_{RSU}}{d_{span}} \ll 1$, $TH_{C,system}$ is relatively independent of d_{RSU}. At shorter d_{RSU} (and thus higher RSU density values), each cell accommodates a lower number of vehicles N_v. Consequently, on one hand, each RSU cell must forward and transmit downlink data traffic that it receives from a higher number of neighboring RSUs. On the other hand, each source flow shares its cell resources with a lower number of mobiles and is thus granted higher bandwidth resources. A mild dependence on d_{RSU} is induced in part by a quantization factor impacting the number of RSUs involved in the dissemination process; it is more amplified under longer d_{RSU} levels. $TH_{C,system}$ attained by the V2VDA scheme is similar to that achieved by the RAMDA scheme. This is caused by the efficient reuse of frequency resources realized between intralane, interlane, and V2I / I2V transmissions. Under this underlying spectral reuse scheme, RAMDA's uplink and downlink transmissions do not require additional bandwidth resources when compared to the resources allocated under the V2VDA scheme. This is noted to be the case as the intralane bandwidth BW_{intra} term is a dominant factor in determining the required value of BW_{total} (Equation (4.1)). BW_{intra} that must be allocated under the RAMDA and V2VDA schemes are noted to attain similar values, as each intralane link must support approximately the same number of V2V packet flows issued by source vehicles resident over d_{span}, whether the packets are guided for transmission to RSU nodes or not. As D_v is increased from 10 m to higher values, assuming $D_v \leq 100$ m, and considering each RSU to accommodate more than one vehicle, the realized data rate remains relatively unchanged, as long as an intralane link stays in an interference dominated mode. Under the latter mode, adjustments in transmit power and antenna gain lead to minor changes in the achieved data rates. Under both the RAMDA and V2VDA schemes, longer D_v generally leads to a significant increase in the throughput capacity level per vehicle $TH_{C,v}$, because fewer flows issued by multiple source vehicles would then share the intralane communication bandwidth (Equation (4.2)).

In accommodating multiple packet types, we note that the system can be loaded at up to the delay-capped throughput rate with critical packets, while the remaining system capacity (i.e., not higher than $TH_{C,system}$) can be used to accommodate non critical packets (when no packet delay limits are imposed). We observe that RAMDA exhibits better packet delay performance than that attained under V2VDA, especially when considering a system loaded by critical messages at lower traffic rate levels. In this case, we assume a requirement of $D_P = 1$ ms. For example, when $d_{RSU} = 50$ m, a maximum critical message throughput rate of 2.4 Gbps can be accommodated by the RAMDA scheme, which is higher than that achieved by the V2VDA scheme, 1.95 Gbps. For other targeted delay values below 1 ms, when $d_{RSU} < 300$ m, RAMDA's overall attained packet delay level is lower than that achieved by V2VDA due to the significantly reduced number of induced V2V multi-hop transmissions, and thus inducing a lower total transmission delay, even when incorporating the fact the additional uplink and downlink hops are used. For example, for a corresponding scenario, we observe that fewer than 60 V2V intralane hops are used under RAMDA vs. 100 V2V intralane hops that are utilized under V2VDA. When $d_{RSU} > 300$ m, the delay performance of V2VDA becomes superior to that exhibited by RAMDA. We have also evaluated the system's performance under the impact of shadow fading effects, using the parameters shown in Table II, observing that such effects can lead to performance degradation. Description of associated performance behavior is however out of scope of this chapter.

4.6 Concluding Remarks

To disseminate data flows among vehicles traveling along the autonomous highway, using mmWave spectral resources, we develop RSU-aided and pure V2V based multicast dissemination networking and scheduling algorithms. We present mechanisms for operating such schemes, noted respectively as RAMDA and V2VDA, for setting the end-to-end routes and for the allocation of bandwidth resources to the links embedded in the routes. We present a process to be used for configuring and sizing the corresponding FDMA / TDMA based scheduling schemes, as employed by multiplexing/multiple-access operations across links and

routes, in a spatial reuse manner. We evaluate the delay-throughput performance behavior of both algorithms as a function of different system parameters, including inter-RSU distance, inter-vehicular range, data rate (and MCS), spatial reuse factors, beamwidths and transmit power levels. We aim to guarantee a strict packet delay requirement for critical packets and accommodate non-critical packets at a high throughput rate. When the RSU density is higher than an identified threshold, the delay performance behavior achieved by RAMDA is shown to be superior to that attained by V2VDA. When the RSU density is lower than a computed threshold, or in regions that lack a RSU infrastructure, use must be made of the V2VDA scheme. We identify the throughput rate that can be achieved for the support of critical messages that are subjected to strict packet delay limits. We determine, under the assumed mmWave system parameters and structures, the maximal achievable value for the throughput rate, when no packet delay constraints are imposed, identified as the system's throughput capacity. Furthermore, we show that both schemes achieve a similar throughput capacity level. Therefore, we note that by using RAMDA, the system's designer can dedicate capacity resources to accommodate critical packets, while still having, up to the full residual throughput capacity level, available resources that can be used to support non critical packets, employing either scheme. We note that packets that belong to certain message classes are required at times to be disseminated not only to other vehicles but also to the RSUs for processing by the infrastructure system. In this case, it is essential to employ a RSU aided scheme such as RAMDA.

CHAPTER 5

Conclusions

This dissertation presents data networking schemes for autonomous vehicle highway. We analyze the performance behavior of the networking schemes by considering cross-layer MAC / PHY parameters, including scheduling and resource allocation schemes and the corresponding spatial reuse factors, data rates and the associated modulation/coding schemes, transmit power levels, antenna beamwidth values. In addition, we also incorporate highway-specific parameters, such as inter-vehicular distance levels, which are particularly relevant for autonomous highway systems that accommodate vehicles in platoons, and the density of roadside unit (RSU) infrastructure.

We develop for autonomous transportation systems vehicular data networking mechanisms that use vehicle to vehicle (V2V) communications for data transmissions over the sub-6 GHz and mmWave bands. In the sub-6 GHz band, V2V data transmissions take place by using a vehicular backbone network which is formed by electing certain vehicles, such as selective platoon leaders, to act as vehicular backbone nodes to facilitate source vehicles which generate packets to multicast packets over a prescribed geographical span in a multi-hop fashion. We find that generally there is a trade off between the inter backbone node distance and the feasible data rate realized across the backbone network. We show that increasing the inter-BN distance reduces the number of dissemination hops (and thus enhancing the data throughput), but in turn reduces the maximum feasible data rate that is realizable over the backbone network (hence reducing the resulting throughput rate). In the mmWave band, our V2V networking scheme uses highly directional hop-by-hop transmissions.

We also study infrastructure-aided data networking for autonomous transportation systems.

We expect that in the upcoming years, many more RSUs will be installed and used to facilitate a highly reliable and high-capacity vehicular communication system. We determine the performance behavior of infrastructure-aided networking schemes under a wide range of RSU density levels in both the sub-6 GHz and the mmWave bands. We analyze the performance behavior of infrastructure aided schemes, showing the non linear dependence of the delay-throughput performance behavior on inter-RSU distance levels. The study provides guidelines for system designers in determining the inter-RSU distance ranges which satisfy the system's data dissemination objectives, as well as to select other data networking parameters.

REFERENCES

[1] C. Diakaki, M. Papageorgiou, I. Papamichail, and I. Nikolos, "Overview and analysis of Vehicle Automation and Communication Systems from a motorway traffic management perspective," *Transportation Research Part A: Policy and Practice*, vol. 75, pp. 147–165, 2015.

[2] S. Ucar, S. C. Ergen, and O. Ozkasap, "Ieee 802.11p and visible light hybrid communication based secure autonomous platoon," *IEEE Transactions on Vehicular Technology*, vol. 67, no. 9, pp. 8667–8681, 2018.

[3] F. Cuomo, I. Rubin, A. Baiocchi, and P. Salvo, "Enhanced VANET Broadcast Throughput Capacity via a Dynamic Backbone Architecture," *Ad Hoc Networks*, vol. 21, pp. 42–59, Oct 2014.

[4] H.-J. Ju and I. Rubin, "Performance analysis and enhancement for backbone based wireless mobile ad hoc networks," in *2nd International Conference on Broadband Networks, 2005.*, Oct 2005, pp. 733–742 Vol. 1.

[5] C.-C. Tan, I. Rubin, and H.-J. Ju, "Multicasting in mobile backbone based ad hoc wireless networks," in *IEEE Wireless Communications and Networking Conference (WCNC)*, vol. 2, April 2006, pp. 703–708.

[6] I. Turcanu, P. Salvo, A. Baiocchi, and F. Cuomo, "An integrated VANET-based data dissemination and collection protocol for complex urban scenarios," *Ad Hoc Networks*, vol. 52, pp. 28 – 38, 2016, Modeling and Performance Evaluation of Wireless Ad Hoc Networks.

[7] F. Yu and S. Biswas, "Self-Configuring TDMA Protocols for Enhancing Vehicle Safety With DSRC Based Vehicle-to-Vehicle Communications," *IEEE Journal on Selected Areas in Communications*, vol. 25, no. 8, pp. 1526–1537, Oct 2007.

[8] Y.-Y. Lin and I. Rubin, "Integrated Message Dissemination and Traffic Regulation for Autonomous VANETs," *IEEE Transactions on Vehicular Technology*, vol. 66, no. 10, pp. 8644–8658, Oct 2017.

[9] G. Pathak, H. Li, C. B. Math, and S. H. de Groot, "Modelling of Communication Reliability for Platooning Applications for Intelligent Transport System," in *84th IEEE Vehicular Technology Conference (VTC-Fall)*, Sep 2016, pp. 1–6.

[10] O. Shagdar, F. Nashashibi, and S. Tohme, "Performance study of CAM over IEEE 802.11p for cooperative adaptive cruise control," in *Wireless Days*, March 2017, pp. 70–76.

[11] S. Santini, A. Salvi, A. S. Valente, A. Pescapé, M. Segata, and R. L. Cigno, "A Consensus-Based Approach for Platooning with Intervehicular Communications and Its Validation

in Realistic Scenarios," *IEEE Transactions on Vehicular Technology*, vol. 66, no. 3, pp. 1985–1999, March 2017.

[12] M. Segata, B. Bloessl, S. Joerer, C. Sommer, M. Gerla, R. L. Cigno, and F. Dressler, "Toward Communication Strategies for Platooning: Simulative and Experimental Evaluation," *IEEE Transactions on Vehicular Technology*, vol. 64, no. 12, pp. 5411–5423, Dec 2015.

[13] B. Liu, D. Jia, K. Lu, D. Ngoduy, J. Wang, and L. Wu, "A Joint Control-Communication Design for Reliable Vehicle Platooning in Hybrid Traffic," *IEEE Transactions on Vehicular Technology*, vol. 66, no. 10, pp. 9394–9409, Oct 2017.

[14] T. S. Dao, C. M. Clark, and J. P. Huissoon, "Distributed platoon assignment and lane selection for traffic flow optimization," in *IEEE Intelligent Vehicles Symposium*, June 2008, pp. 739–744.

[15] J. Lioris, R. Pedarsani, F. Y. Tascikaraoglu, and P. Varaiya, "Platoons of connected vehicles can double throughput in urban roads," *Transportation Research Part C: Emerging Technologies*, vol. 77, pp. 292–305, 2017.

[16] C. Campolo, A. Molinaro, G. Araniti, and A. O. Berthet, "Better Platooning Control Toward Autonomous Driving : An LTE Device-to-Device Communications Strategy That Meets Ultralow Latency Requirements," *IEEE Vehicular Technology Magazine*, vol. 12, no. 1, pp. 30–38, March 2017.

[17] "IEEE Standard for Wireless Access in Vehicular Environments (WAVE) – Multi-Channel Operation," *IEEE Std 1609.4-2016 (Revision of IEEE Std 1609.4-2010)*, pp. 1–94, March 2016.

[18] C. Campolo, A. Molinaro, and A. Vinel, "To switch or not to switch: Service discovery and provisioning in multi-radio v2r communications," in *2016 8th International Workshop on Resilient Networks Design and Modeling (RNDM)*, Sept 2016, pp. 281–287.

[19] Y. Maalej, A. Abderrahim, M. Guizani, B. Hamdaoui, and E. Balti, "Advanced activity-aware multi-channel operations1609.4 in vanets for vehicular clouds," in *2016 IEEE Global Communications Conference (GLOBECOM)*, Dec 2016, pp. 1–6.

[20] M. van Eenennaam, A. Remke, and G. Heijenk, "An analytical model for beaconing in vanets," in *2012 IEEE Vehicular Networking Conference (VNC)*, Nov 2012, pp. 9–16.

[21] M. Hadded, R. Zagrouba, A. Laouiti, P. Muhlethaler, and L. A. Saidane, "An optimal strategy for collision-free slots allocations in vehicular ad-hoc networks," in *Vehicular Ad-hoc Networks for Smart Cities*, A. Laouiti, A. Qayyum, and M. N. Mohamad Saad, Eds. Singapore: Springer Singapore, 2015, pp. 15–30.

[22] H. A. Omar, W. Zhuang, and L. Li, "Vemac: A novel multichannel mac protocol for vehicular ad hoc networks," in *2011 IEEE Conference on Computer Communications Workshops (INFOCOM WKSHPS)*, April 2011, pp. 413–418.

[23] Federal Communications Commission, "Report and Order 03-324," docs.fcc.gov/public/attachments/FCC-03-324A1.pdf, 2004, online; accessed 19 February 2019.

[24] 5G Automotive Association, "Coexistence of C-V2X and 802.11p at 5.9 GHz," 5gaa.org/news/position-paper-coexistence-of-c-v2x-and-802-11p-at-5-9-ghz.

[25] I. Rubin, A. Baiocchi, Y. Sunyoto, and I. Turcanu, "Traffic management and networking for autonomous vehicular highway systems," *Ad Hoc Networks*, vol. 83, pp. 125 – 148, 2019. [Online]. Available: http://www.sciencedirect.com/science/article/pii/S1570870518306164

[26] ETSI, "Intelligent Transport Systems (ITS); STDMA recommended parameters and settings for cooperative ITS; Access Layer Part," ETSI, Tech. Rep. 102 861 v1.1.1, Jan 2012.

[27] "IEEE Standard for Information technology–Telecommunications and information exchange between systems Local and metropolitan area networks–Specific requirements - Part 11: Wireless LAN Medium Access Control (MAC) and Physical Layer (PHY) Specifications," *IEEE Std 802.11-2016 (Revision of IEEE Std 802.11-2012)*, pp. 1–3534, Dec 2016.

[28] M. Sepulcre, J. Gozalvez, and B. Coll-Perales, "Why 6 Mbps is Not (Always) the Optimum Data Rate for Beaconing in Vehicular Networks," *IEEE Transactions on Mobile Computing*, vol. 16, no. 12, pp. 3568–3579, Dec 2017.

[29] W. G. Cassidy, N. Jaber, S. A. Ruppert, J. Toimoor, K. E. Tepe, and E. Abdel-Raheem, "Interference modelling and SNR threshold study for use in vehicular safety messaging simulation," in *26th Biennial Symposium on Communications (QBSC)*, May 2012, pp. 52–55.

[30] "Vehicle safety communications - applications (vsc-a) final report," *U.S. Department of Transportation*, pp. 1–102, Sep 2011.

[31] Q. Xu, T. Mak, J. Ko, and R. Sengupta, "Vehicle-to-Vehicle Safety Messaging in DSRC," in *Proceedings of the 1st ACM International Workshop on Vehicular Ad Hoc Networks*, ser. VANET '04. Philadelphia, PA, USA: ACM, 2004, pp. 19–28.

[32] S. Gräfling, P. Mähönen, and J. Riihijärvi, "Performance evaluation of IEEE 1609 WAVE and IEEE 802.11p for vehicular communications," in *Second International Conference on Ubiquitous and Future Networks (ICUFN)*, June 2010, pp. 344–348.

[33] Y. Ni, J. He, L. Cai, and Y. Bo, "Data uploading in hybrid v2v/v2i vehicular networks: Modeling and cooperative strategy," *IEEE Transactions on Vehicular Technology*, vol. 67, no. 5, pp. 4602–4614, May 2018.

[34] J. Chen, G. Mao, C. Li, W. Liang, and D. Zhang, "Capacity of cooperative vehicular networks with infrastructure support: Multiuser case," *IEEE Transactions on Vehicular Technology*, vol. 67, no. 2, pp. 1546–1560, Feb 2018.

[35] T. Wu, W. Liao, and C. Chang, "A cost-effective strategy for road-side unit placement in vehicular networks," *IEEE Transactions on Communications*, vol. 60, no. 8, pp. 2295–2303, August 2012.

[36] M. Giordani, M. Rebato, A. Zanella, and M. Zorzi, "Coverage and connectivity analysis of millimeter wave vehicular networks," *Ad Hoc Networks*, vol. 80, pp. 158 – 171, 2018. [Online]. Available: http://www.sciencedirect.com/science/article/pii/S1570870518305687

[37] K. Kastell, "Analysis of planning constraints for wireless access in vehicular environments with respect to different mobility and propagation models," in *2016 18th International Conference on Transparent Optical Networks (ICTON)*, July 2016, pp. 1–4.

[38] Z. Song, L. Shangguan, and K. Jamieson, "Wi-fi goes to town: Rapid picocell switching for wireless transit networks," in *Proceedings of the Conference of the ACM Special Interest Group on Data Communication*, ser. SIGCOMM '17. New York, NY, USA: ACM, 2017, pp. 322–334. [Online]. Available: http://doi.acm.org/10.1145/3098822.3098846

[39] H. Chang and I. Rubin, "Optimal downlink and uplink fractional frequency reuse in cellular wireless networks," *IEEE Transactions on Vehicular Technology*, vol. 65, no. 4, pp. 2295–2308, April 2016.

[40] R. Zhang, X. Cheng, L. Yang, X. Shen, and B. Jiao, "A novel centralized tdma-based scheduling protocol for vehicular networks," *IEEE Transactions on Intelligent Transportation Systems*, vol. 16, no. 1, pp. 411–416, Feb 2015.

[41] N. Boulila, M. Hadded, A. Laouiti, and L. A. Saidane, "Qch-mac: A qos-aware centralized hybrid mac protocol for vehicular ad hoc networks," in *2018 IEEE 32nd International Conference on Advanced Information Networking and Applications (AINA)*, May 2018, pp. 55–62.

[42] W. Guo, L. Huang, L. Chen, H. Xu, and J. Xie, "An adaptive collision-free mac protocol based on tdma for inter-vehicular communication," in *2012 International Conference on Wireless Communications and Signal Processing (WCSP)*, Oct 2012, pp. 1–6.

[43] H. Kim, M. Emmelmann, B. Rathke, and A. Wolisz, "A radio over fiber network architecture for road vehicle communication systems," in *2005 IEEE 61st Vehicular Technology Conference*, vol. 5, May 2005, pp. 2920–2924 Vol. 5.

[44] G. M. Abdalla, M. A. Abu-Rgheff, and S. Senouci, "Space-orthogonal frequency-time medium access control (soft mac) for vanet," in *2009 Global Information Infrastructure Symposium*, June 2009, pp. 1–8.

[45] M. Hadded, P. Muhlethaler, A. Laouiti, R. Zagrouba, and L. A. Saidane, "Tdma-based mac protocols for vehicular ad hoc networks: A survey, qualitative analysis, and open research issues," *IEEE Communications Surveys Tutorials*, vol. 17, no. 4, pp. 2461–2492, Fourthquarter 2015.

[46] V. Shivaldova, A. Paier, D. Smely, and C. F. Mecklenbräuker, "On roadside unit antenna measurements for vehicle-to-infrastructure communications," in *2012 IEEE 23rd International Symposium on Personal, Indoor and Mobile Radio Communications - (PIMRC)*, Sept 2012, pp. 1295–1299.

[47] W. Shieh, W. Lee, S. Tung, B. Jeng, and C. Liu, "Analysis of the optimum configuration of roadside units and onboard units in dedicated short-range communication systems," *IEEE Transactions on Intelligent Transportation Systems*, vol. 7, no. 4, pp. 565–571, Dec 2006.

[48] I. Rubin and Y. Sunyoto, "Infrastructure-aided networking for autonomous vehicular systems," in *Proceedings of the Future Technologies Conference (FTC) 2019*, K. Arai, R. Bhatia, and S. Kapoor, Eds. Cham: Springer International Publishing, 2020, pp. 66–86.

[49] M. I. Hassan, H. L. Vu, and T. Sakurai, "Performance analysis of the ieee 802.11 mac protocol for dsrc safety applications," *IEEE Transactions on Vehicular Technology*, vol. 60, no. 8, pp. 3882–3896, Oct 2011.

[50] C. Han, M. Dianati, R. Tafazolli, R. Kernchen, and X. Shen, "Analytical study of the ieee 802.11p mac sublayer in vehicular networks," *IEEE Transactions on Intelligent Transportation Systems*, vol. 13, no. 2, pp. 873–886, June 2012.

[51] J. Gozalvez, M. Sepulcre, and R. Bauza, "Ieee 802.11p vehicle to infrastructure communications in urban environments," *IEEE Communications Magazine*, vol. 50, no. 5, pp. 176–183, May 2012.

[52] S. Djahel and Y. Ghamri-Doudane, "A robust congestion control scheme for fast and reliable dissemination of safety messages in vanets," in *2012 IEEE Wireless Communications and Networking Conference (WCNC)*, April 2012, pp. 2264–2269.

[53] M. Torrent-Moreno, J. Mittag, P. Santi, and H. Hartenstein, "Vehicle-to-vehicle communication: Fair transmit power control for safety-critical information," *IEEE Transactions on Vehicular Technology*, vol. 58, no. 7, pp. 3684–3703, Sep. 2009.

[54] L. Cheng, B. E. Henty, D. D. Stancil, F. Bai, and P. Mudalige, "Mobile vehicle-to-vehicle narrow-band channel measurement and characterization of the 5.9 ghz dedicated short range communication (dsrc) frequency band," *IEEE Journal on Selected Areas in Communications*, vol. 25, no. 8, pp. 1501–1516, Oct 2007.

[55] C. Perfecto, J. Del Ser, and M. Bennis, "Millimeter-wave v2v communications: Distributed association and beam alignment," *IEEE Journal on Selected Areas in Communications*, vol. 35, no. 9, pp. 2148–2162, Sep. 2017.

[56] R. Verdone, "Multihop r-aloha for intervehicle communications at millimeter waves," *IEEE Transactions on Vehicular Technology*, vol. 46, no. 4, pp. 992–1005, Nov 1997.

[57] X. Chen, S. Leng, Z. Tang, K. Xiong, and G. Qiao, "A millimeter wave-based sensor data broadcasting scheme for vehicular communications," *IEEE Access*, vol. 7, pp. 149 387–149 397, 2019.

[58] V. Va, T. Shimizu, G. Bansal, and R. W. Heath, "Beam design for beam switching based millimeter wave vehicle-to-infrastructure communications," in *2016 IEEE International Conference on Communications (ICC)*, May 2016, pp. 1–6.

[59] Y. Sunyoto and I. Rubin, "Infrastructure-based networking for autonomous transportation systems using IEEE 802.11p," in *2019 IEEE Vehicular Networking Conference (VNC) (IEEE VNC 2019)*, Los Angeles, USA, Dec. 2019.

[60] J. Qiao, X. S. Shen, J. W. Mark, Q. Shen, Y. He, and L. Lei, "Enabling device-to-device communications in millimeter-wave 5g cellular networks," *IEEE Communications Magazine*, vol. 53, no. 1, pp. 209–215, January 2015.

[61] Y. Wang, G. de Veciana, T. Shimizu, and H. Lu, "Performance and scaling of collaborative sensing and networking for automated driving applications," in *2018 IEEE International Conference on Communications Workshops (ICC Workshops)*, May 2018, pp. 1–6.

[62] J. Choi, V. Va, N. Gonzalez-Prelcic, R. Daniels, C. R. Bhat, and R. W. H. Jr, "Millimeter wave vehicular communication to support massive automotive sensing," 2016.

[63] 3GPP, "Study on evaluation methodology of new Vehicle-to-Everything V2X use cases for LTE and NR (Rel. 15)," *TR37.885*, June 2018.

[64] V. Va, X. Zhang, and R. W. Heath, "Beam switching for millimeter wave communication to support high speed trains," in *2015 IEEE 82nd Vehicular Technology Conference (VTC2015-Fall)*, Sep. 2015, pp. 1–5.

[65] C. Balanis, "Antenna Theory: Analysis and Design. 4th Edition ," *John Wiley and Sons*, March 2016.

[66] H. Shokri-Ghadikolaei, L. Gkatzikis, and C. Fischione, "Beam-searching and transmission scheduling in millimeter wave communications," in *2015 IEEE International Conference on Communications (ICC)*, June 2015, pp. 1292–1297.

[67] M. Polese, M. Giordani, M. Mezzavilla, S. Rangan, and M. Zorzi, "Improved handover through dual connectivity in 5g mmwave mobile networks," *IEEE Journal on Selected Areas in Communications*, vol. 35, no. 9, pp. 2069–2084, Sep. 2017.

[68] 3GPP, "Study on channel model for frequencies from 0.5 to 100 GHz (Rel. 15)," *TR38.901*, June 2018.

[69] M. Giordani, T. Shimizu, A. Zanella, T. Higuchi, O. Altintas, and M. Zorzi, "Path loss models for v2v mmwave communication: Performance evaluation and open challenges," 2019.

[70] 3GPP, "Service requirements for enhanced V2X scenarios (Rel. 15)," *TS22.186*, June 2018.

[71] B. Coll-Perales, J. Gozalvez, and M. Gruteser, "Sub-6ghz assisted mac for millimeter wave vehicular communications," *IEEE Communications Magazine*, vol. 57, no. 3, pp. 125–131, March 2019.